EINDHOVEN UNIVERSITY OF TECHNOLOGY

The influence of phosphorus on the solid state reaction between copper and silicon or germanium

Citation for published version (APA):
Becht, J. G. M. (1987). *The influence of phosphorus on the solid state reaction between copper and silicon or germanium*. [Phd Thesis 1 (Research TU/e / Graduation TU/e), Chemical Engineering and Chemistry]. Technische Universiteit Eindhoven. https://doi.org/10.6100/IR263751

DOI:
10.6100/IR263751

Document status and date:
Published: 01/01/1987

Document Version:
Publisher's PDF, also known as Version of Record (includes final page, issue and volume numbers)

Please check the document version of this publication:

• A submitted manuscript is the version of the article upon submission and before peer-review. There can be important differences between the submitted version and the official published version of record. People interested in the research are advised to contact the author for the final version of the publication, or visit the DOI to the publisher's website.
• The final author version and the galley proof are versions of the publication after peer review.
• The final published version features the final layout of the paper including the volume, issue and page numbers.

Link to publication

General rights
Copyright and moral rights for the publications made accessible in the public portal are retained by the authors and/or other copyright owners and it is a condition of accessing publications that users recognise and abide by the legal requirements associated with these rights.

• Users may download and print one copy of any publication from the public portal for the purpose of private study or research.
• You may not further distribute the material or use it for any profit-making activity or commercial gain
• You may freely distribute the URL identifying the publication in the public portal.

If the publication is distributed under the terms of Article 25fa of the Dutch Copyright Act, indicated by the "Taverne" license above, please follow below link for the End User Agreement:

www.tue.nl/taverne

Take down policy
If you believe that this document breaches copyright please contact us at:

openaccess@tue.nl

providing details and we will investigate your claim.

Download date: 04. Oct. 2023

THE INFLUENCE OF PHOSPHORUS ON THE SOLID STATE REACTION BETWEEN COPPER AND SILICON OR GERMANIUM

JOHANNA G.M. BECHT

THE INFLUENCE OF PHOSPHORUS ON THE SOLID STATE REACTION BETWEEN COPPER AND SILICON OR GERMANIUM

These investigations have been supported by the Netherlands Foundation for Chemical Research (SON) with financial aid from the Netherlands Organization for the Advancement of Pure Research (ZWO).

THE INFLUENCE OF PHOSPHORUS ON THE SOLID STATE REACTION BETWEEN COPPER AND SILICON OR GERMANIUM

PROEFSCHRIFT

ter verkrijging van de graad van doctor aan de Technische Universiteit Eindhoven, op gezag van de rector magnificus, Prof. dr. F.N. Hooge, voor een commissie aangewezen door het College van Decanen in het openbaar te verdedigen op vrijdag 22 mei 1987 te 16.00 uur

door

JOHANNA GEERTRUIDA MARIA BECHT

geboren te Bergen op Zoom

Druk: Dissertatiedrukkerij Wibro, Helmond.

Dit proefschrift is goedgekeurd door de promotoren:

Prof.dr. R. Metselaar
en
Prof.dr. G. de With

Co-promotor:
Dr. F.J.J. van Loo

aan Frits

1	Introduction	1
1.1	The reaction between copper and silicon	1
1.2	Literature survey on the reaction between Cu and Si	2
1.3	Contents of this thesis	4
	References chapter 1	5
2	Theoretical frame work	6
2.1	Phenomenological description of diffusion	6
2.1.1	Binary systems	6
2.1.1.1	Layer sequence in a binary diffusion couple	6
2.1.1.2	Determination of diffusion coefficients	8
2.1.1.3	Layer thickness	12
2.1.1.4	Reaction kinetics	14
2.1.1.5	Thin films	17
2.1.2	Ternary systems	19
2.2	Diffusion mechanisms	22
2.2.1	Volume diffusion	22
2.2.2	Short circuit diffusion	24
2.3	Temperature dependence of diffusion	24
2.4	Segregation	27
	References chapter 2	32
	appendix A	34
3	Experimental procedures	35
3.1	Materials	35
3.2	Preparation of alloys	36
3.3	Preparation of diffusion couples	37
3.3.1	Preparation of the slices	37
3.3.2	The vacuum furnace	37
3.3.3	Metallographic preparation of the diffusion couples	39
3.3.4	Other diffusion couple techniques	39
3.4	Optical microscopy	40
3.4.1	General remarks	40
3.4.2	Measurement of the thickness of the reaction layers in diffusion couples	41
3.5	X-ray diffraction	42

3.6 Electron Probe Micro Analysis (EPMA) 43
3.6.1 General 43
3.6.2 Correction program 43
3.6.3 Specimen preparation 46
3.7 AES at high temperature 46
3.8 Statistical evaluation of the data 48
References chapter 3 50

4 The influence of phosphorus on the reaction between copper and silicon 51
4.1 Scope of this chapter 51
4.2 Literature survey on the solid state reaction between copper and silicon 53
4.3 The copper-silicon phase diagram 56
4.4 Determination of the composition of the silicides 58
4.4.1 X-ray diffraction 58
4.4.2 Confirmation of the phase diagram 59
4.4.3 Improvement of the analytical procedure 59
4.4.4 Precise determination of the composition of the silicides at 500°C 62
4.5 Initial experiments 65
4.5.1 AES 65
4.5.2 Improvement of the reproducibility 66
4.5.3 Other diffusion couple techniques 67
4.5.4 Initial diffusion experiments 68
4.6 Product formation 69
4.6.1 The composition of the main product, Cu_3Si 69
4.6.2 The presence of Cu_5Si and $Cu_{15}Si_4$ 73
4.7 Determination of the diffusing component 77
4.8 Morphology of the reaction layers 79
4.8.1 Overall morphology 79
4.8.2 The development of the columnar structure 84
4.8.3 Interpretation of the morphology 85
4.9 Kinetics of the reaction 86
4.9.1 The time dependence of the layer thickness 86
4.9.1.1 Diffusion couples between silicon and pure copper 86
4.9.1.2 Diffusion couples between silicon and phosphorus-containing copper 89

4.9.2 Temperature dependence of the reaction rate constant 90
4.10 Oxidation experiments 93
4.11 Discussion and conclusions 95
References chapter 4 100

5 The reaction between copper phosphide and silicon 102
5.1 Introduction 102
5.2 Ternary phase diagram Cu-Si-P 103
5.2.1 Literature survey 103
5.2.2 Determination of the ternary phase diagram at 500°C 105
5.2.3 The Cu_3Si-Cu_3P pseudo binary system 107
5.3 The solid state reaction between Cu_3P and Si in vacuum 108
5.3.1 Product formation 109
5.3.2 The kinetics of the solid state reaction between Cu_3P and Si in vacuum 116
5.3.3 Morphology of the reaction layer in Cu_3P/Si diffusion couples annealed in vacuum 118
5.4 The solid state reaction between Cu3P and Si in a closed system 119
5.5 Conclusions 121
References chapter 5 122

6 The solid state reaction between copper and germanium 124
6.1 Introduction 124
6.2 Phase diagrams 125
6.2.1 Literature survey 125
6.2.2 Determination of the phase diagrams at 500°C 127
6.3 Diffusion reaction between copper and germanium 130
6.3.1 General remarks 130
6.3.2 Time dependence of the reaction between copper and germanium 132
6.3.3 Temperature dependence of the reaction between copper and germanium 132

6.3.4 Determination of the diffusion coefficient in copper-germanium diffusion couples 135
6.4 The reaction between Cu_3P and germanium in a vacuum system 139
6.5 Conclusions 141
References chapter 6 142

7 A comparison between silicon and germanium in their reaction with copper 143
References chapter 7 149
Summary 150
Samenvatting 152
Levensbericht 154
Nawoord 155

chapter 1 introduction

§ 1.1 The reaction between copper and silicon

When we say that we understand a chemical reaction, we usually mean to say, that we can predict the nature and the amounts of compounds , that will be formed from the reactants under certain circumstances. We need to know, which products are thermodynamically possible, and which phase relations exist between the compounds. The mechanism which is followed gives a way to predict the amount of products formed in a certain time and the effect of a change in the reaction conditions on this amount. Materials properties determine the resulting appearance of the products. In heterogeneous reactions also the state of the interface plays an important role. When one of these aspects is not known, the reaction is poorly understood.

Solid state reactions in binary diffusion couples are widely studied and generally well understood. The reactions proceed by diffusion of one or more components caused by a gradient in chemical potential. The phase diagram describing the system shows, which compounds can be expected in a diffusion couple. The parabolic growth law gives a way to predict the amounts of products formed in a certain time. Systems are normally considered to be purely binary, if the amount of impurities is less than, say, 0.1 atomic percent. Hardly any attention has been paid to the influence of a third component present in much lower concentrations, although it has already been demonstrated in oxydic systems, that both the reaction kinetics and the product morphology may be influenced by such an impurity (lit.1).

In this thesis we will describe the influence of phosphorus concentrations on a p.p.m. scale on the reaction between copper and silicon. In preliminary experiments it was found that "pure" copper, obtained from one supplier, already reacts with silicon to Cu_3Si at low temperatures, while "pure" copper from another supplier

hardly reacted at all. The main difference between the two types of copper appeared to be surface segregation of phosphorus, which was found to occur in the reactive type of copper. On the other hand, various investigators who have studied the solid state reaction between copper and silicon found widely scattering results.

One of the aims of this thesis is to explain why the presence of phosphorus has such a large influence on the reaction between copper and silicon. Furthermore we want to find out whether different amounts of phosphorus present in copper might be responsible for the conflicting results found by the former investigators on this reaction.

§ 1.2 Literature survey on the reaction between Cu and Si

In fig 1.1 the phase diagram of the copper-silicon system is shown as given by Hulgren and Desai (lit.2). Based on this phase diagram we expect the formation of Cu_5Si, $Cu_{15}Si_4$ and Cu_3Si in diffusion couples between copper and silicon below 550°C.

Veer and Kolster (lit.3) have studied the reaction between copper and silicon in the temperature range between 350 and 550°C. The only product observed is Cu_3Si. The reaction is a diffusion controlled process, but an incubation time exists. Experiments with inert markers show, that copper is the only diffusing component. The activation energy is 78 kJ/mol.

Onishi and Miura (lit.4) have studied the influence of compressive stress on the thickness of the reaction layer. If this stress is larger than 8MPa, the amount of product is independent of the applied stress. Between 420 and 465°C at 12MPa the reaction is a diffusion limited process with an activation energy of 150kJ/mol. The formation of Kirkendall pores at the copper/silicide interface indicates, that copper is the only diffusing component. Only Cu_3Si has been observed.

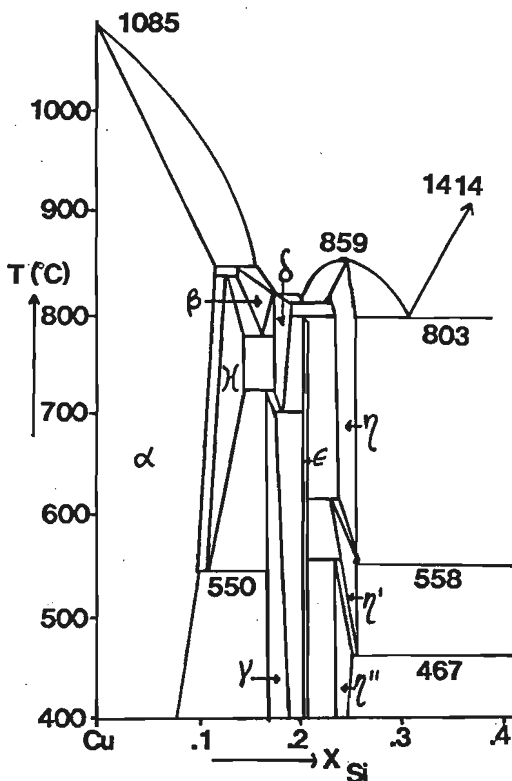

Fig.1.1 The copper-silicon phase diagram according to lit.2.

Ward and Carroll (lit. 5) have electroplated copper onto silicon slices. At low temperatures (between 250 and 350°C) and after short reaction times (≈100s) only Cu_3Si has been formed in a diffusion limited process. The activation energy is 105kJ/mol.

Although we expect the formation of three compounds, in all these investigations only Cu_3Si has been found. Furthermore the results on the reaction rate are conflicting.

§ 1.3 Contents of this thesis

After a brief outline of the theoretical background (chapter 2) and the experimental techniques (chapter 3) the reaction between copper and silicon is described in chapter 4. Attention is being paid to the compounds formed in alloys and diffusion couples. The influence of phosphorus as an impurity in copper is demonstrated and the kinetics of the reation are determined. With these data it will be explained why usually only Cu_3Si has been found and why "pure" copper from different sources react at different rates.

In chapter 5 the reaction between copper phosphide and silicon is studied, in order to get more insight in the phase relations in the ternary system Cu-Si-P. The large influence of the atmosphere, in which the annealing of the alloys and diffusion couples takes place, on the nature and morphology of the reaction products will be described.

Chapter 6 deals with the reaction between copper and germanium, both with and without the presence of phosphorus. Based on the resemblance of the phase relations in the Cu-Ge and Cu-Ge-P systems, compared with the Cu-Si and Cu-Si-P systems, it can be expected that the same type of reactions takes place. As turned out from our experiments, this is not the case. In chapter 7 the reasons for this difference are explained.

References chapter 1

1] P.J.C. Vosters, M.A.J.Th. Laheij, F.J.J. van Loo
R. Metselaar; Oxid.Met. 20(1983),147

2] R.Hultgren, P.D. Desai; Selected thermodynamic values and phase diagrams for copper and some of its binary alloys. International Copper Research Association Inc. (1971)

3] F.A. de Veer, B.H. Kolster, W.G. Burgers;
Trans.Met.Soc.AIME. 242(1968),669

4] M. Onishi, H. Miura;
Trans.Jap.Inst.Met. 18(1977),107

5] W.J. Ward, K.M. Carroll;
J.Electrochem.Soc. 129(1982),227

chapter 2 theoretical framework

In this chapter the theoretical basis for the research described in this thesis will be given. This comprises a phenomenological description of diffusion and some solutions of the differential equation describing diffusion. The consequences for the reaction kinetics are studied. The differences between binary and ternary systems with respect to the layer sequence and the thickness of the product layers will be discussed.

The next subjects are the various diffusion mechanisms and the consequences for the temperature dependence of diffusion.

A few words will be devoted to impurity segregation.

§ 2.1 Phenomenological description of diffusion

§ *2.1.1 Binary systems*

§ *2.1.1.1 Layer sequence in a binary diffusion couple*

If we press two elements together in a diffusion couple at elevated temperatures, a homogenization will occur. After a while a concentration gradient will be observable, which is continuous if the two elements form a complete solid solution in the whole concentration range.

However, if the two elements react according to the hypothetical phase diagram of fig.2.1, reaction layers will be formed, like schematically represented in the right hand side of fig.2.1.

The discontinuity in the concentration gradient arises from the fact that local chemical equilibrium is assumed. A straight-lined interface between α and γ develops, which stems from the phase rule:

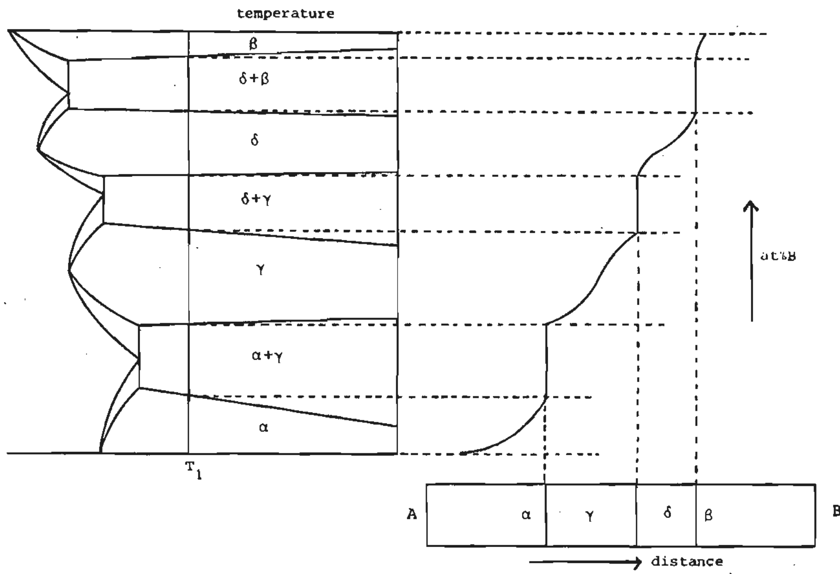

Fig.2.1 Relation between a hypothetical phase diagram and the product layers formed in a diffusion couple, after annealing at temperatuur T_1.

$$F = C - P + 2 \qquad [2.1]$$

where F is the number of degrees of freedom
C is the number of components
P is the number of phases allowed to be in equilibrium with each other.

In a binary system, there are 2 components; in a diffusion couple temperature and pressure are fixed. When two phases are in equilibrium, no degree of freedom is left for the thermodynamic potential (or in a binary system the concentration) to adapt itself. Since an adaptation of the thermodynamic potential is essential for the diffusion process, only single-phased regions can be formed. Only straight-lined interfaces are allowed, under the condition that local equilibrium exists, that is: nucleation is fast compared with the diffusion process. If however nucleation is hindered, phases may be absent and the phases that are formed may show supersaturation.

2.1.1.2 Determination of diffusion coefficients.

We define the origin of the coordinate system applying to a planar diffusion couple, x=0, fixed with respect to the non-diffused left hand side of the diffusion couple. If the total volume remains constant we can express the inter-diffusion flux $\tilde{J}_i$ of component i across any plane in a diffusion couple, fixed with respect to the origin, by Fick's first law, eq.[2.2].

$$\tilde{J}_i = -\tilde{D} \left(\frac{\delta c_i}{\delta x}\right) \qquad [2.2]$$

where the gradient has been taken parallel to the x-axis. $\tilde{D}$ is called the chemical or interdiffusion coefficient, expressed in m^2/s and c_i is the concentration of compound i in mole particles i/m^3.

In a diffusion couple however a steady state will not exist, that is, the concentration and its gradient are changing with time. In that case Fick's second law of diffusion [2.3] is a more convenient form to determine $\tilde{D}$. It has been derived from combining the first law with the law of mass conservation for constant partial molar volumes of both components.

$$\frac{\delta c_i}{\delta t} = \frac{\delta}{\delta x} \left(\tilde{D} \frac{\delta c_i}{\delta x}\right) \qquad [2.3]$$

Various solutions to this differential equation exist, depending on the problem studied. The most common case is that the diffusion coefficient is a function of the concentration. The differential equation [2.3] becomes an inhomogeneous one. It can be transformed into a homogeneous equation by the substitution originally made by Boltzmann (lit.1), $\lambda = x/t^{0.5}$.

Matano (lit.2) has applied this substitution to interdiffusion problems, which allows $\tilde{D}(c_i)$ to be calculated from an experimental $c_i(x)$ plot. The boundary conditions for the differential equation for a semi-infinite diffusion couple are, that the compositions at the ends of the couple halves, this is c_i^- and c_i^+ (see fig.2.2) do not change during the reaction.
The origin of the x-axis is defined by:

$$\int_{c_i^-}^{c_i^+} x \, dc_i = 0 \qquad [2.4]$$

The plane where x = 0 is called the Matano plane.

With this definition the interdiffusion coefficient $\tilde{D}(c_i*)$ can be obtained with equation [2.5], which can be solved graphically from the measured penetration curve as is shown in fig.2.2.

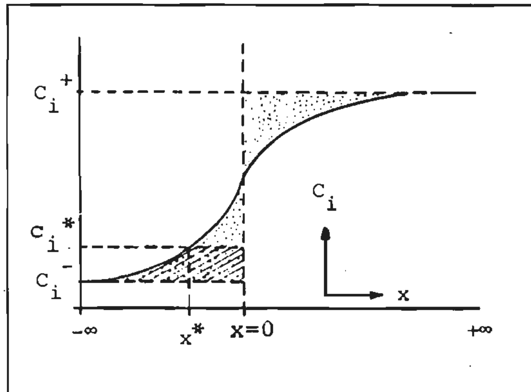

Fig.2.2. Solution of [2.5] by graphical means. Both dashed areas have equal size. They determine the position of the Matano plane, x=0. The shaded area gives the value for the integral in [2.5] at x.*

[2.5]

$$\tilde{D}(c_1*) = -\frac{1}{2t}\left(\frac{dx}{dc_1}\right)_{c_1=c_1*} \int_{c_1^-}^{c_1*} x \, dc_1$$

The diffusion coefficient $\tilde{D}(c_i)$ describes the overall process.

Kirkendall and Smigelskas (lit.3) have marked the original contact interface in a copper-brass diffusion couple with molybdenum wires. After an annealing treatment the markers have moved with respect to the Matano plane towards the brass side. This effect, called the Kirkendall effect, can only be explained if we assume that the components, copper and zinc, have unequal diffusion coefficients, a concept introduced by Darken (lit.4).

Then the interdiffusion flux of component i has two components: firstly there exists an intrinsic flux of atoms which is determined by the concentration gradient of component i; secondly, since the intrinsic diffusion coefficients differ contraction occurs at the side of the fastest moving component, expansion at the other side, resulting in a net displacement of lattice planes, shown by the marker displacement. The expression for the interdiffusion coefficient can now be generalised to (lit.5) :

[2.6]

$$\tilde{D} = c_2\bar{v}_2D_1 + c_1\bar{v}_1D_2$$

where $\bar{v}_i$ denotes the partial molar volume of component i. The intrinsic diffusion coefficients D_i can be determined from the marker displacement x_m and the concentration profile.

If at least one of the starting materials is a pure component, e.q. $c_1^- = 0$, a simple expression for the intrinsic diffusion coefficient exists, as is shown by van Loo (lit.5):

[2.7]

$$D_i(x=x_m) = \frac{1}{2t}\left(\frac{dx}{dc_i}\right)_{x=x_m} \int_{-\infty}^{x_m} c_i\,dx$$

More general expressions have been derived by van Loo (lit.5) and Bastin (lit.6). Application of the various equations depends on the characteristics of the system studied.

Sauer and Freise (lit.7) have derived an expression for the interdiffusion coeffient in case of a binary system in which the partial molar volumes V_m are concentration dependent [2.8]:

[2.8]

$$\tilde{D}(Y^*) = \frac{V_m(Y)^*}{2t}\left(\frac{dx}{dY}\right)^* \left[(1-Y^*)\int_{-\infty}^{x^*} \frac{Y}{V_m(Y)}\,dx + Y^* \int_{x^*}^{+\infty} \frac{(1-Y)}{V_m(Y)}\,dx\right]$$

where $Y = \dfrac{N_i - N_i^-}{N_i^+ - N_i^-}$

and N_i denotes the mole fraction of component i.

All previous given solutions for the determination of diffusion coefficients are dependent on the existence of a concentration gradient in the phase studied. If however the homogeneity range is very small the gradient becomes virtually zero and dx/dc_i becomes infinite, leading to infinite diffusion coefficients when determined with the previous equations. To escape this problem Wagner (lit.8) has defined a new variable, called an integrated diffusion coefficient:

[2.9]

$$D^{y}_{int} = \int_{N_i(y')}^{N_i(y'')} \tilde{D} \, dN_i$$

where $N_i(y'')$ and $N_i(y')$ are the -unknown- limiting mole fractions of component i in compound y. For a line compound y with a layer thickness d_y and
$N_i(y') \tilde{=} N_i(y) \tilde{=} N_i(y'')$
Wagner derives from [2.8]

[2.10]

$$D^{y}_{int} = \frac{(N_i(y)-N_i^-)(N_i^+-N_i(y))}{N_i^+ - N_i^-} \left(\frac{d_y^2}{2t}\right) +$$

$$\frac{d_y}{2t}\left[\frac{N_i^+-N_i(y)}{N_i^+-N_i^-}\int_{-\infty}^{x(y-1,y)}\frac{V_m(y)}{V_m}(N_i-N_i^-)\,dx + \frac{N_i(y)-N_i^-}{N_i^+-N_i^-}\int_{x(y,y+1)}^{+\infty}\frac{V_m(y)}{V_m}(N_i^+-N_i)\,dx\right]$$

where $x(y-1,y)$ and $x(y,y+1)$ are respectively the positions of the left-hand and right-hand boundaries of the y-layer. If no gradient exists outside the y layer the term between the square brackets becomes zero.

§ *2.1.1.3 Layer thickness*

Within a binary diffusion couple the thickness of the product layers will be adjusted in such a way, that a reaction layer where the diffusing component has a low diffusion coefficient, will be thin compared with a layer where the diffusion coefficient is high.

Changing the reaction conditions will be a solution if

one decides to study a layer with a low diffusion coefficient. The most frequently applied method is to change the composition of the starting materials. Instead of pure elements, compounds are used. With the aid of equation [2.10] and using the fact that the integrated diffusion coefficient is a material constant for each phase, it can be shown that in this case a thicker layer will develop.

Assume that two layers develop, both without a concentration gradient, as is experimentally often the case, and that the molar volume is constant throughout the whole couple.

N_y is the mole fraction of component B in compound y which forms a very thin layer (d_y^{I}) in a couple between the pure elements (situation I, see fig. 2.3), N_δ is the mole fraction of B in the main product δ in that same diffusion couple, with thickness d_δ^{I}. We get the following equation:

[2.11a]

$$D^{y}_{int} = \frac{(N_y - N_A)(N_B - N_y)}{(N_B - N_A)} * \frac{(d_y^{I})^2}{2t^{I}} + \frac{d_y^{I}}{2t^{I}} * \left[\frac{N_y - N_A}{N_B - N_A} * d_\delta^{I} * (N_B - N_\delta) \right]$$

In a diffusion couple between A and δ (situation II) only y develops, with a layer thickness d_y^{II}.

The following equation applies:

[2.11b]

$$D^{y}_{int} = \frac{(N_y - N_A)(N_\delta - N_y)}{(N_\delta - N_A)} * \frac{(d_y^{II})^2}{2t^{II}}$$

Since D^{y}_{int} is a material constant, [2.11a] equals [2.11b]. We take $t^{I} = 2t^{II}$.

Furthermore $N_A = 0$ and $N_B = 1$, since pure elements are used. We can deduce a relation between d_δ, d_y^{I} and d_y^{II}:

[2.12]

$$(d_y^{II})^2 = \frac{(1 - N_y) * N_\delta}{N_\delta - N_y} * (d_y^{I})^2 + \frac{(1 - N_\delta) * N_\delta}{N_\delta - N_y} * d_y^{I} * d_\delta^{I}$$

It can be shown that $d_y^{II} > \delta_y^{I}$ (appendix A).

The practical application of this technique will be discussed in § 4.5.2.

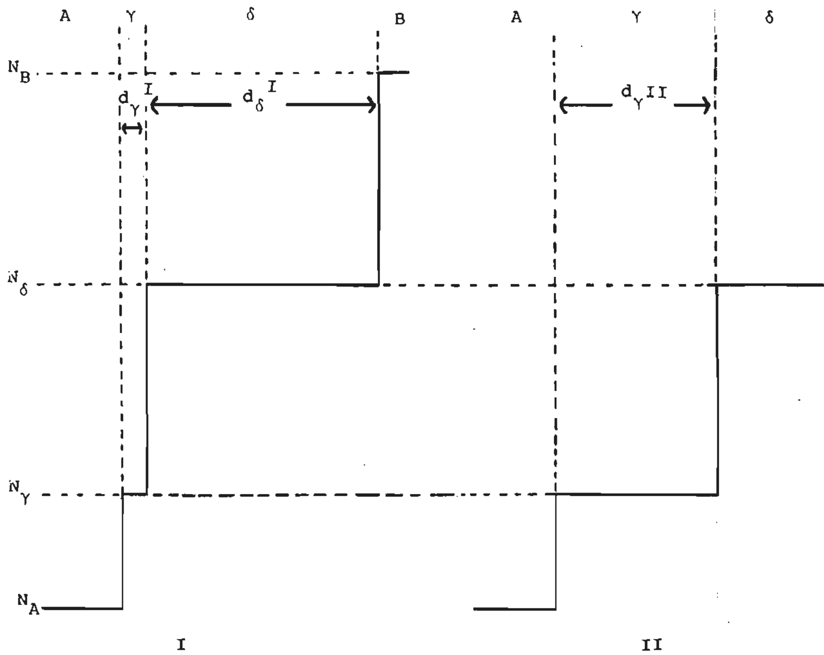

Fig.2.3 Penetration curve for two hypothetical diffusion couples; I = a couple between the pure elements A and B, II = a couple between a compound δ and the pure element B.

§ *2.1.1.4 Reaction kinetics*

The Boltzmann substitution $\lambda = x/t^{0.5}$ has physical meaning, since λ is only a function of the concentration c. Therefore all concentrations, including the phase boundary concentrations, move proportionally with the square root of time. This is the well known parabolic growth law :

$$d^2 = k.t \qquad [2.13]$$

with k is the reaction rate constant.

Although sofar nothing has been said about the diffusion mechanism, an exception has to be made here. Formally the parabolic growth law only applies for a volume diffusion limited process. When the reaction layer grows by grain boundary diffusion the situation is different, since only a small part of the interface area is involved in the supply of reactants. Stark (lit.9) has demonstrated that, in case of grain boundary diffusion through the reaction layer and infinitely fast lateral diffusion at the reaction interface, $d\ln d/d\ln t = 11/20$ which is experimentally indistinguishable from $d\ln d/d\ln t = 1/2$.

It has to be stressed that equation [2.13] is valid for a diffusion limited process. In practice several deviations can occur. If the reaction layer is porous, as for instance in oxidation reactions may happen, direct contact between the reactants is maintained and no limitation by diffusion through the reaction layer occurs. The layer thickness is a linear function of time.

Another situation appears when a reaction barrier exists. We can think of non-porous oxidation layers or deformed layers at the reaction interface. The reaction rate then is determined by the transport of the components across the interface. The diffusion in the reaction layer is again not rate determing.

Often the reaction barrier will be removed, after an incubation time t_0 and the reaction rate of the process will be limited by the diffusion through the reaction layer. From that point of time the thickness of the reaction layer follows a modified parabolic growth law:

$$d^2 = k\,(t-t_0) \qquad [2.14]$$

In equation [2.14] it is assumed, that no product layer has been formed during the incubation time.

A consequence of the presence of an incubation time is, that a plot of the layer thickness as a function of the square root of time gives a false impression of the reaction kinetics. This can be demonstrated with fig.2.4. Here the

layer thickness, for a diffusion limited process calculated from [2.14] with $k = 10^4$ and $t_0 = 5$, is plotted as a function of $t^{1/2}$.

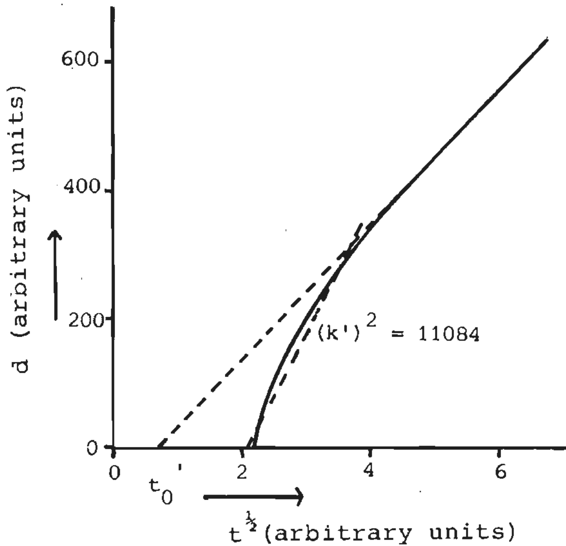

Fig.2.4 A plot of d as a function of $t^{1/2}$; d calculated from $d^2 = k(t-t_0)$, with $k = 10^4$, $t_0 = 5$.

Fig.2.4 shows that the layer thickness is not a linear function of $t^{1/2}$. Furthermore the reaction rate constant derived from the beginning of such a plot is too high: if only data up to $t^{0.5}=4$ are measured, an apparant rate constant $(k')^2=11000$ is found, which is 10% too high. In fig.2.4 it is obvious that an incubation time exists, but for smaller t_0 the scatter in the experimental data will obscure its presence. This may be the reason why incubation times are hardly found when the thickness is plotted against $t^{1/2}$. And IF an incubation time is found it can not be accompanied with a linear relationship (lit.10), because this would imply that $(t-t_0)^{1/2} = t^{1/2} + K$. Therefore plotting the squared thickness as a function of the reaction time is the best way to determine the reaction kinetics.

2.1.1.5 Thin films

In the previous sections semi-infinite diffusion couples are discussed. The semi-infinity is essential, because then the condition is fulfilled that the composition at the end of the diffusion couple does not change during the annealing treatment. Since the 1970's , however, thin layer diffusion couples have become of great interest, especially in micro electronic device industry, where contacts are constructed on silicon wafers. So the reactions between metal films and bulk silicon slices are intensively studied. The remarkable finding in these studies is, that inter-diffusion and reactions in thin films can be observed at a much lower temperature than in bulk couples. This is due to the purity of the interface between thin films, highly defective microstructures and better detection sensitivity in thin film analytical techniques (lit.11). In compound formation, the stable compounds tend to form sequentially, i.e. they grow one by one in thin film bilayers, instead of growing together as in bulk cases. One essential difference between a thin layer and a bulk specimen is the influence of the surface in the thin film case: about 10% of the atoms in a film of 20 nm thick have to be considered to be surface atoms, with possible differences in bonding, mobility and lattice positions. These aspects have not be considered in the previous discussion, and will not be discussed here.

Gösele et al (lit.12) have shown that in diffusion couples a layer has to exceed a critical thickness before a second phase can develop. In the nickel-silicon system the critical thickness for the Ni_2Si layer is estimated to be 2 μm, a value that will not be reached in structures with layers of about 100 nm. Therefore no other compounds are expected in these thin film couples for kinetic reasons.

The reactions in thin film couples are often terminated because one of the reactants is depleted. The continuation of the reaction depends on the reactant left, as is shown in fig.2.5., where the reactions in the nickel-silicon system are summarized. The first layer is Ni_2Si. If

silicon is depleted the formation of Ni_5Si_2 starts, until all Ni_2Si is consumed. Then the formation of Ni_3Si begins. On the other hand, if nickel is depleted Ni_2Si is converted into NiSi and the reaction is concluded with $NiSi_2$.

It cannot be predicted which compound appears first, although it is sometimes suggested that it is that compound which has the highest melting point, i.e. the most stable compound (lit.13).

In conclusion : the results found in thin layer couples can not be translated to bulk diffusion couples and vice-versa. The concept of critical thickness however may be useful in bulk diffusion couples although the layer thicknesses usually will exceed these critical values.

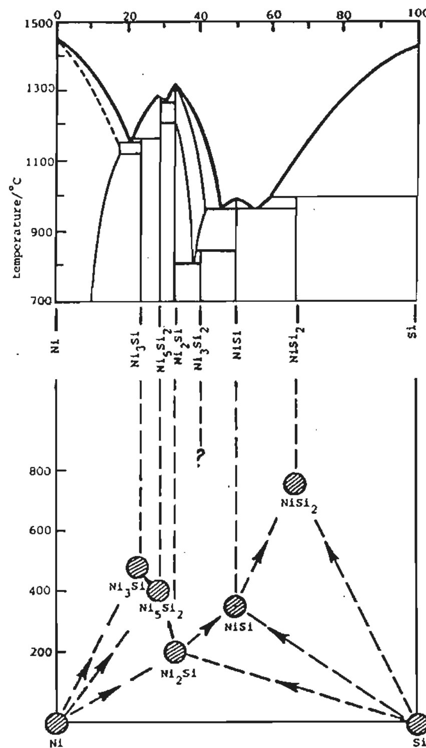

Fig.2.5. Formation map of thin film Ni silicides showing the sequence of phase formation against formation temperature. The schematic phase diagram Ni-Si is shown on top for comparison (after Tu, lit.11). Note that the phase diagram cannot be correct omn a number of points.

§ 2.1.2 Ternary systems

In a binary, isobaric and isothermic system we have one degree of freedom, a concentration N_a, defining the acticity of the components. In a ternary, isobaric and isothermic system we have an additional degree of freedom. A system is defined by two concentrations N_a and N_b. The chemical potential of a component is dependent on the concentrations of both other components. The definition of diffusion coefficients in a ternary system is a complicated matter, since not a single diffusion coefficient but a complex system of coefficients exists. Because this thesis will not deal with diffusion coefficients in ternary systems, we will not go further into the diffusion equations for ternary systems. Although in binary systems the concentration gradient may be taken as the driving force for diffusion, in ternary systems it is clear that the driving force is a gradient in chemical potential. This is demonstrated with an experiment conducted by Darken (lit.14), where a diffusion couple is made from a Fe-C and a Fe-C-Si alloy, both with the same carbon content. In fig.2.6 the results are shown. It is clear that a redistribution of carbon has occurred. If the chemical potential of carbon is plotted (see fig.2.6) as a function of distance it becomes clear the carbon diffusion is not in conflict with thermodynamic rules.

The additional degree of freedom also has a consequence for the layer formation. Two phased regions are allowed. Whether they occur, depends on the thermodynamics and the relative diffusion coefficients in the system. Consider a diffusion couple between B and AX, where BX and A are formed. Rapp (lit.15) has extensively studied the stability of an original planar interface between BX and A in case of an accidental perturbation, in oxidic systems, i.e. X = oxygen. Whether this perturbation grows or vanishes depends on the element diffusing in the rate limiting step. If the BX layer is locally thinner and the diffusion of B through BX is rate limiting, the growth of the BX phase at this particular

place will be faster than in the surroundings until a uniform thickness has been reached, so the perturbation vanishes, see fig.2.7.I.a. If the diffusion of X through A is rate limiting however, in this area where BX is thinner (and so the A layer is thicker) the supply of X will be retarded compared with the surroundings. Therefore a perturbation will be retained and develops into a two phased region (fig.2.7.I.b). Rapp's model only applies for systems with the layer sequence B/BX/A/AX. However in sulphidic systems also the layer sequence B/A/BX/AX has been observed (lit.16), (Fig.2.7.II).

Van Loo (lit.17) has developed a model, which enables us to predict whether layer sequence I or II will occur. It states that the layer sequence depends on the slope of the tie lines between the metal phase(s) and the phases AX and BX. If this sign is the same throughout the whole phase diagram (fig.2.8.a) the sequence AX/A/BX/B is found. If the sign of the slopes changes (fig.2.8.b) the sequence AX/BX/AB/B is the only one thermodynamically allowed. Component X endures a rise in chemical potential and is therefore stationary. For details of this model one is referred to the original literature.

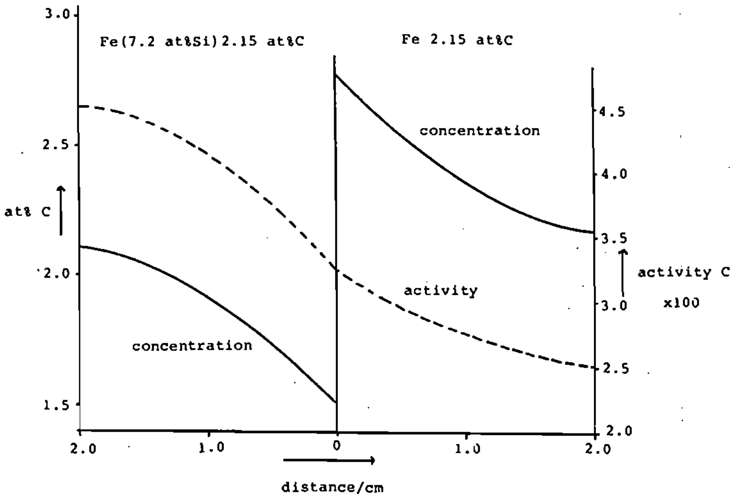

Fig.2.6 The carbon penetration curve and the carbon activity for a diffusion couple, annealed for 13 days at 1050°C, after Darken (lit.14).

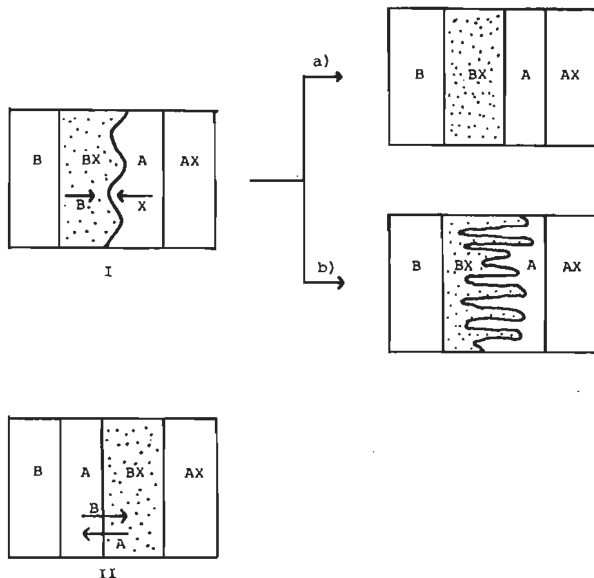

Fig.2.7. Possible morphologies for B/AX diffusion couples.

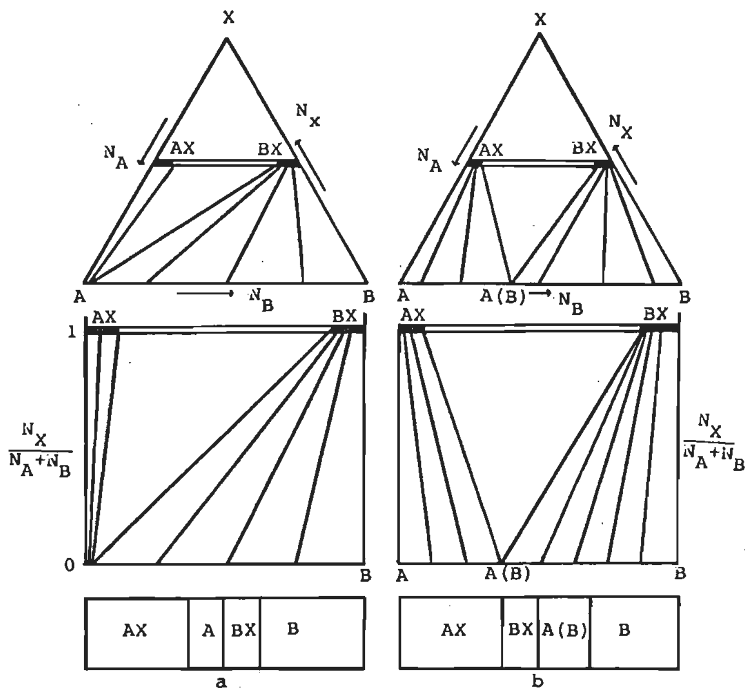

Fig.2.8 Schematic phase diagrams and the layer sequences that are related with them, after van Loo (lit.17).

Besides thermodynamic and kinetic considerations, in a ternary system always the mass balance has to be obeyed, which states that in a reaction between AX and B the same number of moles of BX and A have to be formed. If the phases A and BX are formed in parallel layers, this results in a fixed ratio of the layer thicknesses for A and BX, depending on the molar volumes. The total thickness will be determined by the slowest diffusion in one of the layer. If the reaction layer is built up as a two-phased mixture of A and BX the total thickness will depend on the diffusion characteristics of the matrix phase.

§ 2.2 Diffusion mechanisms

So far nothing has been said about diffusion on microscopic scale. We have to distinguish two groups of mechanisms: diffusion through the bulk of a phase and short circuit diffusion. Both types will be discussed briefly.

§ *2.2.1 Volume diffusion*

In volume diffusion the motion of a diffusing atom takes place through the lattice. In crystalline solids the atoms occupy well defined equilibrium positions; they move by jumping succesively from one equilibrium site to another. Several mechanisms are possible:

a) exchange mechanisms.

In the direct exchange mechanism two neighbouring atoms exchange their positions (fig.2.9.a). In dense structures this mechanism would involve large distortions and hence large activation energies. A cyclic exchange mechanism (fig.2.9.b) would involve less energy, but this mechanism remains unlikely, because of the constraint imposed by the collective motion. There is no experimental support for this mechanism in crystalline solids, although in metallic liquids and in amorphous alloys cooperative motions are more likely operating (lit.18).

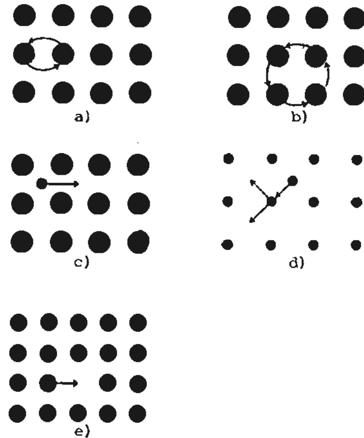

Fig.2.9
Schematic presentation of the various diffusion mechanisms,
a) exchange mechanism,
b) ring exchange mechanism,
c) interstitial mechanism,
d) interstitialcy mechanism,
e) vacancy mechanism.

<u>b] mechanisms involving point defects</u>

A solid in thermal equilibrium always contains point defects like interstitials and vacancies. These defects offer the possibility for atoms to move without too large lattice distortions. Small interstitial atoms, like hydrogen and carbon in metals, diffuse through the lattice by motion from one interstitial site to another interstitial site, obviously called interstitial mechanism (fig.2.9.c). A second mechanism involving interstitials is the interstitialcy mechanism (fig.2.9.d): the atoms move from interstitial sites to substitutional sites and vice-versa. This mechanism is important when the material is out of equilibrium, for instance after plastic deformation or irradiation.

Near the melting point the vacancy concentration can be as high as 10^{-3} site fraction. These empty sites allow neighbouring atoms to move easily (fig.2.9.e). It is this vacancy mechanism that provides an explanation for the Kirkendall effect (§ 2.1.1.2): the atoms of one component exchange their positions with vacancies more often than the other atoms. A nett displacement of the lattice results, since the equilibrium number of vacancies will be maintained. The vacancy flux will be sustained because dislocations and surfaces act as sources and sinks for vacancies. If the supply of vacancies is too large to be absorbed pores will be formed, the so-called Kirkendall pores. This happens

often near the original interface, in the couple halfwith the highest concentration of the fastest diffusing component.

§ 2.2.2 *Short circuit diffusion*

All those regions in a lattice which have lost their perfect ordered structure can serve as short circuits. We can think of grain boundaries, interfaces, dislocations and surfaces. Notably grain boundaries are well studied (lit.19, lit.20). It is established that diffusion takes place involving vacancies in the grain boundary, with an activation energy lower than for bulk diffusion.

It is often difficult to distinguish between volume diffusion through vacancies on the one hand and short circuit diffusion through dislocations on the other hand. Especially in highly defective structures with fast diffusion directions the distinction gets vague: in both cases "bulk" diffusion occurs and a low activation energy is experimentally found.

§ 2.3. Temperature dependence of diffusion

The interdiffusion coefficient can experimentally often be described with an Arrhenius equation, although the interdiffusion coefficient in a binary intermetallic system is the sum of two terms (equation [2.6]), each with their own temperature dependence,

$$\tilde{D} = D_0 * \exp(-Q/RT) \qquad [2.15]$$

where Q is the activation energy, and D_0 is the frequency factor.

This rather simple temperature dependence can be explained by several reasons:

a] the diffusion process is almost entirely determined by the diffusion of one component,

b] the activation energies for both components are equal,

c] the temperature range in which the experiments are conducted is short. An apparant linear relation between lnD and 1/T is easily found then within the experimental error.

If the temperature range is very large, deviations from [2.15] are found: the plot between ln D and 1/T is curved or two distinct slopes are observed. In the first case two competative processes occur, while in the second case a different process becomes rate determining. This second, low temperature process is generally grain boundary diffusion, which becomes important at low temperatures because of its low activation energy, i.e. its weak dependence on temperature.

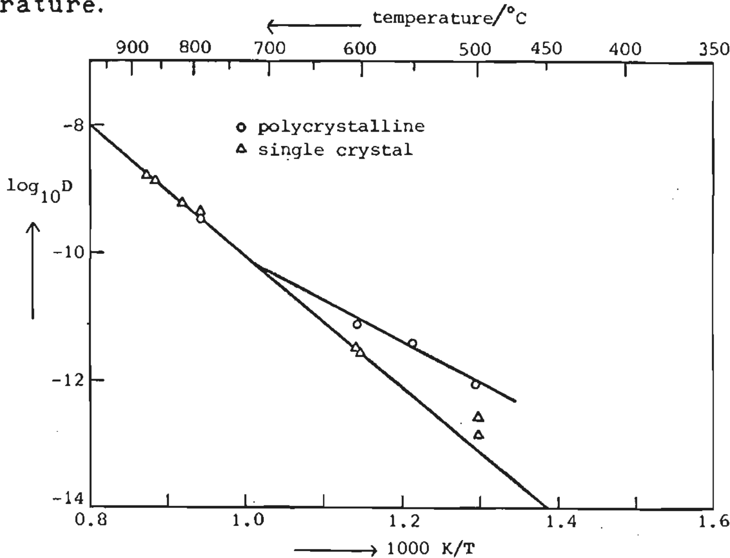

Fig.2.10 Self diffusion in silver as a function of temperature, determined for two types of specimens: a single crystal an poly crystalline material.

$D_{gb} = 2.3 * 10^{-5} \exp(Q_{gb}/RT)$ (cm^2/s)

$D_l = 0.895 \exp(Q_l/RT)$ (cm^2/s)

$Q_{gb} = 11*10^4$ J/mol, $Q_l = 19*10^4$ J/mol

This is very nicely demonstrated by Turnbull (lit.21) for the self diffusion of silver (fig.2.10). We see the large difference between polycrystalline and single crystal material. Below 700°C the diffusivity in the grain boundaries is so high relative to the lattice diffusivity, that the grain boundaries contribute substantially in polycrystalline material. Of course at high temperatures also diffusion takes place in the grain boundaries, but since the temperature dependence is small, this will only contribute a small fraction to the total transport. Besides, the amount of grain boundary surface quickly gets smaller at high temperature due to recrystallisation.

The branching of the ln D versus 1/T plot occurs around 700°C, which is at about 0.75 T_m (melting point in Kelvin). It is often found, that below $T \cong 0.75\ T_m$ grainboundary diffusion becomes important (lit.22). It should however be stressed that the extent in which grain boundary diffusion contributes to the transport, depends on the grain size. We can think of a coarse grained silver specimen in the Turnbull experiment where grain boundary diffusion only contributes significantly below, say 500°C, while in a single crystal grain boundary diffusion will obviously not occur.

Since the reaction rate constant (as defined in equation [2.13]) contains even more temperature dependent variables (lit.23), it is surprising that even then one process is so overwhelmingly important, that a simple Arrhenius plot often is found. The activation energy, determined from the reaction rate constant is an experimental value for the overall process. It can not be attributed to a single process, unless it is certain from other evidence, that it is indeed this single process that determines the reaction rate.

§ 2.4 Segregation

Segregation is the phenomenon that causes the composition of a grain boundary or a surface to differ from the bulk composition. Although grain boundary and surface segregation are based on the same thermodynamic principles, they are often described by different models. A rough division (which is certainly not true for all cases) can be made between two types of approximations: grain boundary segregation is described by phenomenological models, often based on adsorption theories, while surface segregation is studied with atomistic models, where the electronic structure of the segregant is stressed.

These differences in approach stem from the fact that grain boundary and surface segregation are encountered in different fields. Grain boundary segregation is studied in relation with material properties like brittleness in metals caused by non metallic impurities such as carbon, phosphorus and sulphur in iron. On the other hand surface segregation is important for heterogeneous catalysis, where a detailed description of the alloy surface is necessary for the understanding of the catalyst behaviour.

Here only a brief survey on some aspects of segregation will be given. For a more comprehensive treatment of this subject the reader is referred to the numerous reviews (lit. 24 and 25) and books (lit. 26) published on this subject.

Segregation is already discussed by Gibbs, who observed that a phase has boundaries, and that these boundaries will contribute to the total free energy of a system. He developed his theory for liquids, but already noticed that the same would apply for solids (lit.27), both for free surfaces and for internal boundaries like grain boundaries.

The central equation is the Gibbs Adsorption Equation:

$$d\gamma = -S^{s}dT - \Gamma_A d\mu_A - \Gamma_B d\mu_B \qquad [2.16]$$

where γ is the surface energy, S^s is the specific surface excess entropy, Γ_A and Γ_B are the surface excess concentra-

tions and μ_A and μ_B are the chemical potentials of component A and B in the alloy, respectively. Thus equation [2.23] gives a relation between surface composition (expressed indirectly in terms of Γ's), bulk composition (expressed in terms of μ's) and temperature. In order to apply this equation it is necessary to know the surface energy of the alloy as a function of temperature and bulk composition.

Unfortunately it is difficult to determine the surface energy of a solid and the relation between the observable quantities and those in equation [2.16] is not a simple one (lit.28). Therefore approximations have been developed.

The general procedure is to write down the total free energy of a system and minimize this free energy with respect to the composition of the phases. The general result for a binary system can be written as:

[2.17]

$$\frac{N_A^s}{1 - N_A^s} = \frac{N_A^b}{1 - N_A^b} \exp(- \Delta H_a/RT)$$

where N_A^s and N_A^b are respectively the atom fractions of component A in the surface layer and the bulk phase. ΔH_a is the enthalpy of adsorption or segregation.

McLean (lit.29) has postulated that the strain energy, E_{el} associated with a solute atom in a solid solution (arising from the difference in atomic volume) will be eliminated by segregation of the solute atom. Thus:

[2.18]

$$\Delta H_a = -E_{el} = \frac{24\ \pi K G r_0 r_1 (r_0 - r_1)}{3 K r_1 + 4 G r_0}$$

with K is the bulk modulus of the solute, G is the shear modulus of the solvent and r_0 and r_1 are the appropriate radii for the solvent and solute atoms respectively. Within a factor 2 the values arising from this equation agree with the experimentally determined values (lit.24).

McLean has made the assumption that monolayer segregation occurs, in analogon with the Langmuir adsorption isotherm. The analogon can be extended to a BET (Brunauer-Emmett-Teller) isotherm (lit.30). The interaction between solute and solvent can be taken into account and more component systems can be described by these approximations (lit.31).

Another way to determine ΔH_a is calculation of the change in the total free energy when atomic bonds are broken (broken bond model)(lit.32). A point of discussion is the number of atomic layers where the composition differs from the bulk composition. For ideal solutions the surface layer comprises one atomic layer (lit.32), but for regular solutions 3 (lit.33) to 7 (lit.34) layers are influenced by the presence of the surface.
Expressions like [2.19] are derived

$$\Delta H_a = \frac{Z_v}{2} (\epsilon_{BB} - \epsilon_{AA}) + 2\omega Z_l (N_A{}^b - N_A{}^s) + 2\omega Z_v (N_A{}^b - 1/2) \qquad [2.19]$$

with Z_l is the number of lateral bonds of the atom within its layer (parallel to the surface), Z_v is the number of out of plane bonds, ϵ_{ij} is the bond energy between atom i and j and ω is the alloy parameter, its precise definition depending on which model is used to describe the solution. As a consequence the various models also take different atomic bonds into account.

It is clear that any realistic description of segregation should include all contributions: surface energies, alloy interactions, and solute strain energy. A first approximation is a simple summation of all contributions leading to [2.20] (lit.35).

$$\Delta H_a = (\gamma_A - \gamma_B)\sigma + \frac{2\ \Delta H_m}{Z N_A^b (1 - N_A^b)} \{Z_1 (N_A^b - N_A^s) + Z_v (N_A^b - 1/2)\} - \frac{24\ \pi K G r_0 r_1 (r_0 - r_1)^2}{3Kr_1 + 4Gr_0} \qquad [2.20]$$

where γ_i is the surface energy of the pure component i, σ is the surface area per atom, ΔH_m is the enthalpy of mixing and Z is the coordination number. This equation has since been extended to concentrated solutions (lit.36) and multilayer segregation (lit.37).

Evidently, the mathematics involved is rather complicated. Several models are developed to predict segregation behaviour on simpler data, like the shape of the phase diagram (lit.38), but these are not always satisfactory.

Fortunately the experimental determination of surface (and of grainboundary) segregation has experienced a large evolution since the developement of surface sensitive techniques like AES (Auger Electron Spectroscopy), LEIS (Low Energy Ion Spectroscopy) and SIMS (Secondary Ion Mass Spectroscopy) (lit.39).

So far nothing has been said about the time necessary to develop an equilibrium surface concentration. McLean (lit.29) has combined equations for diffusion with those for segregation. The most simple solution, for a monolayer coverage by an impurity, is depicted in fig.2.11. Here is α the enrichment factor, d the thickness of an atomic layer. It follows that for a hypothetical system with $D=4*10^{-11}$ cm^2/s and $\alpha = 10^3$ already after 10 seconds 60 % of a monolayer is formed. The physical basis for the very short times necessary to reach equilibrium concentrations is the fact that only a small amount of material is involved and that the distances are very short. So in practical situations the surface of an alloy at elevated temperatures will always be covered with a segregating element.

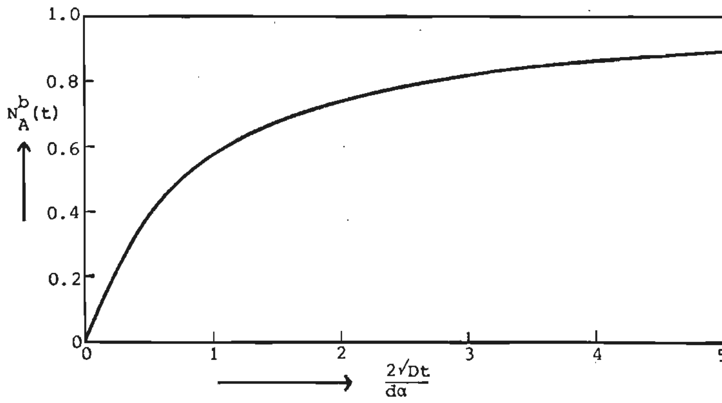

Fig.2.11. Time dependence of segregation after McLean (lit.29).

References chapter 2

1] L. Boltzmann; Ann.Physik. 53(1894),960.
2] C. Matano; Japan.Phys. 8(1933),109.
3] A.D. Smigelskas, E.O. Kirkendall; Trans.Met.Soc.AIME 171(1947),130
4] L.S.Darken; Trans.Met.Soc.AIME 175(1948),184
5] F.J.J. van Loo; Thesis Technische Hogeschool Eindhoven (1971)
6] G.F. Bastin; Thesis Technische Hogeschool Eindhoven (1972)
7] F. Sauer, V. Freise; Z.Elektrochem. 66(1962),353
8] C. Wagner; Acta.Met. 17(1969),99
9] J.P. Stark; Acta.Met.32(1984),535
10] F.A. Veer, B.H. Kolster, W.G. Burgers; Trans.Met.Soc.AIME 242(1968),669
11] K.N. Tu; Ann.Rev.Mater.Sci. 15(1985),147
12] U. Gösele, K.N. Tu; J.Appl.Phys. 53(1982),3252
13] F.M. D'Heurle; Thin Films and Interfaces II; ed. J.E.E. Baglin, D.R. Campbell, W.K. Chu; MRS Symp.Proc. 25(1984),3
14] L.S. Darken; Trans.Met.Soc.AIME 180(1949),430
15] R.A. Rapp, A.Ezis, G.J.Yurek; Met.Trans. 4(1973),1283
16] J.A. van Beek, P.M.T. de Kok, F.J.J. van Loo; Oxid.Met. 22(1984),147
17] F.J.J. van Loo, J.A. van Beek, G.F. Bastin, R. Metselaar; Diffusion in solids; pp 231-259 eds. M.A. Dayananda, G.E. Murch (1985) Metallurgical Society AIME, Warrendale (PA)
18] J.L. Bocquet, G. Brébec, Y. Limoge; Physical Metallurgy, eds. R.W. Cahn, P. Haasen; North Holland Physics Publishing Amsterdam 3rd version (1983)
19] R.W. Baluffi; Metall.Trans.B 13B(1982),527
20] N.L. Peterson; Int.Met.Rev. 28(1983),65
21] D.Turnbull; Atom Movements A.S.M. Cleveland(1951)
22] P.G. Shewmon; Diffusion in Solids, McGraw-Hill Book Company Inc. New York (1963)
23] G.V. Kidson; J.Nucl.Mater. 3(1961),21

24] M.P. Seah; J.Phys.F 10(1980),1043

25] E.D. Hondros; Pure Appl.Chem. 56(1984),1677

26] Interfacial Segregation; ed. W.C. Johnson, J.M. Blakely; ASM Metals Park Ohio (1979)

27] W.H.M. Sachtler, R.A. van Santen; Appl.Surf.Sci. 3(1979),121

28] P. Wynblatt, R.C. Ku, p 115 of reference 26.

29] D. McLean; Grainboundaries in Metals, Oxford University Press (1957)

30] M.P. Seah, C. Lea; Phil.Mag. 31(1975),627

31] M. Guttmann; Surf.Sci. 53(1975),213

32] F.L. Williams, D. Nason; Surf.Sci. 45(1974)377

33] D. Kumar, A. Mookerjee, V. Kumar; J.Phys.F 6(1976),725

34] A. Cruq, L. Degols, G. Lienard, A. Frennet; Surf.Sci. 80(1979),78

35] P. Wynblatt, R.C. Ku; Surf.Sci. 65(1977),511

36] C. Molinari, J.C. Joud, P. Desne; Surf.Sci. 84(1979),141

37] J.W. Lee, H.I. Aaronson; Surf.Sci. 95(1980),227

38] J.J. Burton, E.S. Macklin; Phys.Rev.Lett. 37 (1976),1433

39] H.J. Grabke; Oberflächenanalytik in der Metallkunde; ed. H.J.Grabke; Deutsche Gesellschaft für Metallkunde (1983)

APPENDIX A

In § 2.1.1.3 it has been deduced that:

[A. 1]

$$(d_y^{II})^2 = \frac{(1-N_y)*N_\delta}{N_\delta - N_y} * (d_y^I)^2 + \frac{(1-N_\delta)*N_\delta}{N_\delta - N_y} * d_y^I * d_\delta^I$$

If $d_y^I \not\leq 0$ then

$$\frac{(d_y^{II})^2}{(d_y^I)^2} = \frac{(1-N_y)*N_\delta}{N_\delta - N_y} + \frac{(1-N_\delta)*Nd}{N_\delta - N_y} * \frac{d_\delta^I}{d_y^I}$$

$$= \frac{(1-N_y)N_\delta + A(1-N_\delta)N_\delta}{N_\delta - N_y}$$

$$= \frac{1-\{N_y - A(1-N_\delta)\}}{1 - {}^{N_y}/N_\delta}$$ [A. 2]

with $A = d_\delta^I / d_y^I > 1$

$d_y^{II} > d_y I$ if the right hand side of [A. 2] > 1

This is true when:

$$N_y - A(1-N_\delta) < {}^{N_y}/N_\delta$$ [A. 3]

Since $N_y < N_\delta < 1$ it follows that:

$$N_y - A(1-N_\delta) < N_y$$

and

$$^{N_y}/N_\delta > N_y$$

So d_y^{II}/d_y^I for all cases.

chapter 3 experimental procedures

§ 3.1 Materials

The research described in this thesis is concerned with the influence of impurities on reaction diffusion. For this reason we have obtained copper from various sources, containing different amounts of impurities. In table 3.1 a summary is given on the composition of the types of copper.

table 3.1 Chemical analysis of the different types of copper

copper type	P content	S content
MRC, MARZ qual.	< 1 ppm[a]	< 1 ppm[a]
MRC, VP qual.	< 5 ppm[a]	< 5 ppm[a]
Drijfhout	32 ppm[b]	1.5 ppm[b]
Preussag	5 ppm[b]	3.4 ppm[b]
Cu1P	1 at%[c]	not determ.

[a] = as stated by the supplier
[b] = determined by mass spectrometry
[c] = as prepared

Copper phosphide has been supplied by Alpha Products (Ventron) in the form of balls that contain 15 wt% phosphorus according to the supplier. Some of the balls contain an excess of copper.
Cu1P is prepared by melting Cu MRC VP with copper phosphide to a total phosphorus content of 1 at%.
The poly-crystalline n-type silicon rod has been supplied by Vieille Montagne and germanium by Ventron, m6N purity.

§ 3.2 Preparation of the alloys

Alloys have been prepared of lumps of raw materials instead of powders. Powders have the advantage that they can be thoroughly mixed before melting, but may introduce a large oxygen contamination in the alloys. The lumps on the other hand have less surface area and this area can be cleaned by grinding before melting in order to remove the oxidation layer. The lumps are melted three times by an electric arc in an argon atmosphere. This results in completely homogenized alloys. Alloys are prepared with Cu MRC VP.

The alloys are checked for weight losses after melting. Phosphorus has a strong tendency to evaporate especially in low copper alloys. Binary Cu-Si and Cu-Ge alloys are prepared without losses. The alloys are equilibrated in evacuated silica capsules for 3 weeks (binary Cu-Si and Cu-Ge alloys) to 2 months (ternary Cu-Si-P and Cu-Ge-P alloys) at temperatures between 400 and 600 °C. After the heat treatment the alloys are water quenched.

Samples are metallographically prepared as follows: they are mounted in resin (manufactured by Struers) which has been made electrically conductive with iron powder (iron:resin = 2:1 by weight). Polishing is executed on successive types of SiC paper and on nylon cloth with diamond paste (6, 3, 1 µm) and finished with a short treatment with alumina (0.05 µm) on soft cloth.

The morphology is studied with optical microscopy, the composition of the constituting phases is determined with electron probe micro analysis (EPMA).

§ 3.3 Preparation of diffusion couples

§ 3.3.1 Preparation of the slices

Diffusion couples are prepared with slices cut from the raw materials with a SiC saw. The silicon slices are 1*1*0.2 cm^3, copper slices are circular with a diameter of 0.9 cm. The slices are ground on SiC paper, polished on nylon cloth with diamond paste and on soft cloth with alumina. For each type of material a different cloth has been used, which has only been used for that specific material, in order to avoid contamination. Between the various steps the slices are cleaned with alcohol or refined petrol. As a final step the slices are washed with aceton and carefully but quickly dried in order to limit oxidation. After preparation the slices are immediately placed in the vacuum furnaces again to limit oxidation to a minimum. The whole procedure takes about 5 minutes.

§ 3.3.2 The vacuum furnace

The diffusion experiments are conducted in specially designed vacuum furnaces (lit.1). In fig.3.1. a schematic view is given. The main body of the furnace is a molybdenum block. The diffusion couple is placed on top of this. Two thermocouples are placed inside the block close to the surface to measure and controle the temperature of the diffusion couple. The furnace is heated by a thermocoax element. Around the heating element radiation shields are placed, firstly to reduce heat losses, but secondly to prevent the warming up of the rubber leaktight rings. The platelets of the diffusion couple are pressed together with a weight of 20 kg that rests via a half alumina ball on the diffusion couple, resulting in a compressive stress of 3 MPa. The furnace is evacuated with an oil diffusion pump, to a pressure lower than 0.1mPa, which is good enough to prevent oxidation of the diffusion couples during

annealing. An experiment, where the vacuum pump has failed shows that this vacuum is a prerequisite.

The couples are placed in the furnace, which is then evacuated. When the minimum pressure has been reached the heating is put on. Experiments are conducted between 375 and 650 °C; the temperature is controlled within 2 °C. The furnace reaches the desired temperature after about 15 minutes. The moment the furnace has attained that temperature is taken as zero time for the reaction. After the annealing treatment the furnace is switched off. The initial cooling rate is about 250°C/h. Depending on the original temperature the cooling takes 2 to 4 hours.

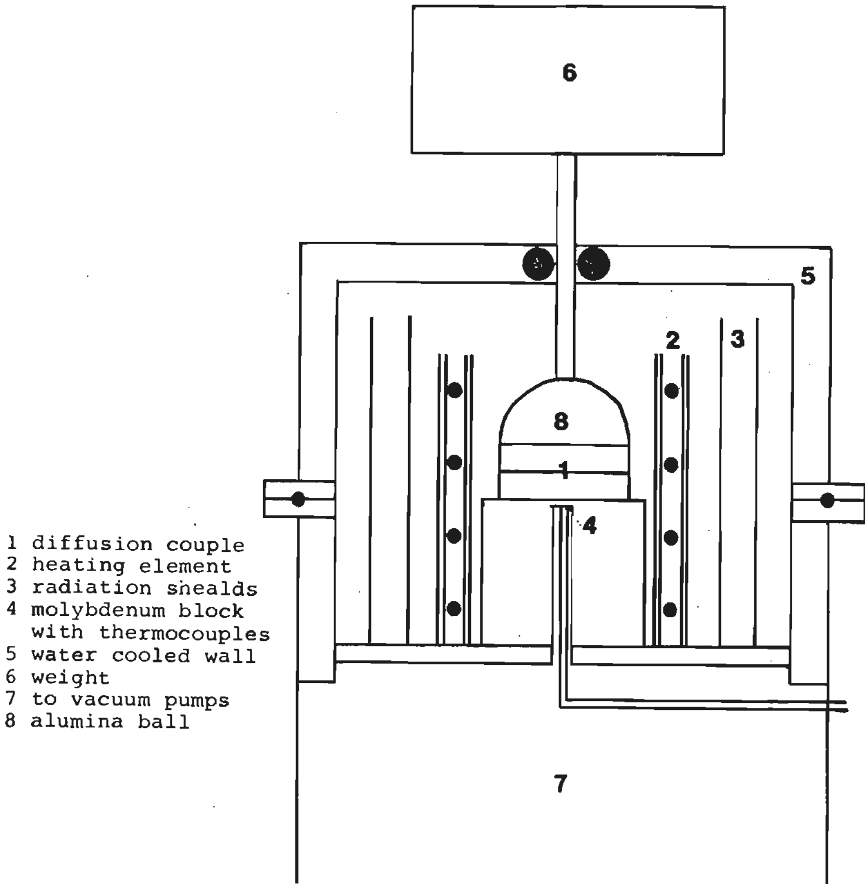

Fig.3.1 Vacuum furnace.

§ 3.3.3 Metallographic preparation of the diffusion couples

After annealing the diffusion couples are embedded in the resin described in § 3.2. The specimen is ground perpendicular to the reaction layer, until a constant thickness has been reached. Next the couples are polished. The couples are studied both with optical and electron microscopy. The morphology of the silicide layers is studied after etching in dilute nitric acid (nitric acid 60% : water = 2 : 1 by volume) for about 15 seconds. No solution has been found that gives satisfactory results in etching germanides.

In the next chapters the following code is used to identify a diffusion couple between material A and B, annealed at X °C for Y hours : A/B;X,Y. Sometimes a serial number is included, when several specimens prepared under identical conditions exist. So: Cu1P/Ge;500,24,II means a couple between copper containing 1at%P, and germanium, annealed at 500 °C for 24 hours, and this specific couple is the second duplicate.

§ 3.3.4 Other diffusion couple techniques

The vacuum furnace is not the only technique available to prepare diffusion couples. On rare occasions the following techniques are used.

a) a spring tube.

The platelets are placed inside a tube as depicted in fig.3.2. where they are pressed together by a spring, which remains outside the hot part of the furnace. To prevent oxidation an inert gas (helium) is passed through the tube. This procedure has two disadvantages : the major one is that the compressive stress that can be applied is insufficient for the system studied. Secondly the inert gas will always contain some oxygen and the continuous flow will oxidize the specimens.

b) a clamp.

A clamp consists of two platelets made of stainless steel between which the diffusion couple is placed and the whole is screwed together (fig.3.3). The clamp is annealed inside an evacuated silica capsule. The disadvantage is that the compressive stress is not reproducible.

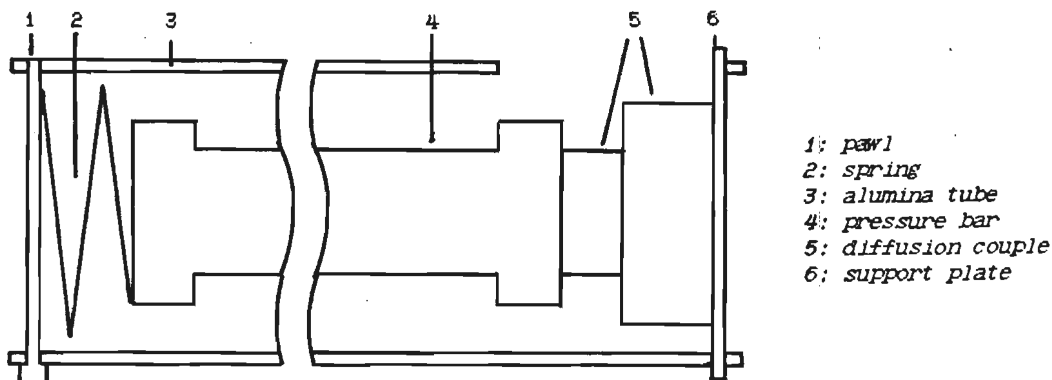

Fig.3.2 Spring tube

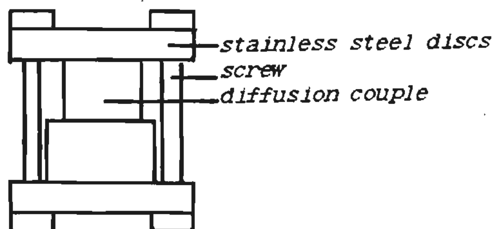

Fig.3.3 Clamp

§ 3.4 Optical microscopy

§ 3.4.1 General remarks

Alloys and diffusion couples are studied with optical microscopy, both with normal and polarized light (Reichert MeF2) to determine the number of phases formed in a specimen, the morphology of the reaction layers in diffusion couples and the thickness of the reaction layers. The fact that Cu_3Si and Cu_3Ge are coloured under polarized light greatly facilitated the identification of the phases.

§ 3.4.2 *Measurement of the thickness of the reaction layers in diffusion couples*

A Reichert metal-microscope equipped with a calibrated eye piece is used to measure the thickness of the reaction layers. Since some of the diffusion layers have a lens-shaped form (see chapter 4), the diffusion couples are ground until a maximum thickness has been reached. The shape of the reaction layers might lead to values of the thicknesses that are systematically too low.

The random uncertainty in the thickness has three sources :

a) When the zero-line and the read-out line are set, the read-out suffers from the usual errors in estimation the final decimal. These magnitude of the error in thickness depends on the magnification of the object lens as is shown in table 3.2.

Table 3.2 Error in thickness as a function of the thickness

Thickness	Error
< 150 µm	0.05 * 15 -> 1 µm
150 - 300 µm	0.05 * 30 -> 2 µm
300 - 760 µm	0.05 * 76 -> 4 µm
760 - 1540 µm	0.05 * 154 -> 8 µm
> 1540 µm	3*0.05 * 154 -> 23 µm

The relative error is about 1% in the whole range.

b) Independent measurements on the same series of experiments show a variation of approximately 25 µm in the range of 760-1540 µm, originating from differences in setting of the read-out line in the eye piece.

For these two sources together the total uncertainty is considered to be 2 % of the value. Since the value of the thickness is squared for some type of numerical analysis, this causes uncertainties up to 4% in d^2.

c) Especially in couples where an incubation time for the layer growth is present, irregular layers may be formed, since growth begins at different times for various parts of the contact area. The uncertainty in the layer thickness is reflected in the uncertainty in the reaction rate constant.

§ 3.5 X-ray diffraction

Although X-ray diffraction has, after all, only been used in a qualitative sense, several techniques have been applied to study the structures of the phases formed.The X-ray diffraction studies are hampered by the high oxidation rate of the silicides, which excluded the general use of powders for analyses. Slices are used because here the oxidation layer can easily be removed, but usually the crystals in the specimen are very large. This results in diffractograms where intensities are changed due to preferential orientation.

Diffractograms are recorded with a Philips PW 1010 or PW 1120 diffractometer, equipped with a rotating specimen holder. An evacuated Guinier camera has been used for powder diagrams, with alumina as an internal standard. A micro beam has been used to record transmission X-ray diffraction patterns through the edge of a wedge-shaped diffusion couple. High temperature diffraction has been conducted in an evacuated diffractometer equiped with an electrically heated platinum belt. The differences between the various Cu_3Si phases can not be distinguished with these techniques.

The possible texture in the reaction layers is determined with a cylindrical camera. No texture has been found. In all experiments Cu $K\alpha$ radiation has been used.

§ 3.6 Electron Probe Micro Analysis (EPMA)

§ 3.6.1 General

When a metal is irradiated with electrons of sufficient energy a vacancy will be created in one of the electron core levels of the atoms. This vacancy will be filled with an electron from a higher level and the energy can be released in the form of characteristic X-rays. The wavelength of the X-rays is independent of the environment of the atom, unless the vacancy has been created in a bonding level as is the case in ultra light atoms like boron and carbon. Special problems arise then (lit.2), but we will not deal with them here since the elements involved in this research, Cu, Si, Ge, P all have higher atomic numbers.

The X-rays that are emitted from the target originate from a tear drop like volume, having the size of about $1\mu m^3$, therefore micro analyses are possible.

Analyses are performed with a Jeol 733 Superprobe, usually operating with an acceleration voltage of 20 kV and a beam current of 10 nA, although sometimes also 30 nA has been used.

§ 3.6.2 Correction program

Since X-rays are characteristic they can be used to identify the elements present in the irradiated volume (qualitative analyses). Quantitative analyses are also possible if we compare the measured intensities with a standard intensity. Several corrections have to be made in order to convert these ratios to concentration units. These corrections are concerned with the effects of atomic number, absorption and fluorescence. In this research the so-called BAS program is used (lit.3). This program is based on a description of the X-ray distribution as a function the depth of the specimen with a $\Phi(\rho z)$ curve in which

Φ represents the ionization and ρz the mass depth of the sample.

Although this program in general is superior over other programs (lit.4) several remarks have to be made here. In all correction programs wavelengths are parametrized, as well as critical excitation voltages. Mass absorption coefficients (MAC's) are generally calculated using parametrizations, which may not be fully optimalized, since MAC's are usually not known with sufficient accuracy. This results in large variation in data for specific systems, for instance the mass absorption coefficient for Si Kα in Cu ranges from 3513 according to Frazer (lit.5) to 3212 according to Heinrich (lit.6) which is a scatter of 10%. The BAS program uses the Frazer parametrization, all other parametrizations being adapted to these values.

Due to limitations in the computer capacity atomic numbers are given as whole numbers, thus the BAS program works with an atomic number of 63 for copper, while in fact it is 63.54. The influence on the program, where the atomic number is a variable, is difficult to estimate. This limitation will be removed in a future version of the program.

These problems and other possible errors in the correction program can be circumvented by choosing a standard sample, which composition lies close to the unknown. The advantages will be demonstrated in chapter 4.

Another advantage of this choice is that the optimal detector setting can be used for both the standard and the unknown. This can be demonstrated with the histograms depicted in fig.3.4. Here count rates are normalized to the average value. The specimen is silicon rich Cu_3Si. Calibration is executed either on elemental copper and silicon or on a standard Cu_3Si compound. The distribution for Si Kα after calibration on Cu_3Si is much narrower than after calibration on elemental silicon. That especially silicon is vulnerable for this phenomenon is partly caused by the fact that the count rate in pure silicon is 20 times as high as in Cu_3Si. So calibration on pure silicon involves detector settings optimal for high

count rates to be used for low count rates in the samples. Calibration on Cu_3Si allows the use of detector setting optimal for low count rates both for the standard as for the samples. Copper is less vulnerable since copper forms some 88 wt% of Cu_3Si and the countrates between pure copper and Cu_3Si do not differ much.

It is, however, striking that the silicon distribution is always wider than the copper distribution. This must be related to the fact that silicon has a lower atomic number, so the absorption correction is appreciable. Si Kα is more surface sensitive than Cu Kα. The scatter then is caused by by the surface condition: roughness or oxidation layers.

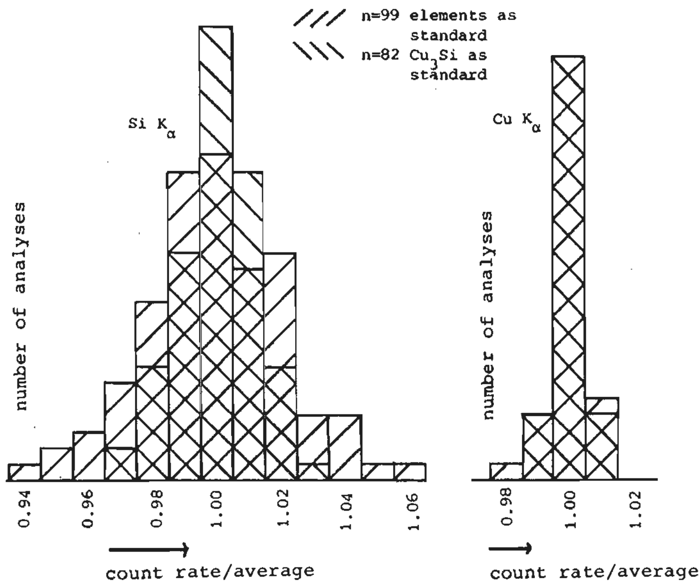

Fig.3.4 Comparison of the count rates for copper and silicon Kα in Cu_3Si, after calibration on elements and Cu_3Si. For each analysis the CuKα and SiKα have been counted for 10 sec. The count rates are normalized with respect to the average count rate obtained for the whole series.

§ 3.6.3 Specimen preparation

Quantitative analyses with EPMA require a conductive specimen. Not only the sample itself needs to be conductive, without insulating gaps or interlayers, but also the sample holder has to be conductive. This is achieved by mixing the resin with metal powder. Commonly copper is used, but this may be spread out over the sample surface during polishing. Since our samples contain copper this may lead to misinterpretations. To avoid confusion the resin is mixed with iron powder, which can clearly be identified as originating from the sample holder in case some contamination with the sample might occur.

Samples have to be flat, scratch free and clean. During the analyses it appeared that silicon is easily oxidized and Cu_3Si is notorious for its high oxidation rate. Therefore all specimen are polished immediately before analysis.

§ 3.7 AES at high temperature

Auger Electron Spectroscopy uses Auger electrons to study the compositions of surfaces (lit.7).

The incident electron beam creates a vacancy in a core level (fig.3.5), which is immediately filled by another electron. The energy E_K-E_L from this transition can be released in the form of characteristic X-rays (the basis for EPMA) or can be transferred to another electron, e.g. in the L_2 level, which is ejected as an Auger electron. The kinetic energy of Auger electrons lies in the range of 20 -

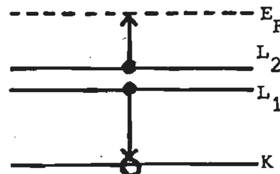

Fig.3.5 Energy levels involved in an Auger transition

2500 eV. These electrons have a limited mean free path (about 1 nm), resulting in a high surface sensitivity of AES. Because of this high surface sensitivity AES is performed in ultra high vacuum systems, in order to reduce carbon and oxygen contamination. Even at a pressure of 10^{-7} Pa an appreciable fraction of a monolayer of carbon and oxygen can be adsorbed on the surface of the specimen in a period of 30 minutes.

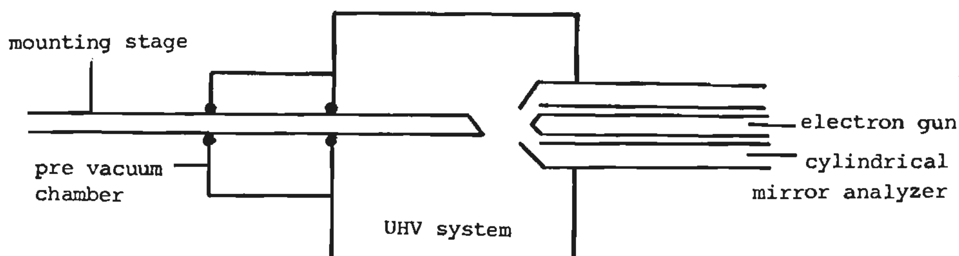

Fig.3.6 Schematic view of the high temperature AES apparatus

High temperature AES is performed by heating a specimen inside the UHV system (fig.3.6). Auger spectra are recorded while the specimen is hot. A different technique constitutes in heating the specimen in the prevacuum chamber and introducing it in the UHV after cooling down. The results, discussed in chapter 4, prove, that this technique would give a false impression of the materials studied in this thesis.

At the time of our experiments our sample introduction system consisted of a long bar, which is kept outside the vacuum system, when out of use. Heating this bar inside the UHV results in a severe deterioration of the vacuum. Since AES is only used as an indication of the impurities involved in the diffusion experiments we have not tried to reduce the carbon level.

§ 3.8. Statistical evaluation of the data.

Several statistical equations are used to evaluate the data. Since these techniques are standard only the formulas and the definitions will be given (lit.8).
The mean of n values $\bar{x}$ is given as

[3.1]

$$\bar{x} = \frac{\sum_{1}^{n} x}{n}$$

The sample standard deviation σ_x of x is given by:

[3.2]

$$\sigma_x^2 = \frac{\Sigma(x_i - \bar{x})^2}{n-1}$$

The standard deviation σ of $\bar{x}$ is given by:

[3.3]

$$\sigma^2 = \frac{\Sigma(x_i - \bar{x})^2}{n*(n-1)} = \frac{\sigma_x^2}{n}$$

The 70 % confidence interval of $\bar{x}$ is given by $\bar{x} \pm \sigma$.

Regression lines for $y = ax + b$ are calculated from:

[3.4]

$$a = \frac{n \cdot \Sigma(x \cdot y) - \Sigma x \cdot \Sigma y}{n \cdot \Sigma x^2 - (\Sigma x)^2}$$

[3.5]

$$b = \frac{\Sigma x^2 \cdot \Sigma y - \Sigma x \cdot \Sigma(x \cdot y)}{n \cdot \Sigma x^2 - (\Sigma x)^2}$$

where y is the value measured as a function of x, which is accurately known.
The 70 % confidence interval for the slope a and intercept b can be calculated from

$$(\Delta a)^2 = \frac{\dfrac{\Sigma[y - f(x)]^2}{(n-2)}}{\Sigma x^2 - (\Sigma x)^2/n} \qquad [3.6]$$

$$(\Delta b)^2 = (\Delta a)^2 \cdot \Sigma x^2/n \qquad [3.7]$$

where y is the measured value and f(x) = ax + b

References chapter 3

1] G.F. Bastin;
Thesis Technische Hogeschool Eindhoven (1972)

2] G.F. Bastin, H.J.M. Heijligers;
J.Microsc.Spectrosc.Electron. 11(1986),215

3] G.F. Bastin, F.J.J. van Loo, H.J.M. Heijligers;
X-ray Spectr. 13(1984),91

4] G.F. Bastin, H.J.M. Heijligers, F.J.J. van Loo;
Scanning 6(1984),58

5] J.Z. Frazer; Publ. 67-29, Inst. for the Study of Mat.,
Univ. of Calif., la Jolla (1967)

6] K.F.J. Heinrich in: Electron Microscope,
ed. T.D. McKinley, K.H.F. Heinrich, D.B. Wittry,
John Willey, New York (1966)

7] Methods of Surface analysis, ed. A.W. Czanderna;
Elsevier Scientific Publ.Comp. Amsterdam (1975)

8] D.P. Shoemaker, C.W. Garland, J.I. Steinfeld, J.W.Nibler;
Experiments in Physical Chemistry, McGraw Hill New York.
4th edition (1981)

chapter 4 the influence of phosphorus on the reaction between copper and silicon

§ 4.1 Scope of this chapter

As is explained in chapter 1 we are interested in the solid state reaction between copper and silicon because neither the product formation nor the reaction kinetics are understood.

Since the influence of impurities on solid state reactions has been observed before (lit.1), we have related the impurity content of the various types of copper with the product formation and the kinetics in the reaction between copper and silicon. Although the impurity contents in the original copper types (Cu Drijfhout, Cu Preussag) seem rather similar (tab 3.1) AES at high temperatures indicates a strong phosphorus segregation in case of Cu Drijfhout (for details see § 4.5). Cu Preussag shows sulphur segregation. Sulphur segregation has been reported before (lit.6). Preliminary experiments with dopes of phosphorus and sulphur added to the copper starting material have suggested that the presence of phosphorus is more important than that of sulphur. Therefore our attention has been focussed on the influence of phosphorus on the reaction between copper and silicon.

The central questions are : a]: in what way are the reaction kinetics influenced by phosphorus and b]: is the absence of Cu_5Si and $Cu_{15}Si_4$ kinetically determined or caused by the presence of phosphorus?

Cu_5Si and $Cu_{15}Si_4$ may be absent for kinetical reasons, which means that the layers are present in principle, but are too small to be observed. These products will then be found, when the reaction conditions are changed. On the other hand : the presence of phosphorus

might change the phase diagram applying to the reaction in such a way that the diffusion path does not reach Cu_5Si or $Cu_{15}Si_4$. In fig.4.1 a schematic phase diagram is shown, which explains the absence of the other silicides. The essential feature of this diagram is that no tie lines exist between Cu_3P and $Cu_{15}Si_4$ or Cu_5Si. In § 4.6.2 it will be argued that this phase diagram can not be correct.

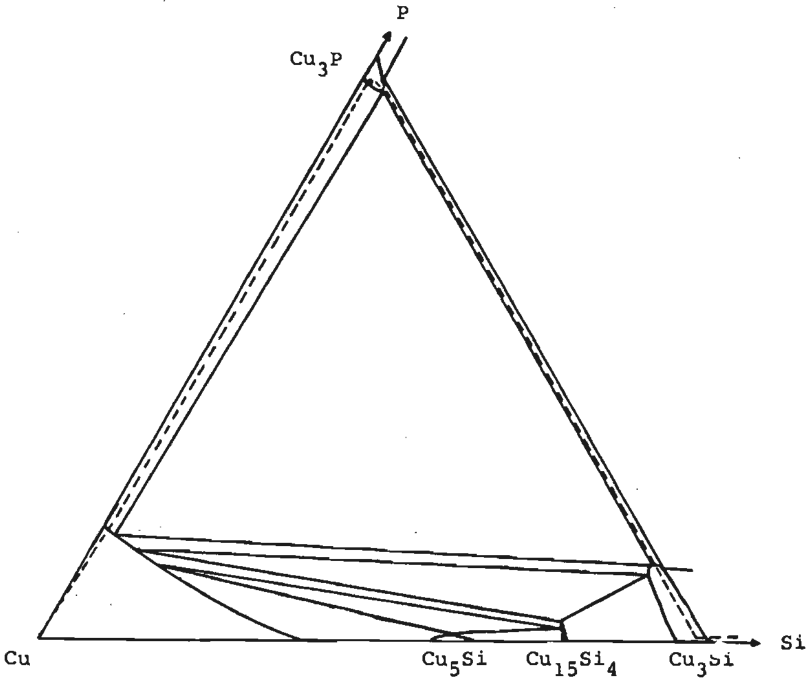

Fig.4.1 Possible ternary phase diagram , which excludes the formation of Cu_5Si and $Cu_{15}Si_4$ in Cu/Si diffusion couples in the presence of phosphorus. In § 4.6 it will be argued that this diagram can not be correct.

In this chapter the following subjects will be discussed:

- literature survey on the solid state reaction between copper and silicon in § 4.2.
- the Cu-Si phase diagram as reported in the literature (§ 4.3) will be compared with results obtained in binary alloys (§ 4.4) and with the products formed in diffusion couples (§ 4.6).
- after a few remarks on the initial experiments (§ 4.5), the diffusing component will be determined (§ 4.7) and the morphology of the reaction layers will be discussed (§ 4.8).
- the reaction kinetics (§ 4.9) in copper-silicon diffusion couples, both with phosphorus free and phosphorus-containing copper has been determined and the effect of oxidation of the silicon slices has been studied (§ 4.10).
- the influence of the phosphorus on the solid state reaction between copper and silicon will be discussed and a comparison with data reported in the literature will be made (§ 4.11).

§ 4.2 Literature survey on the solid state reaction between copper and silicon

The solid state reaction between copper and silicon has been studied before by other workers and their results agree with the general picture given in chapter 1: only one product is formed and there is disagreement on the reaction kinetics.

Veer and Kolster (lit.2) have used clamps to press the copper and siliconplatelets together. Only Cu_3Si is found. In the temperature range between 350 and 550°C the reaction proceeds in a diffusion controlled process, after an incubation time. It is noted here that the layer thicknesses are plotted as a function of the square root of time, which thwarts the correct determination of the incubation time as explained in chapter 2.

The activation energy for the diffusion coefficient has been calculated by Veer et al. (lit. 2) to be 78 kJ/mol, while Kolster (lit. 3) gives 88 kJ/mol. The difference between these valuse stems from a difference in diffusion coefficient derived from the same diffusion couples, shown by a comparison of table 1 in lit. 2 with table 7.1 in lit. 3. Ward (lit. 4) has reexamined the original data of Veer et al. and finds an activation energy of 107 kJ/mol for the reaction rate constant, defined as $k=d^2/t$ ($\mu m^2/h$).

The reaction proceeds by exclusive copper diffusion through the already formed silicide layer. Kolster (lit. 3) proposes a bulk diffusion mechanism. The low activation energy is attributed by the high defect concentration in Cu_3Si.

Onishi and Miura (lit.5) have employed a furnace with the same general design as the one used in our work. They have examined the influence of the compressive stress on the layer thickness (fig.4.2a). At low stresses they have found a non-linear relation between d and $t^{1/2}$. However, if we replot their data as d^2 as a function of t (fig.4.2b) we see, that when higher stresses are applied, the incubation time reduces and the reaction rate constant increases. The fact that the diffusion seems to be accelerated by higher stresses is explained by them by the observation of Kirkendall pores at the copper-silicide interface, when low stresses are applied. High stresses keep the pores closed, so that the reaction proceeds without hindrance. When the applied stresses are higher than 8 MPa the layer thickness is a linear function of the square root of time and the reaction rate becomes stress independent.

Between 420 and 465°C, at 12 MPa, the reaction is a diffusion limited process with an activation energy of 150 kJ/mol, which is ascribed to bulk diffusion of copper through Cu_3Si. No other phases are observed.

Ward et al (lit.4) have used a different technique to study the reaction. Silicon slices are etch-cleaned and electroplated with a thin layer of copper. This couple is allowed to react for a short time (≈ 100 s) at temperatures

between 250 and 350°C. The remaining copper is etched away and the thickness of the Cu_3Si layer is measured. No incubation time is observed. The activation energy of 105 kJ/mol, is relatively low and is ascribed to grain boundary diffusion. The difference in activation energy between this work (lit.4) and Onishi's (lit.5) is explained by Ward et al.by the different temperature range in which the experiments are conducted : at higher temperatures bulk diffusion plays a larger role than at low temperatures where Ward has experimented. Furthermore the different experimental technique may cause differences in nucleation of Cu_3Si : when the grains are smaller, and more boundaries exist grain boundary diffusion will play a larger role than in the case of larger grains.

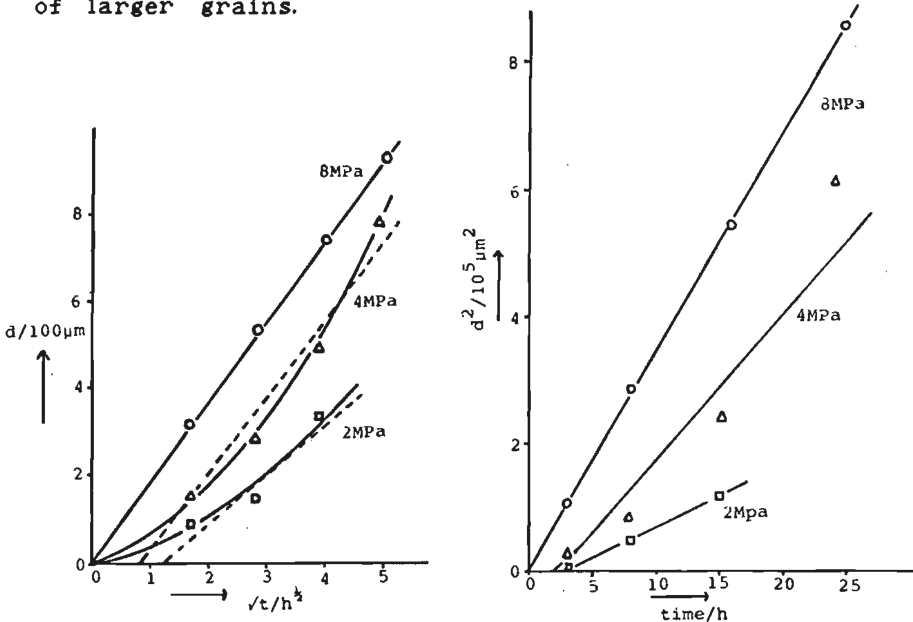

Fig. 4.2a The influence of the compressive stress on the layer thickness in Cu/Si diffusion couples according to lit.2 at 450°C.

Fig. 4.2b The data of Fig. 4.2a plotted as the thickness squared as function of time, clearly showing the presence of an incubation time at low stresses. Note the advantage this plot offers in the determination of the reaction rate constant.

§ 4.3 The copper-silicon phase diagram

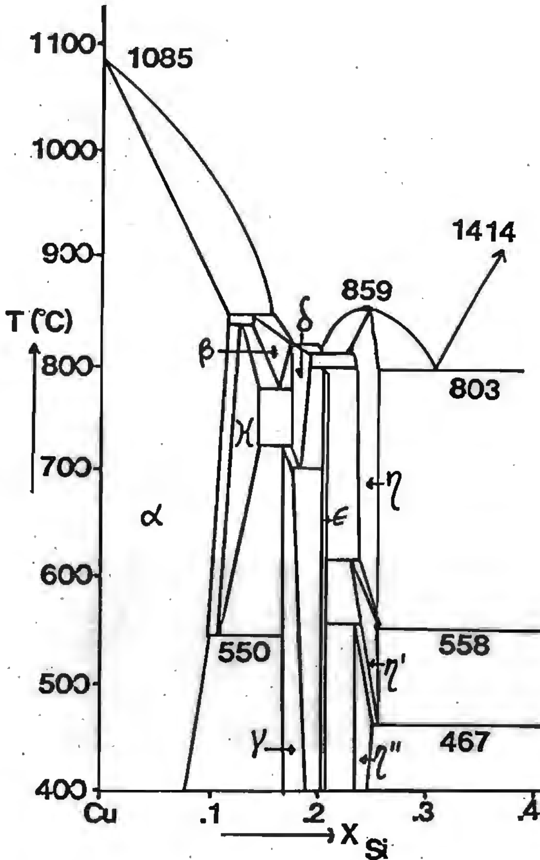

Fig.4.3 The binary copper-silicon phase diagram according to lit.7.

The copper-silicon phase diagram according to lit.7 is shown in fig.4.3. The existence of the high temperature compounds κ, β, and δ is of no concern for this work. Our attention is focussed on the γ, ϵ and η phases, which are the only existing compounds at temperatures below 550°C. The solubility of silicon in copper is quite large, about 11at% at 800°C; while the solubility of copper in silicon is negligible on this scale : 0.00009at%

at 800°C (lit.8). The γ-phase has a cubic structure, β-Mn type, a_0 =0.6222nm (lit.9). The γ-phase shows a homogeneity range from 16.8 to 18.1at% silicon at 500°C, acccording to this diagram. The alternative name Cu_5Si implies a silicon content of 16.7at%. The ε-phase has been subject of a discussion concerning the existence of this phase. The existence has been affirmed by Mukherjee et al.(lit.10). The ε-phase has a cubic structure, a_0 = 0.9615nm. They report some transformation near 600°C, but this is not confirmed by Hultgren and Desai (lit.7). Hultgren et al. (lit.7) state the silicon content to be 20.1at%, while Hansen (lit.9) defines the ε-phase as a 15:4 electron compound, with 21.1at% silicon. This is quite close to the value of 21.2at% that Mukherjee et al. have found (lit.10).

The data concerning the η, η'and η'' phases are contradictory. The low temperature transformations as shown in the diagram are not always found (lit.8). According to Kolster (lit.3) a third transformation occurs around 200°C. Mukherjee et al. (lit.10) have found a low temperature phase η' with a complex tetragonal cell. At high temperatures there are drastic changes in the intensity of some diffraction lines, indicating some sort of transformation between 550 and 700°C.

Solberg (lit.11) has determined the structure of precipitates in silicon by means of transmission electron diffraction. The crystal structure is determined to be based on a trigonally distorted bcc arrangement. The η'' lattice is orthorhombic (C) and is a two-dimensional long period superlatice, a = 7.676nm, b = 0.700nm, c = 2.194nm. The high temperature forms η and η' are both related to this structure. They have trigonal spacegroups R3m and R3 respectively with lattice parameters a(η) = 0.247nm, α(η) = 109,74°; a(η') = 0.472nm, α(η') = 95.72°.

The η-phases are commonly referred to as Cu_3Si, suggesting a composition with 25at% silicon. As shown in the phase diagram the η-phases contain less silicon : according to Hultgren et al.(lit.7) the homogeneity region ranges

from 23.0 to 24.8 at% silicon. Kolster (lit.3) does not examine the boundary concentrations, but indicates that an alloy with 24.2 at% silicon is a homogeneous one. Onishi (lit.5) takes respectively 23.2 and 24.3 at% Si as the homogeneity boundaries of the Cu_3Si layer found in diffusion couples between 400 and 460°C. Neither Veer (lit.2) nor Ward (lit.4) give exact determinations of the silicon concentration in their reaction layers.

§ 4.4 Determination of the composition of the silicides

In order to confirm the copper-silicon phase diagram binary alloys containing 5 - 30 at% silicon have been prepared by arc-melting (see § 3.2 for practical details). Both two-phased and homogeneous alloys have been studied.

§ 4.4.1 *X-ray diffraction*

X-ray diffraction is only used in a qualitative sense.

The diffraction patterns of Cu_5Si and $Cu_{15}Si_4$ are similar to those reported in the literature. Experiments with Cu_3Si are hampered by the high oxidation rate of this silicide. Since powdered specimens have a large surface area which results in high amounts of oxidation products, we are obliged to use platelets that can easily be cleaned by polishing. The use of platelets has the disadvantage that preferential orientation may occur. This will result in intensities of the diffraction lines that deviate from those given in the literature.

During high temperature diffraction experiments on powdered Cu_3Si samples in vacuum we have observed a change in intensity of the diffraction lines around 200°C, confirming a structure change as suggested by Kolster (lit.3). Another small alteration occurs between 465 and 470°C in a sample containing silicon-rich Cu_3Si and silicon, indicating the transformation $\eta'' \rightarrow \eta'$. These alterations are only recognized during heating of the

specimen; on cooling no changes can be observed to what is probably the stable room temperature form. But if a specimen is kept at room temperature for prolonged time, the diffraction pattern differs from a freshly annealed sample, so some transformation occurs at room temperature. Because of the irreversible nature of the experiments, we have not tried to interpret the patterns.

§ 4.4.2 *Confirmation of the phase diagram*

For the determination of the composition of the silicides we rely totally on electron probe micro analysis (EPMA) and inspection by optical microscopy.

In early analyses we have used elementary copper and silicon as a calibration standard for EPMA. The BAS $\Phi(\rho z)$ correctionprogram (lit.12) is used to calculate the composition of the samples from the measured X-ray intensities.

These analyses confirm the existing phase diagram in the temperature range between 400 and 500°C. The solubility of silicon in copper is 10at%, Cu_5Si, $Cu_{15}Si_4$ and Cu_3Si contain respectively 17, 22 and 24at% silicon on average. No other compounds are found.

§ 4.4.3 *Improvement of the analytical procedure*

During these analyses a major problem has emerged: the oxidation of the standards as well as the samples. Especially the silicon standard is vulnerable to oxidation, which may cause deviations as large as 10 % in the calibration. The reproducibility is improved when freshly polished standards are used.

Again the high oxidation rate of Cu_3Si causes problems. Not only because the correction program used for the analyses cannot handle specimens covered with a thin layer of a second phase, but also because a concentration

gradient is created in the alloy (fig.4.4). It has been reported (lit.13), that copper-silicon alloys are covered with a SiO_2 layer, leaving a copper enriched layer beneath. So it is not sufficient to polish away the oxidation layer, but a deeper layer ought to be removed. In a sample, known to contain about 24 at% silicon we have measured 16 at% silicon after superficial polishing.

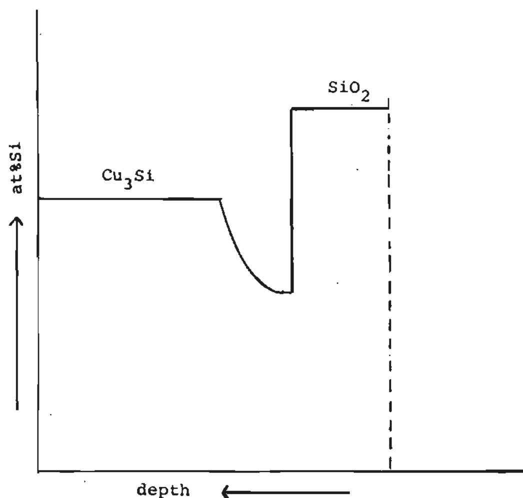

Fig.4.4 A schematic view of the silicon concentration profile in an oxidized alloy.

In order to eliminate these oxidation problems in the samples we have adopted the following procedure: a specimen is abraded on 600 Grit SiC paper (mesh 25 μm), quickly polished with 6μm and 1μm diamond paste, washed with refined petrol and ethanol and immediately, covered with ethanol, inserted in the pre-vacuum chamber of the electron microscope. Here the specimen is allowed to dry under vacuum. This procedure results in samples that show no discoloration. Polishing with alumina seems to be particularly hazardous for the samples.

For a precise determination of the phase boundaries of Cu_3Si we have used a homogeneous Cu_3Si alloy containing 23.6at% silicon (as weighted, melted and annealed without losses) as calibration standard. The use of a standard with comparable composition to the unknown has the advantage

that the count rates of the standard and the sample are quite alike, which strongly improves the counting statistics Furthermore uncertainties in the correction program like absorption coefficients have less influence on the composition calculated as is explained in chapter 3. The disadvantage is that a bias may be created in the analyses: if the standard alloy has a deviation in its composition all the analyses will deviate in the same direction. But relative concentrations will be more reliable : if two concentrations differ, say 2 at%, this number has a greater confidence when it is measured against a compound with about the same composition than when elements are used as standards.

The improvement in the counting statistics is clarified by comparing fig.4.5.a with fig.4.5.b. Fig.4.5.a shows a histogram of 75 analyses of the concentration measured with EPMA, calibrated with elementary copper and silicon. The alloy consists of Cu_3Si, with some $Cu_{15}Si_4$, so point measurements have been taken in the copper rich

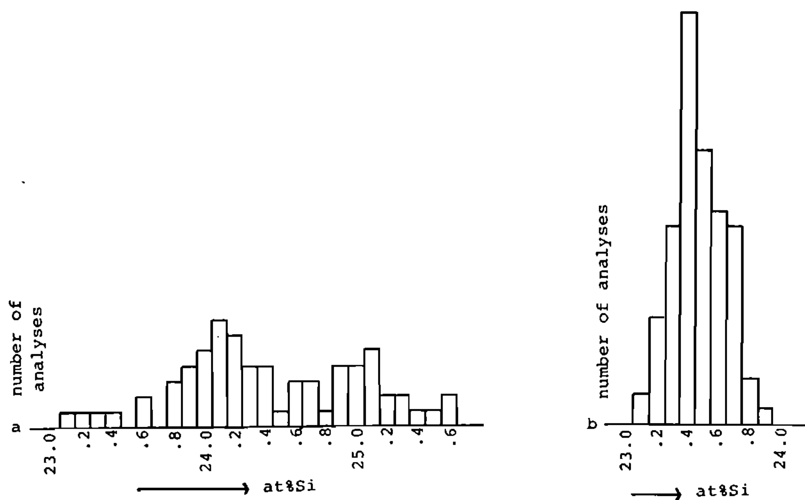

Fig.4.5.a Copper rich side of Cu_3Si, measured against elementary copper and silicon.

$\bar{x}$ = 24.44at% Si, σ_x = 0.6, n = 75, σ = 0.07

Fig.4.5.b Copper rich side of Cu_3Si measured against Cu_3Si containing 23.6at% Si.

$\bar{x}$ = 23.46at% Si, σ_x = 0.17, n = 99, σ = 0.02.

Cu_3Si phase. The concentrations calculated span a range of more than 2at%. Fig.4.5.b shows a histogram of 99 analyses of the same compound, but now after calibration on the 23.6 at% Si alloy. The latter histogram is much narrower and approaches a normal distribution. The standard deviation σ_x in a single measurement has been reduced from 0.6 (fig.4.5.a) to 0.17 at% (fig.4.5.b). The mean value of the silicon concentration $\bar{x}$ is shifted from 24.44 to 23.46at% in the latter case. This may be the bias that is introduced by the alloy, although it is more probable that $\bar{x}$ after calibration on elementary silicon (fig.4.5.a) deviates from the real composition because of errors in the correction program.

§ 4.4.4 *Precise determination of the composition of the silicides at 500°C*

The use of the 23.6at% Si alloy as a calibration standard, together with the special procedure to avoid the oxidation of the samples, opens the possibility to determine the width of the homogeneity range of Cu_3Si. For that purpose two alloys are analysed : Cu_3Si with some $Cu_{15}Si_4$ (the copper rich side of Cu_3Si) and Cu_3Si with silicon precipitates (the silicon rich side of Cu_3Si). Both alloys are equilibrated at 500°C for 2 months. The results are summarized in fig.4.6.

The measurements on both alloys are clearly separated, when calibrated with respect to the 23.6at% alloy. If we compare these results with the calculated range of composition after calibration on the elements (fig.4.5.a), we see that it would be impossible to separate the two compositions of Cu_3Si in the later case. Now we can calculate the average composition of both alloys which results in a silicon concentration of 23.46 +/- 0.02at% for the copper rich side of Cu_3Si and 24.23 +/- 0.03at% for the silicon rich side. The homogeneity range is 0.8at% wide. Cu_3Si

contains less silicon than this simple formula suggests. If we compare our results with the published phase diagram (fig.4.3) we see that Cu_3Si contains less silicon according to our results, and that our homogeneity region is smaller. Our results agree reasonably well with those of Onishi et al.(lit.5).

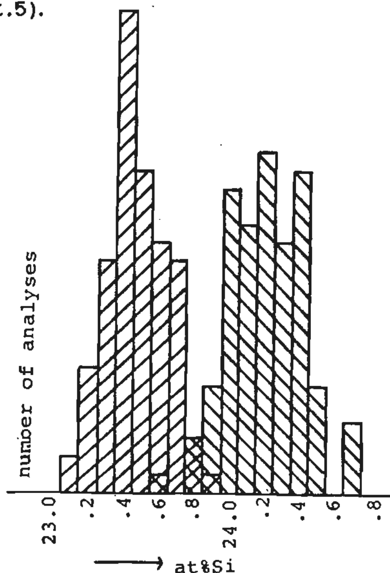

fig.4.6 Analyses of copper rich, respectively silicon rich Cu_3Si with EPMA, calibrated on 23.6at% Si.

	$\bar{x}$	σ_x	σ	n
Cu rich	*23.46*	*0.17*	*0.02*	*99*
Si rich	*24.21*	*0.26*	*0.03*	*99*

The same analytical procedure is applied to other alloys, containing α + Cu_5Si, Cu_5Si + $Cu_{15}Si_4$, $Cu_{15}Si_4$ + Cu_3Si, equilibrated at 500°C, which gives the limits in the concentration of all phses at that temperature.
The results are summarized in tab.4.1.

Table 4.1 Summary of the phase boundaries in the copper-silicon system at 500°C, measured with EPMA, calibrated on a 23.6at% Si alloy.

alloy	phase boundary	silicon content at%
$\alpha+Cu_5Si$	α (Si rich)	10.02 +/- 0.06
14.7at%Si	Cu_5Si (Cu rich)	16.72 +/- 0.05
$Cu_5Si+Cu_{15}Si_4$	Cu_5Si (Si rich)	17.54 +/- 0.05
20.8at%Si	$Cu_{15}Si_4$ (Cu rich)	21.70 +/- 0.04
$Cu_{15}Si_4+Cu_3Si$	$Cu_{15}Si_4$ (Si rich)	21.86 +/- 0.06
23.0at%Si	Cu_3Si (Cu rich)	23.46 +/- 0.02
Cu_3Si + Si	Cu_3Si (Si rich)	24.23 +/- 0.03
29.5at%Si		

We can compare our results with the published phase diagram. The homogeneity range of Cu_5Si seems to be smaller; the composition fits the formula Cu_5Si and this compound is able to absorb a small amount of silicon. $Cu_{15}Si_4$ has a very narrow homogeneity region, with a small excess of silicon compared to this formula.

§ 4.5 Initial experiments

The initial experiments are primarily concerned with the determination of the possible impurity governing the reaction between copper and silicon, and with increasing the reproducibility of the diffusion experiments.

§ 4.5.1 *AES*

Auger spectra are recorded with the apparatus described before (§ 3.7). The profiles are shown in fig 4.7. They are recorded during heating of the sample in the ultra high vacuum chamber. Both profiles show a rather large carbon contamination, which is related with the construction of the mounting stage. The main feature is the large phosphorus segregation in Cu Drijfhout (bulk concentration 30 ppm). During heating both sulphur and phosphorus segregate to the surface, but the driving force for phosphorus segregation seems to be higher in case of Cu Drijfhout. The concentration of phosphorus at the surface, calculated after correction for the carbon contamination, is about 25at%. This resembles a Cu_3P surface. The segregation ratio is about 10^4, a value not exceptionally high (lit.14). The behaviour of Cu MRC VP (bulk concentration phosphorus < 5 ppm) is quite different. The most important difference is that, the phosphorus signal does not change during the experiment, while the sulphur signal is rather strong. The segregation of sulphur to a copper surface is well documentated, since sulphur is a rather common impurity in "pure" copper (lit.6).

The strong phosphorus segregation challenged us to test the hypothesis that phosphorus is the impurity that influences so strongly the reaction between copper and silicon.

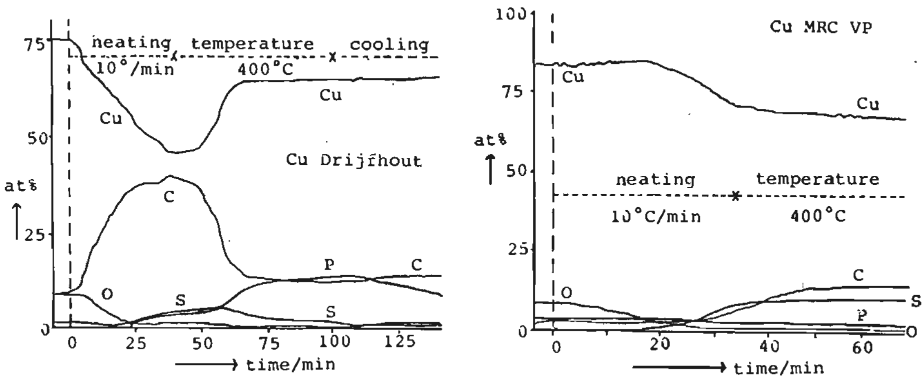

Fig.4.7 AES profile during hot stage experiment;
a) Cu Drijfhout, containing 30 ppm P,
b) Cu MRC VP, containing <5 ppm P.

In passing we note that the phoshorus signal quickly reduces when the heating power is switched off. This implies that studying segregation behaviour by heating the specimen in the pre-vacuum chamber and recording the surface composition after cooling, might give a false impression of the surface composition at high temperature.

§ 4.5.2 Improvement of the reproducibility

The reproducibility is greatly improved after the recognition of the fact that copper from various sources might react differently because of different impurity contents.

Further improvements have been gained after changing the preparation procedure, in that way that contamination with other elements is avoided. Flat mirror like slices are used and oxidation is reduced to a minimum (see §3.3 for details).

Attention has been paid to the compressive stress applied during a annealing treatment. A compromise between the values advised by Onishi et al. (lit.5), the compressive stress ought to be larger than 10MPa, and the practical

possibilities of our equipment has been reached : a constant stress during all experiments of 3 MPa. This is achieved by using larger silicon slices than copper slices, so that the contact area is determined by the surface of the copper slice. The size of the copper slices is determined by the bar in which copper has been supplied. In principle it is indeed possible to use smaller silicon slices, which would result in higher stresses. Several disadvantages exist however: smaller slices are difficult to manipulate and side effects become more important. The lens-shape of the reaction layer, as will be discussed in § 4.8.1 favors the use of platelets as large as possible. When smaller slices are used, we observe a stress dependence similar to the one observed by Onishi et al. (lit.5).

The furnace is operated with a vacuum pressure of less than 0.1mPa, which proves to be sufficient to avoid oxidation of the diffusion couples during annealing. An experiment during which the vacuum system has failed, has proven that this vacuum is a necessity for good results.

§ 4.5.3 *Other diffusion couple techniques*

The applicability of other techniques than the vacuum furnaces has been tested.

The (traditional) clamps, as described in § 3.3, cannot be used, since a copper-silicon couple shrinks during reaction. This is caused by the fact that the resulting Cu_3Si takes 11% less space than the original copper and silicon (lit.3,15). This contraction is caused by the change from the relatively open silicon structure to the dense, nearly bcc Cu_3Si structure.

A second possible technique is a spring tube (described in § 3.3). The results are unsatisfactory. Firstly because the stress that can be applied is insufficient. Secondly because the experiments have to be conducted in an inert atmosphere. The continuous flow of gas, containing a very small amount of oxygen, results in discoloration of the copper platelets by oxygen contamination.

The contraction during the formation of Cu_3Si creates large stresses in the silicon platelet, which shows cracks after the reaction. The fissures so developed make it impossible to reheat a diffusion couple in order to study the cummulative growth. So all experiments are conducted with different couples.

§ 4.5.4 Initial diffusion experiments

The hypothesis, that phosphorus as found in Cu Drijfhout (§ 4.5.1) is the impurity that strongly influences the reaction between copper and silicon, is tested by conducting experiments with copper doped with 1at% P, which will be further denoted as Cu1P. Fig.4.8 shows the results. Cu Drijfhout en Cu1P show the same behaviour in the low temperature range : fast reaction with regular diffusion layers. No essential difference is observed between the layer thicknesses of Cu Drijfhout and Cu1P. Cu MRC Marz does not show any regular diffusion reaction at all below 465°C, while Cu MRC VP, with intermediate phosphorus content, shows some reaction above 450°C.

On the basis of these experiments we have decided to perform all the other experiments with Cu MRC Marz and Cu1P.

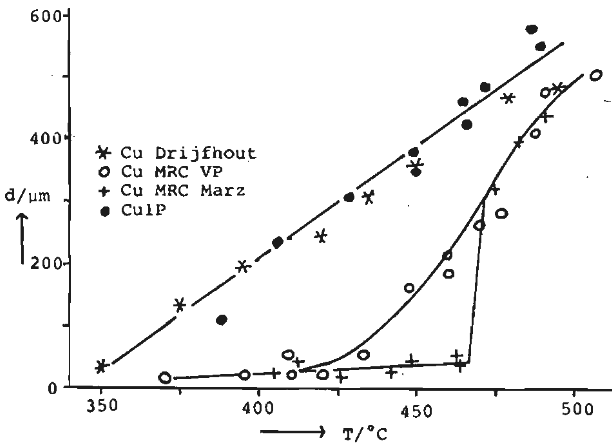

Fig.4.8 Thickness of the Cu_3Si layer in Cu/Si diffusion couples after 4 h annealing for various types of copper.

§ 4.6 Product formation

§ 4.6.1 The composition of the main product, Cu_3Si

As reported before (lit.16) we confirm the observation that Cu_3Si is the main product.

We have determined the composition of this layer by EPMA. Since we want to determine the homogeneity range of Cu_3Si in diffusion couples, we have made analyses of both sides of the reaction layer. A property of EPMA is, that analyses near a boundary have less reliability. So the actual analyses are executed at about 5µm from the, sometimes scaly, copper/silicide interface and at about 3 µm from the silicide/silicon interface. Fig.4.9 shows the analyses for a diffusion couple annealed at 500°C, for 8 hours; resulting in a layer of about 600µm. If we compare the results with those discussed in § 4.4.4 it strikes that both sides of the silicide layer have the same composition of 23.18at%Si, although we would expect that the full homogeneity range is formed in a diffusion layer. Furthermore we see that the layer seems to contain more copper than the copper rich side of Cu_3Si found in alloys, which contains 23.46at%Si.

This difference might be accounted for by the consideration that the analyses are performed separately, so a systematic error may be introduced, based on differences in calibration procedure, conductivity and flatness of the specimen. It can however not be excluded, that supersaturation of Cu_3Si occurs when $Cu_{15}Si_4$ does not nucleate.

It is interesting to note here, that in a diffusion couple, where locally $Cu_{15}Si_4$ has nucleated (Cu Marz /Si;500,65), the silicon concentration in the Cu_3Si phase at these places is 0.37 ± 0.06 at% higher than at places where $Cu_{15}Si_4$ is absent.

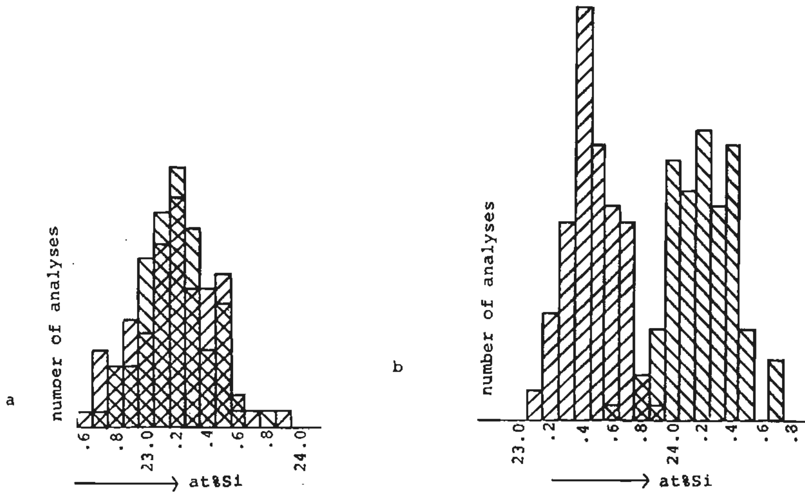

Fig.4.9 Composition of Cu_3Si formed in a diffusion couple (Cu Marz/Si;500,8) at the boundaries of the reaction layer a), compared with the homogeneity boundaries in alloys at 500°C b).

Cu_3Si at the Cu_3Si/copper interface:
x = 23.17 +/- 0.03 at% Si, n = 82
Cu_3Si at the Cu_3Si/silicon interface:
x = 23.19 +/- 0.03 at% Si, n = 80
Cu_3Si, copper rich phase boundary:
x = 23.46 +/- 0.02 at% Si
Cu_3Si, silicon rich phase boundary:
x = 24.23 +/- 0.03 at% Si

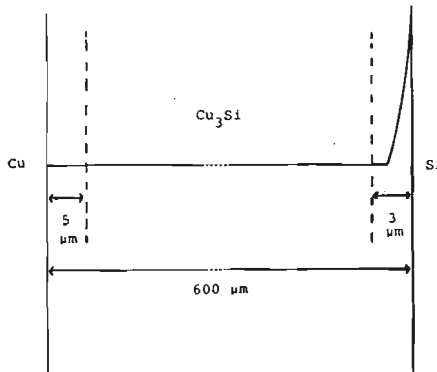

Fig 4.10 Proposed concentration profile in Cu/Si diffusion couples.

The fact that both sides of the diffusion layer have the same composition can be explained by the concentration profile given in fig.4.10. If the diffusion through the silicon rich side of Cu_3Si is very slow, a high concentration gradient will occur in the final few micrometers. Unfortunately this gradient in composition will be too steep to be observed by conventional profiling. Therefore we only have indirect prove for this concentration profile.

In diffusion couples with doped copper Cu_3P is formed next to Cu_3Si (fig.4.11). This layer is formed by Cu_3P precipitates left behind when copper diffuses away to react with silicon. The phosphorus content in Cu_3Si is below the detection limit of the conventional analyses (less then 0.02 at% P).

2.8 inch

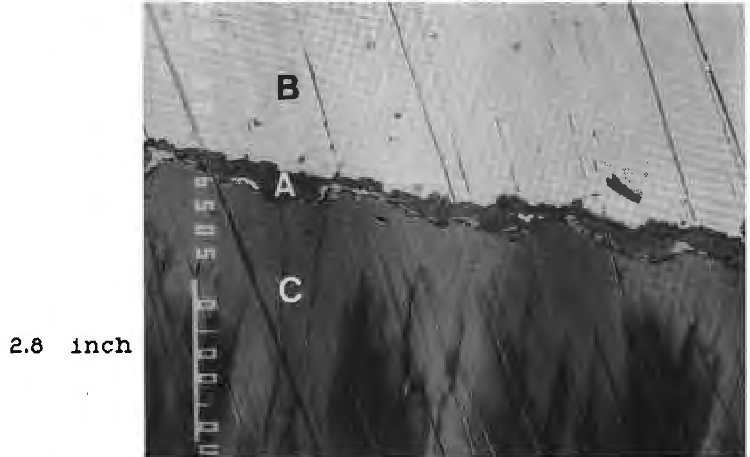

Fig.4.11 Cu_3P^A formed at the $copper^B$/$silicide^C$ interface in a diffusion couple between Cu1P and silicon, annealed at 400@C for 68 hours (back scattered electron image). Bar indicates 100μm

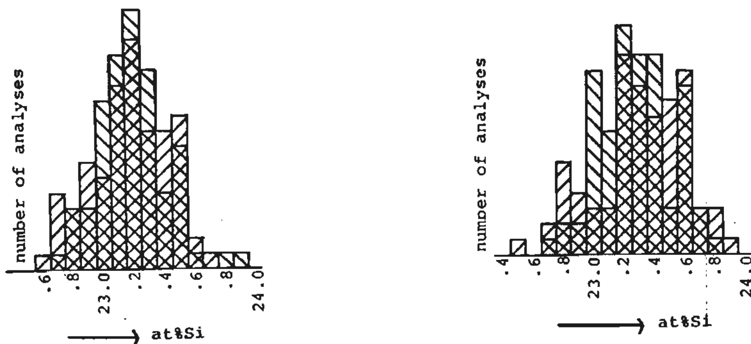

Fig.4.12 The composition of the Cu_3Si layer in a Cu1P/Si diffusion couple as determined with EPMA, compared with the composition of this layer in a Cu Marz/Si diffusion couple (calibration is performed with a 23.6at%Si alloy).

a]: Cu Marz/Si;500,8:

Cu-side: $\bar{x}$ = 23.17 +/- 0.03 at%Si, σ_x = 0.26, n = 82

Si-side: $\bar{x}$ = 23.19 +/- 0.03 at%Si, σ_x = 0.22, n = 80

b]: Cu1P/Si;500,4:

Cu-side: $\bar{x}$ = 23.29 +/- 0.03 at%Si, σ_x = 0.30, n = 81

Si-side: $\bar{x}$ = 23.27 +/- 0.03 at%Si, σ_x = 0.24, n = 84

In fig.4.12 a comparison is made between the composition of Cu_3Si in doped diffusion couples with that in undoped couples. Two conclusions can be derived: a] also in the phosphorus doped couples both sides of the Cu_3Si have the same composition, and b] this composition is different from the one found in undoped couples. The silicon content is shifted from 23.18 to 23.28at%. This difference is most probably not caused by systematic errors, since both diffusion couples are contained in the same sample, and calibration procedure, conductivity and flatness are the same. The difference in composition is significant with 99 % confidence. (student t-test; $\bar{x}_1$=23.18, n_1=162, $\bar{x}_2$=23.28, n_2=165, σ=0.26; this gives t=3.477. This is larger than t(0.995) = 2.59. Therefore $\bar{x}_1$ unequals $\bar{x}_2$). Also in other diffusion couples has this tendency for higher silicon concentration been observed.

§ 4.6.2 The presence of $Cu_{15}Si_4$ and Cu_5Si

Usually $Cu_{15}Si_4$ and Cu_5Si are absent in copper- silicon diffusion couples. As explained before this may be caused either by thermodynamic or by kinetic reasons.

The presence of phosphorus as the reason for the absence of $Cu_{15}Si_4$ and Cu_5Si is contradicted by the, admittedly rare, observation of the formation of these phases in Cu1P/Si diffusion couples, as shown in fig. 4. 13. Here a small layer of $Cu_{15}Si_4$ has been formed between Cu_3P and Cu_3Si. So in principle $Cu_{15}Si_4$ can be formed in the presence of a trace of phosphorus. Both $Cu_{15}Si_4$ and Cu_5Si are formed in a diffusion couple between Cu_3P (containing some free copper) and Cu_3Si as demonstrated in fig. 4. 14. So even in the presence of a large amount of phosphorus the other silicides can be formed.

These observations prove that a ternary phase diagram as proposed in fig. 4. 1 cannot describe the diffusion in the copper-silicon system in the presence of phosphorus. In chapter 5 we will go further into the details of the ternary phase diagram.

Since $Cu_{15}Si_4$ and Cu_5Si are not absent for thermodynamic reasons, it may be the kinetics of the reaction that prohibits the formation of these silicides. An indication that the absence is determined by the reaction kinetics is the observation that the formation of $Cu_{15}Si_4$ is accompanied by an overall retarded growth rate of Cu_3Si (fig. 4. 15). This suggests that if the growth of Cu_3Si is disturbed at the silicide/silicon interface, the reaction between Cu_3Si and copper starts and $Cu_{15}Si_4$ can be formed.

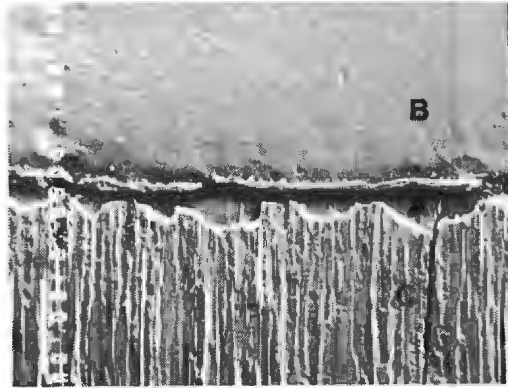

Fig.4.13 Secondary electron image of the formation of $Cu_{15}Si_4$^A in a phosphorus containing diffusion couple: Cu1P/Si;400,40. Bar indicates 100 μm. B=Cu1P, C=Cu_3Si.

3.9 inch

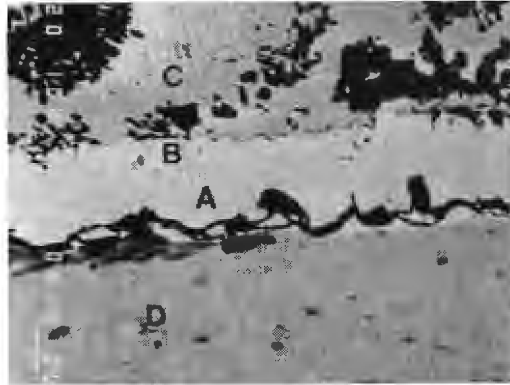

Fig.4.14 The formation of $Cu_{15}Si_4$^A and Cu_5Si^B in a diffusion couple between Cu_3P^C and Cu_3Si^D, annealed at 500@C for 16 hours (back scattered electron image). Bar indicates 10 μm.

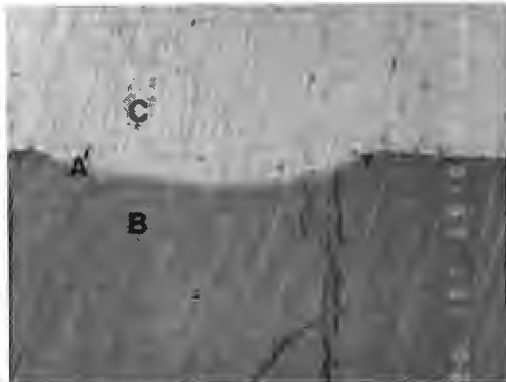

Fig.4.15 The formation of $Cu_{15}Si_4$^A accompanied with an overall retarded growth rate; Cu Marz/Si;400,100; BEI. Bar indicates 100 μm. B=Cu_3Si, C=Cu

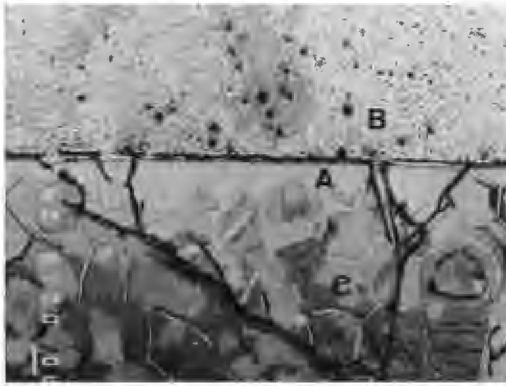

Fig.4.16 The formation of $Cu_{15}Si_4$^A in a diffusion couple between CuP^B and a Cu-Si alloy^C containing 23.1 at% Si; 500°C,16 h, BEI. Bar indicates 100 µm.

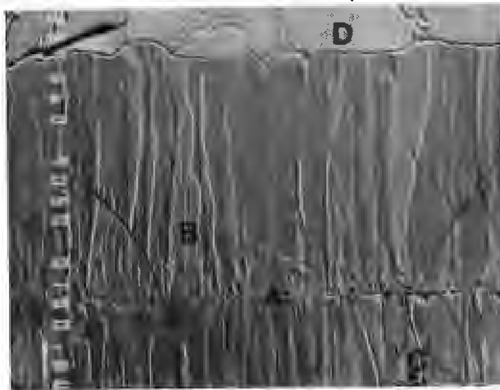

Fig.4.17 The marker plane^A in the Cu_3Si^B layer a diffusion couple between silicon^C and an alloy^D containing 18at% silicon, separating Cu_3Si formed by decomposition of Cu_5Si (top) and Cu_3Si formed by diffusion of copper towards silicon (bottom). Bar indicates 100 µm.

A way to study the formation of $Cu_{15}Si_4$ is to prepare diffusion couples between Cu_3Si and Cu. Cu_3Si is very quickly oxidized and covered with SiO_2 (lit.13). As will be explained in § 4.10 this SiO_2 layer hampers the reaction with pure copper, but not the reaction with phosphorus-containing copper. Therefore the reaction between Cu1P and Cu_3Si has been studied. The reaction is carried out with an alloy containing 23.1at% Si, which implies that already some $Cu_{15}Si_4$ is present at the grain boundaries of Cu_3Si.

After 16 hours at 500°C about 120 μm of $Cu_{15}Si_4$ and 12 μm of Cu_5Si has been formed, see fig. 4.16. Since virtually no concentration gradient exists in the diffusion couples, we can apply the integrated diffusion coefficient as defined by Wagner (lit. 17). As derived in chapter 2 there exists a relation between the thickness of a product layer in a diffusion couple between two elements (d_ϵ^I) and the thickness of that same product layer in a couple between an element and a compound (d_ϵ^{II}), eq. [2.12].

$$(d_\epsilon^{II})^2 = \frac{(1-N_\epsilon)N_\eta}{N_\eta - N_\epsilon} * (d_\epsilon^I)^2 + \frac{(1-N_\eta)N_\eta}{N_\eta - N_\epsilon} * d_\epsilon^I * d_\eta^I$$

where ϵ denotes the $Cu_{15}Si_4$ phase and η the Cu_3Si phase.
The ϵ phase contains 21.7 at% silicon (§ 4.4.4).
The η phase contains 23.5 at% silicon in diffusion couples.
So: $N_\epsilon = 0.217$ and $N_\eta = 0.235$.
In a diffusion couple between copper and silicon at 500 @ after 16 hours 1200 μm of Cu_3Si will be formed, so d_η^I = 1200 μm. Since in the diffusion couple between copper and the compound η 120 μm of $Cu_{15}Si_4$ has been formed (d_ϵ^{II} = 120 μm), we calculate the formation of 1 μm $Cu_{15}Si_4$ in a diffusion couple between copper and silicon at 500°C, when the Cu_3Si layer is 1200 μm thick. At shorter reaction times and lower temperatures even less $Cu_{15}Si_4$ will be formed. So in general the amount of $Cu_{15}Si_4$ will be too small to be detected by the usual techniques.

This is corrobarated by comparing the integrated diffusion coeficients D_{ϵ}^{int} and D_{η}^{int}, which can be calculated according to eq [2.11b]. In case of the Cu/Si diffusion couple with $d\eta$ = 1200 μm after 16 hours, it follows that $D_{\eta}^{int} = 2.2*10^{-8} cm^2/s$. While from the Cu_3Si/Cu couple with: d_{ϵ} = 120 μm after 16 hours it follows that $D_{\epsilon}^{int} = 1.6*10^{-11}$ cm^2/s. So the integrated diffusion coefficient in the ε phase is more than 1000 times as small as the integrated diffusion coefficient in the η phase.

For the ε phase, with a homogeneity range of 0.16 at% (§4.4.4) we can make an estimation for the value of the interdiffusion coefficient $\tilde{D}_{\epsilon} \approx D_{\epsilon}^{int}/\Delta N_{\epsilon} \approx 1*10^{-8}$ cm^2/s. This value differs from the published value of the diffusion coefficient in $Cu_{15}Si_4 \approx 2*10^{-13}$ cm^2/s at 500°C extrapolated from higher temperatures (lit.18). This can be an indication that in the ε phase grain boundary difusion occurs.

It may be concluded that kinetic reasons prevent the formation of $Cu_{15}Si_4$ in copper/silicon diffusion couples : the layer is indeed formed, but it is too small to be observed unless the reaction between copper and silicon at the Cu_3Si/Si interface is disturbed, in which case copper reacts with Cu_3Si to form $Cu_{15}Si_4$ with an overall retarded growth rate.

§ 4.7 Determination of the diffusing component

The solid state reaction between copper and silicon can, at least in principle, proceed by three mechanisms : diffusion of copper through the already formed silicide layer, diffusion of silicon through this layer or diffusion of both components.

The third mechanism can be ruled out immediately, since it would lead to the formation of a markerplane inside the silicide layer, which is not observed. The presence of natural markers (pores, inclusions) suggest that the copper-silicide interface is the markerplane. The same conclusion has been reached by Onishi (lit.5), based on the position of

the Kirkendall pores and by Kolster (lit.3) who used tungsten wires as markers. This latter method has the disadvantage that the diffusion couple suffers from deformation around the wires.

A more accurate technique is the study of a diffusion couple between silicon and a copper-silicon alloy, where Cu_3Si is formed in two ways : by decomposition of the alloy and by diffusion. The two products can easily be distinguished by a markerplane (fig.4.17), where crystals nucleated from both sides meet. If only silicon diffuses this marker plane would coincide with the silicon-silicide interface. If only copper diffuses, we can calculate the ratio between the thicknesses of the two layers. If both components would diffuse the markerplane would be somewhere in between.

The alloy used in this experiment is a two-phased alloy with 18at% silicon consisting of Cu_5Si (17.5at% Si, $Cu_{825}Si_{175}$) and a small amount of $Cu_{15}Si_4$, not uniformally distributed over the alloy.
Like in other diffusion couples Cu_3Si is formed, which contains 23.2 at% Si: $Cu_{768}Si_{232}$.
If only copper diffuses, we can derive the following set of equations:
a] decomposition of Cu_5Si:

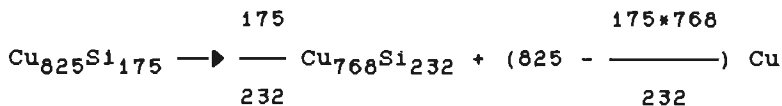

$$Cu_{825}Si_{175} \longrightarrow \frac{175}{232} Cu_{768}Si_{232} + (825 - \frac{175*768}{232})\ Cu$$

b] reaction of the diffused copper with silicon:

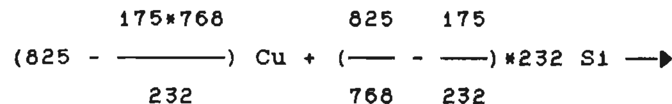

$$(825 - \frac{175*768}{232})\ Cu + (\frac{825}{768} - \frac{175}{232})*232\ Si \longrightarrow$$

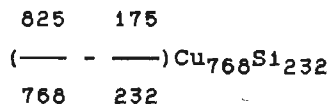

$$(\frac{825}{768} - \frac{175}{232}) Cu_{768}Si_{232}$$

The ratio between the layers formed according to a] and b]

is: $\frac{175}{232} : (\frac{825}{768} - \frac{175}{232}) = 0.754 : 0.320 = 2.36 : 1$

If we take $Cu_{82}Si_{18}$ as a material, the ratio is 2.66:1. The observed ratio varies between 2.33 and 2.65, which can be explained by the non uniform distribution of $Cu_{15}Si_4$ through the alloy. These results confirm the hypothesis that only copper diffuses in Cu_3Si.

§ 4.8 The morphology of the reactionlayers

§ 4.8.1 Overall morphology

In general the Cu_3Si layer formed in Cu/Si diffusion couples has a columnar structure and well defined, straight lined interfaces. Fig 4.19 illustrates this. If the silicon slice is smaller than the copper slice (as is the case for the couple shown in fig.4.19) reaction layer follows the contours of the silicon slice. If, however, the silicon slice is larger, then a lens shaped reaction layer is formed. Fig.4.20 gives a schematic view, while fig.4.21 shows a detail for a real diffusion couple.

Both ends of the silicide layer have lost direct contact with the copper slice, and are only embedded in the silicon slice. This indicates that the surface diffusion of copper along the surface of the Cu_3Si crystals must be very fast. This lens-shaped layer is sometimes accompanied by curved columns, as illustrated in fig.4.22, where the nuclei grow perpendicular on the copper/silicide interface. It is not clear which variables favors this morphology. A consequence of this lens-shape is that the layer thickness in the middle of the couple is larger than near the edges. For this reason the couples are abraded until a constant (maximal) thickness is found.

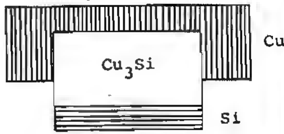

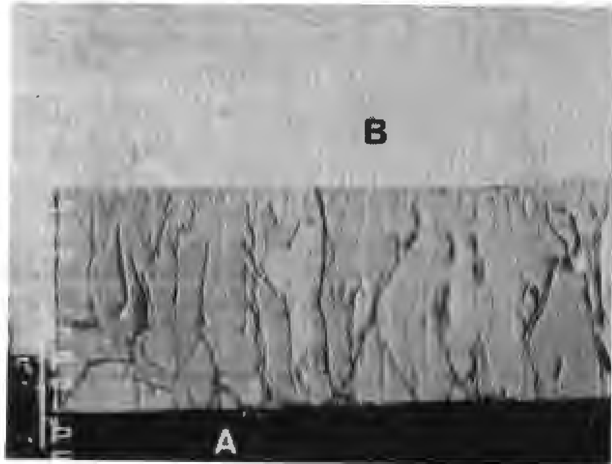

Fig.4.18 A schematic view of a straight lined reaction layer, developing when the silicon slice is smaller than the copper slice.

Fig.4.19 A real diffusion couple where silicon[A] is smaller than copper[B], Cu Marz/Si; 500,25I. SEI, bar indicates 1000 μm. C = Cu_3Si.

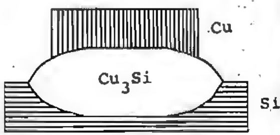

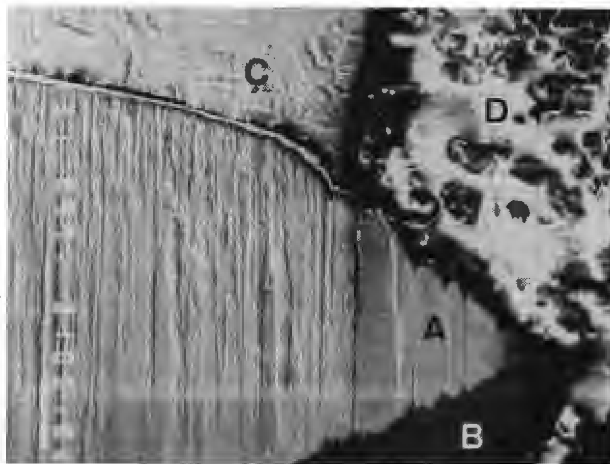

Fig.4.20 A schematic view of lens-shaped reaction layer.

Fig.4.21 Cu Marz/Si;420,195I; Cu_3Si-crystals[A] only in contact with silicon[B]. Bar indicates 100 μm, SEI. C=copper, D= embedding resin.

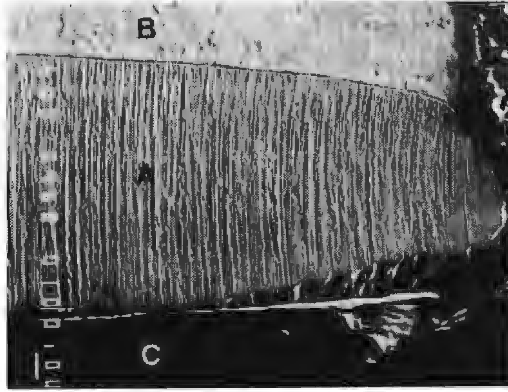

Fig.4.22 Cu Marz/Si;430,89; The reactionlayer^{A} consists of curved columns. Secondary electron image, bar indicates 100 μm. B = Cu, C = Si.

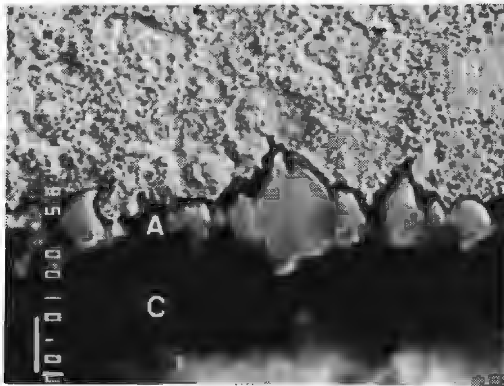

Fig.4.23 Cu Marz/Si;400,161I; single crystals of Cu_3Si^{A} formed between Cu^{B} and Si^{C}. Bar indicates 10 μm.

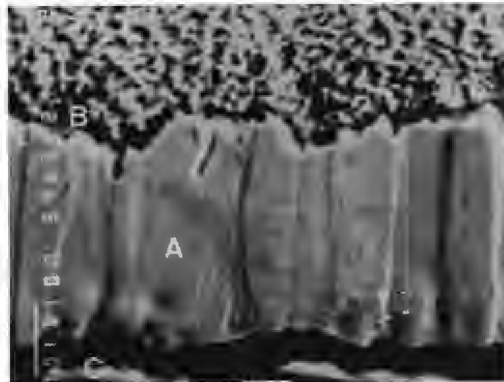

Fig.4.24 Cu Marz/Si;464,4I; early form of a Cu_3Si diffusion layer^{A} between Cu^{B} and Si^{C} bar indicates 10 μm.

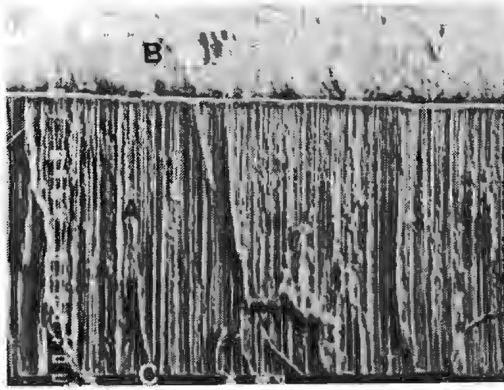

Fig.4.25 Cu Marz/Si;430,65; thin columns of Cu_3Si^A between Cu^B and Si^C. Bar indicates 100 μm.

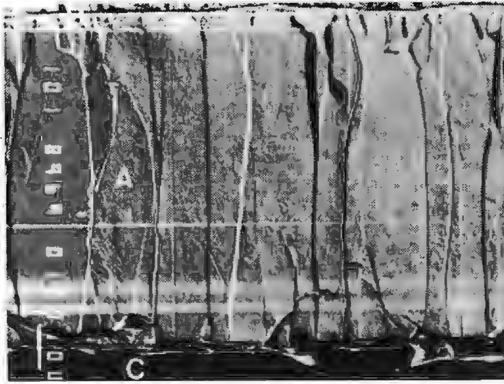

Fig.4.26 Cu Marz/Si;500,8; thick grains of Cu_3Si^A between Cu^B aand Si^C. Bar indicates 100 μm.

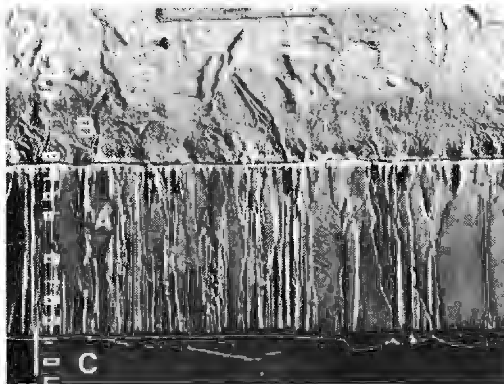

Fig.4.27 Cu Marz/Si;483,4; thin and thick columns of Cu_3Si^A between Cu^B and Si^C. Bar indicates 100 μm.

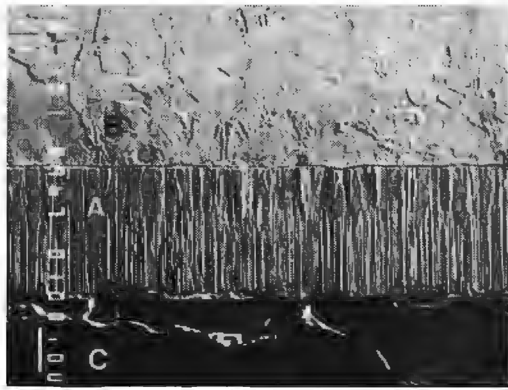

Fig.4.28 Cu Marz/Si;472,4II; thin and thick columns of Cu_3Si^A between Cu^B and Si^C. Bar indicates 100 µm.

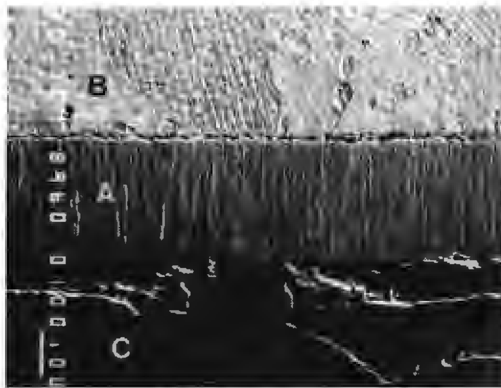

Fig.4.29 CuiP/Si;519,4; thin columns of Cu_3Si^A between $CuiP^B$ and Si^C. Bar indicates 100 µm.

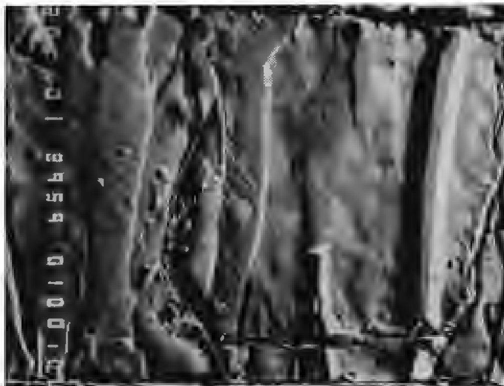

Fig.4.30 CuiP/Si;528,4; thick columns of Cu_3Si between CuiP and Si . Bar indicates 100 µm.

§ 4.8.2 *The development of the columnar structure*

As can be seen from figs.4.21-22 the reaction layer has in general a columnar structure. This structure has some definite stages of development. After short reaction times no layer is formed, but small separate crystals develop, as shown in fig.4.23. These crystals indicate that the diffusion limited process has not yet started. This morphology will be used as an indication that the annealing time is smaller than the incubation time at that particular temperature.

In the early stage of the diffusion limitation a uniform layer of single crystals is formed, with similar length and width, typically 5μm (fig.4.24). At low temperatures the next stage in the development is the formation of thin columns, both in doped and undoped couples. The average column diameter is less then 10μm (fig.4.25).

In undoped couples this morphology is found until about 470°C. Above 500°C thick columns are formed, with a diameter as large as 100μm (fig.4.26). In the range between 470 and 500°C both thick and thin columns can be formed in the same diffusion couple. Two morphologies are found, as illustrated by fig.4.27 and fig.4.28. Fig.4.27 shows a diffusion couple in which both thick and thin columns grow next to each other, while fig.4.28 shows a couple in which suddenly thin crystals nucleate on the older thicker grains at the copper side of the layer. The inverse morphology with the thicker grains at the silicon side has not been found.

In phosphorus containing diffusion couples the general picture is the same, but the temperature range in which the change from thin to thick columns occurs is different. Below 520°C only thin columns are found (fig.4.29), while above 520°C thick grains are formed (fig.4.30). No diffusion couples with both forms are observed.

§ 4.8.3 Interpretation of the morphology

The formation of the small single crystals is interpretated as the occurrence of another than a diffusion limited process, so the annealing time is smaller than the incubation time for the particular reaction conditions.

In fig.4.31 the grain size is plotted as a function of temperature. At high temperatures large grains are formed: the reaction is so fast, that already the first formed nuclei grow to form a closed layer. Only a few grain boundaries are present in the layer, so the diffusion must proceed by a bulk diffusion mechanism. At low temperatures the grain size is small: the reaction is relatively slow, so many nuclei will be formed before a closed reaction layer has been formed. The resulting reaction layer contains many grain boundaries, and therefore a grain boundary diffusion mechanism will probably prevail.

At medium temperatures we see that the grain size in diffusion couples with pure copper is larger than when phosphorus is present. The presence of phosphorus at the copper surface seems to induce so many nuclei, that a closed layer with many thin grains can be formed. and fast layer growth by grin boundary diffusion occurs (§ 4.9). In the absence of phosphorus the reaction becomes relatively fast compared with the nucleation rate, so fewer nuclei are present in a closed layer. A bulk diffusion mechanism will become more important, giving rise to a slower layer growth.

A columnar morphology is often considered to be the result of anisotropic diffusion in the product layer. Nuclei with a favourable orientation grow much faster than the others, forming columnar crystals with a more or less identical crystallographic orientation (texture) parallel to the diffusion direction (lit.19). This mechanism, however, does not apply to the growth of the Cu_3Si layer, since, although the morphology is strongly columnar, no crystallographic texture has been found.

Fig.4.32 The grain size of Cu_3Si in copper-silicon diffusion couples as a function of temperature both in presence and absence of phosphorus in copper.

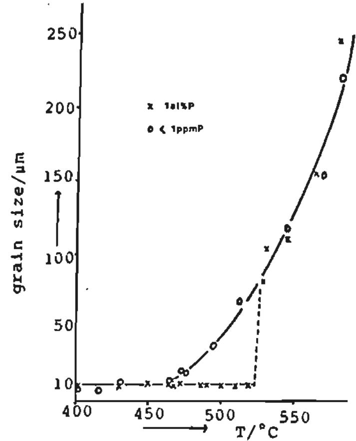

§ 4.9 Kinetics of the reaction

§ 4.9.1 *The time dependence of the layer thickness*

The relation tested in this paragraph is the parabolic growth law. In a diffusion limited process the layer thickness will show the following dependence on the reaction time

$$d^2=k*(t-t_0)$$

Here t_0 is the incubation time, the time necessary for the process to become limited by diffusion through the product layer. During the incubation time, the layer growth is very slow compared with the growth after the incubationtime.
k is the reaction rate constant in $\mu m^2/h$.

§ 4.9.1.1 Diffusion couples between silicon and pure copper

There exists a great difference in time dependence of the layer thickness between doped and undoped couples.

In the couples with pure copper a large incubation time exists, before the reaction proceeds in a diffusion limited way, obeying the parabolic growth law, fig.4.32. The occurrence of the incubation time means that a reaction

barrier exists. The time necessary to remove this layer is reduced when the temperature is raised : at 400°C the incubation time may be as large as 25 hours, at 415°C it is about 15 hours, while at 430°C it is reduced to 5 hours. Above about 465°C no incubation time exists, as demonstrated by the layer thickness as a function of temperature at 500°C in fig.4.33. The morphology of the reaction product clearly shows whether the annealing time is shorter than the incubation time: small crystals are formed instead of a continuous layer, as discussed in § 4.8.2. The occurrence of such large incubation times also explains the early observations (§ 4.5.4): 4 hours anneal is too short to start the proper diffusion process. In §4.10 we will go deeper into the nature of this barrier.

The incubation time is not a constant, but slightly changes from experiment to experiment. It causes the relative large deviation in the measurements as shown in fig.4.32. The fragility of the diffusion couples inhibits the reheating of a diffusion couple, which would give the opportunity to study the time dependence in one couple, with one incubation time.

But in all cases, after some time the reaction is diffusion limited and the reaction rate constant can be determined, although with a relatively large experimental error due to the variability of the incubation time. With the least-squares method we come to the following results:

at 400°C k = 3600 +/- 400 $\mu m^2/h$ (ln k = 8.2 +/- 0.1).
at 415°C k = 7900 +/- 2300 $\mu m^2/h$ (ln k = 9.0 +/- 0.4).
at 430°C k = 9400 +/- 800 $\mu m^2/h$ (ln k = 9.2 +/- 0.1).

At 415°C the reproducibility is not very good, resulting in a large error.

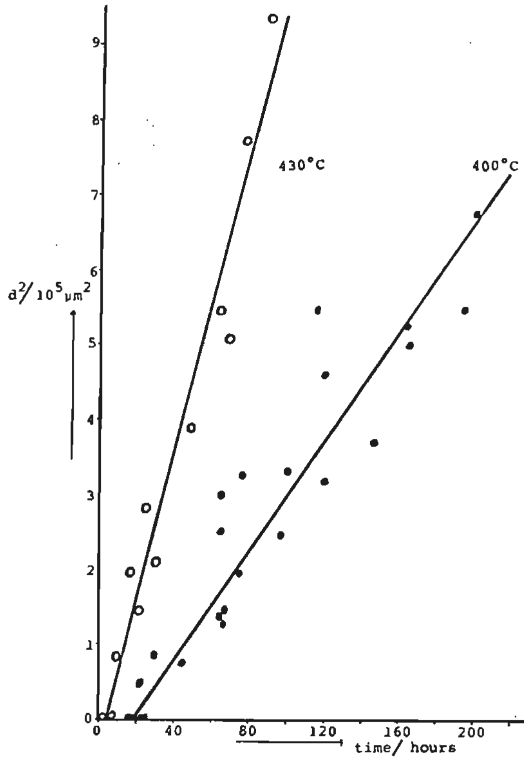

Fig.4.32 The thickness of the reaction layer as a function of time for undoped diffusion couples at low temperatures.

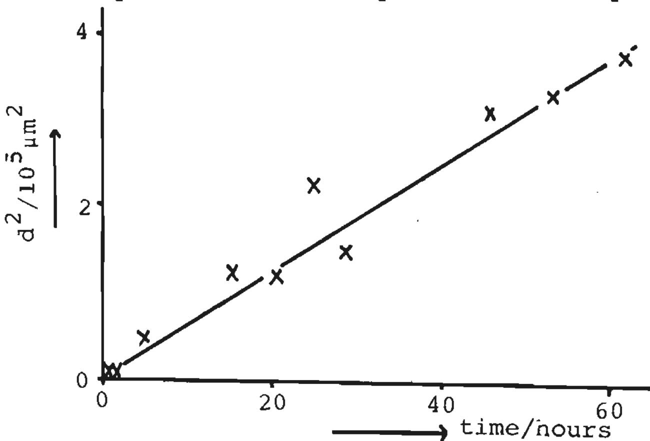

Fig.4.33 Thickness of the Cu_3Si layer in Cu/Si diffusion couples in the absence of phosphorus as a function of time, 500 °C.

§ 4.9.1.2 *Diffusion couples between silicon and phosphorus-containing copper*

The time dependence is completely changed if phosphorus is present in the copper. The amount of phosphorus is not of great influence, both 30ppm and 1at% act in the same way: the incubation time is eliminated, fig.4.34. This means that the reaction barrier is removed by the segregation of phosphorus to the copper surface during the start up of the furnace (about 20 minutes). From the AES experiments (§ 4.5.1.) we know that the copper surface is covered with phosphorus in circa 30 minutes, so the segregation of phosphorus is fast enough to occur during the initial phases of a heat treatment.

Furthermore the reaction rate constant in the presence of phosphorus is much larger than in the undoped case (at 400°C k = 10500 +/- 200 $\mu m^2/h$; ln k = 9.26 +/- 0.02).

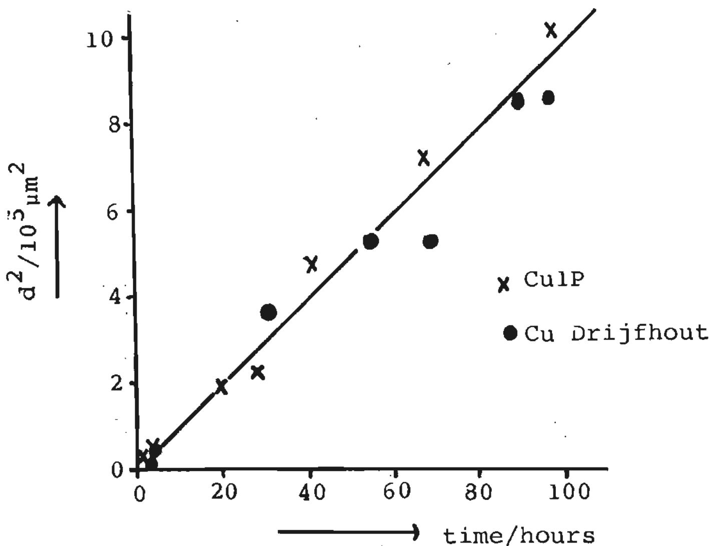

Fig.4.35 Layer thickness of Cu_3Si as a function of time in the presence of phosphorus at 400°C.

§ 4.9.2 *Temperature dependence of the reaction rate contstant*

The reaction rate constants are determined in two ways, depending on the type of copper and on the temperature. At low temperatures, in the absence of phosphorus, the constant is determined by the least squares method from the time dependence of the layer thickness according to the formula :

$$d^2 = k*(t-t_0)$$

At higher temperatures (above 470°C), after confirmation of the absence of an incubation time, the layer thickness is only determined at one reaction time. This procedure is followed for the whole temperature range for the doped couples. The values so determined agree very well with those from a full time dependence determination.

Fig.4.35 shows the temperature dependence of the reaction rate constant, plotted as an Arrhenius plot: the natural logarithm of the constant versus the reciprocal temperature. Such a plot gives the activation energy of the rate determining step of the process. We have already proven that the reaction is diffusion limited (from the parabolic growth law) and that the diffusing component is copper, so here we determine the activation energy of the diffusion of copper through the Cu_3Si layer, assuming that the concentration limits of Cu_3Si are temperature independent.

There is a distinct difference between pure copper and copper, that contains phosphorus. At high temperatures the activation energy of the copper diffusion is 175 +/- 3 kJ/mol, both for undoped and doped copper. Undoped copper reacts with this activation energy down to temperatures as low as 470°C. Then the activation energy changes to a much lower value: 110 +/- 12 kJ/mol. These values are interpreted in the following way : at high temperatures copper diffuses by a bulk diffusion mechanism, while at low tempe-

ratures grain boundary diffusion occurs, a process known to involve a lower activation energy. The same conclusion has been reached in § 4.8.3 on basis of the morphology of the reaction layer: at high temperatures thick grains are formed while at low temperatures thin grains occur, which results in a faster supply of copper through the boundaries. The temperature where the change from grain boundary to bulk diffusion occurs determined from the activation energy, coincides with the temperature where very small grains are formed (fig.4.31).

In doped diffusion couples the situation is somewhat different: already at 530°C the mechanism is changed from bulk diffusion to grain boundary diffusion, which is shown both by the grain size (fig.4.31) and by the temperature dependence of the reaction rate constant. The presence of phosphorus implies the early nucleation of many crystals, so that grain boundary diffusion can provide already at high temperatures a substantial part of the copper supply. This means that the preexponential factor, which is not temperature dependent, is larger in case phosphorus is present. This preexponential factor contains terms like the number of sites available for diffusion. From our results we have to conclude that the presence of phosphorus induces the formation of more nuclei, resulting in more grain boundaries available for diffusion.

The activation energy at low temperature in the presence of phosphorus is 92 +/- 4 kJ/mol. On basis of our data we cannot conclude whether the activation energies in the presence and in the absence of phosphorus (110 +/- 12 kJ/mol) are equal within experimental error. There is no theoretical basis for the two values to be equal: we are discussing grain boundary diffusion of copper and the phosphorus will be present on these grain boundaries. So in principle the two processes may proceed with different activation energies and preexponential factors.

The conclusion from these experiments is that already a trace of phosphorus (30 ppm) eliminates the appearance of incubation times at low temperature and, between 470 and

530°C, changes the diffusion process from a bulk mechanism to a grain boundary mechanism . Related with this the morphology of the reaction product is changed from coarse-grained to fine-grained.

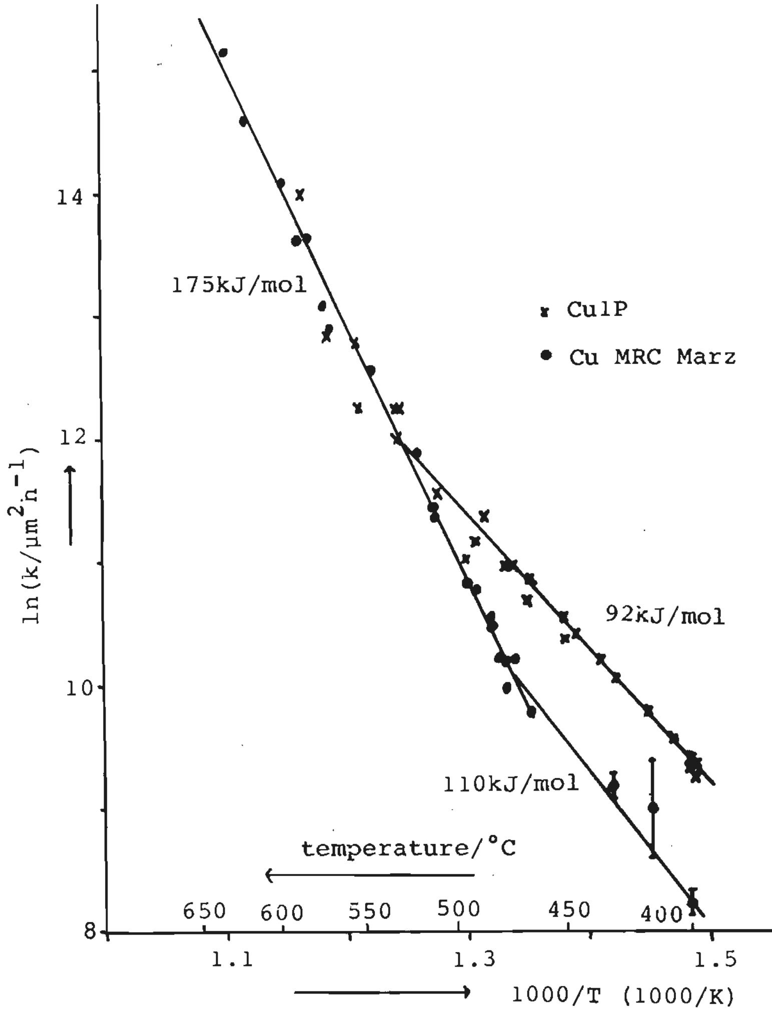

Fig.4.36 Arrhenius plot of the reaction rate constant versus temperature, both for doped and undoped copper-silicon diffusion couples.

§ 4.10 Oxidation experiments

As shown in § 4.9.1 there exists a major difference in the time dependence of the layer thickness between doped and undoped diffusion couples: at temperatures below 470°C pure copper reacts after an incubation time, while doped copper reacts immediately. This incubation time suggests that a reaction barrier exists in clean couples which is removed by phosphorus.

A reaction barrier that will always be present is most probably an oxidation layer. Especially the presence of a silicon dioxide layer on silicon is very likely. It is known that silicon is always covered with a thin layer of oxide, even when extreme precautions are taken. This layer has a thickness in the range of 2nm (lit.21).

In order to find out, whether it is indeed this oxidation layer, that hampers the reaction, we have conducted experiments with pre-oxidized silicon slices. Polished silicon slices are oxidized in a furnace at 1000°C, for half an hour under pure oxygen. This results in a violet discoloration of the slices. The reaction barrier then created is so large that pure copper does not react at all, even at 500°C after 65 hours.

The situation is completely different for copper which contains phosphorus. Both at 400 and 500°C the reaction layer thickness is comparable to the results of the experiments with non-preoxidized silicon. After 16 hours at 500°C a layer of 1050 μm is formed, while in regular diffusion experiments a layer of 1200 μm is expected. For 400°C and 66 hours annealing the numbers are : 680 μm formed, and 830 μm expected in the usual set-up.

We have to conclude from these experiments, that the oxidation layer on silicon is indeed a barrier for the reaction between copper and silicon. It is known (lit.22) that the diffusion of copper through silicon dioxide is a very slow process.

We can think of several ways in which phosphorus removes the reaction barrier: it might be that phosphorus induces crystallisation in the amorphous silicon dioxide layer, so that copper can diffuse through the grain boundaries. Another way is the formation of volatile phosphorus oxides, which are then removed by the vacuum system. A third possibility is the formation of silicon phosphates. Formation of $SiO_2.P_2O_5$ in the bulk phase has been described (lit.23). We have observed the formation of a compound containing Si, P and O during a reaction between phosphorus powder and silica in the presence of copper powder. The presence of copper seems to be necessary, since no product has been found in the absence of copper.

When phosphorus is absent the oxide layer has to dissolve in copper, a process which is apparently slow.

The effect of a silicon dioxide layer on the reaction with copper has also been demonstrated by experiments with Cu_3Si alloys. These alloys are covered with a silicon dioxide layer and do not react with pure copper, only with phosphorus doped copper, a reaction in which $Cu_{15}Si_4$ and Cu_5Si are formed. So also in this case the presence of silicon dioxide prevents the reaction of pure copper.

§ 4.11 Discussion and conclusions

In § 4.1 we have asked ourselves two questions : firstly, why are two products missing in copper-silicon diffusion couples, or why is Cu_3Si the only product formed, and secondly can the presence of phosphorus explain, that various types of copper react so differently.

If we study our diffusion couples carefully, we see that sometimes $Cu_{15}Si_4$ and Cu_5Si are formed, even in phosphorus containing diffusion couples. If we change the reaction conditions and allow copper to react with Cu_3Si, $Cu_{15}Si_4$ and Cu_5Si are formed, in small amounts. From the layer thickness in these experiments we can calculate, that in the regular copper-silicon diffusion couples the $Cu_{15}Si_4$ and Cu_5Si layers will be too thin to be observed. The rare observation of these layers in normal diffusion couples is caused by an obstruction at the reaction interface, so that copper reacts with the already formed Cu_3Si.

In the literature $Cu_{15}Si_4$ and Cu_5Si are never found in diffusion couples. This can be accounted for by two reasons : the reaction times are too short, and no diffusion couples between Cu_3Si and copper have been described.

The layer thickness of Cu_3Si obeys the parabolic growth law, although sometimes an incubation time exists (§ 4.9.1). The rate limiting step in the formation of Cu_3Si is the diffusion of copper through the already formed layer (§ 4.7). From the temperature dependence of the reaction rate constant we can calculate the activation energy of the diffusion of copper through the already formed silicide layer.

We observe two different activation energies related to two different diffusion processes. The temperature range in which the reaction follows one of the reaction mechanisms is dependent on the amount of phosphorus present. At high temperature (above 530°C) both with and without

phosphorus, the reaction has a high activation energy 175 +/- 3 kJ/mol and the reaction layer consistes of very thick crystals: the reaction proceeds by bulk diffusion of copper.

If phosphorus is present the activation energy changes to a much lower value at about 530°C. The activation energy then is 92 +/- 4 kJ/mol and based on this lower value and the morphology of the layers we conclude that the mechanism changes to a grain boundary diffusion mechanism at low temperature.

If phosphorus is absent, however, the bulk diffusion mechanism is preserved till about 470°C. At lower temperatures also a grain boundary diffusion mechanism is operative, the activation energy being 110 +/- 12 kJ/mol.

The preexponential factor for grain boundary diffusion changes in presence of phosphorus. This is probably related to a difference in the number of grain boundaries present, so it is related to the nucleation process of Cu_3Si.

In case of pure copper, at low temperatures, an incubation time exists. This is caused by a reaction barrier, notably a silicon dioxidelayer present on silicon. In case phosphorus-containing copper is used, phosphorus segregates to the reaction interface and removes this reaction barrier.

In fig.4.36 a comparison is made between the results of this work and those from the literature, recalculated to the same scale. Although different techniques and materials are used, we see a great resemblance between the results. Ward et al. (lit.4) have found a low activation energy at very low temperatures. Their reaction rate constants coicides with an extrapolation of our results for the phosphorus containing diffusion couples. The lack of incubation time can be accounted for by consideration of the experimental technique: the silicon slices are etch-cleaned and electroplated with copper. No oxidation layer will be formed. The preexponential factor is quite similar to the one found in this work.

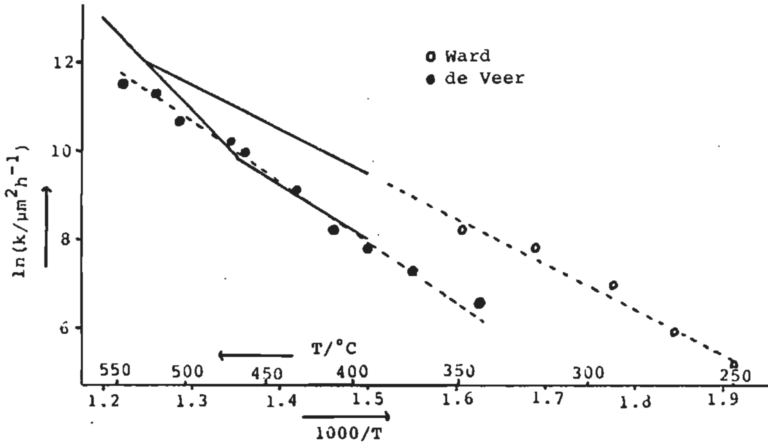

Fig.4.36 Comparison between this work (solid lines) and results of Veer et al.(lit.2) and Ward et al.(lit.4) on the reaction in copper-silicon diffusion couples.

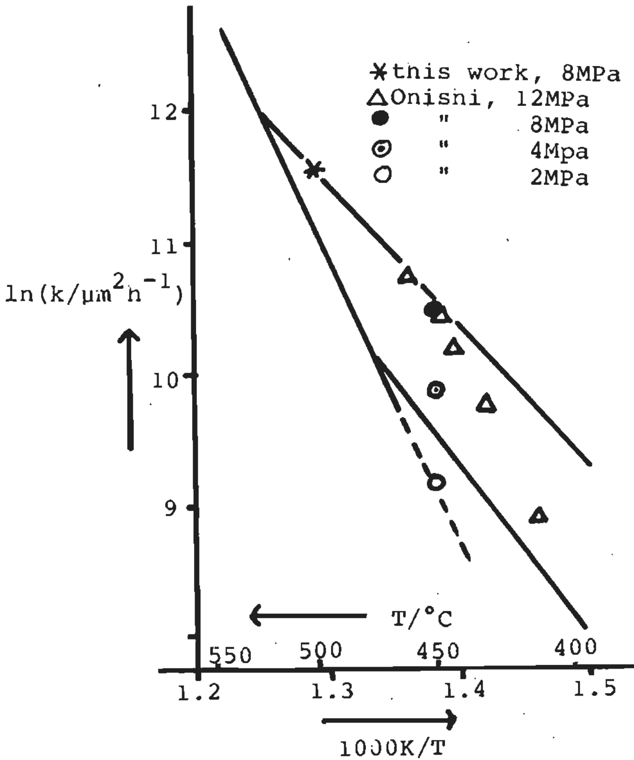

Fig.4.37 Comparison between this work and the data of lit.5.

The results of Veer et al.(lit.2), and Kolster (lit.3) are similar to ours for phosphorus free diffusion couples, although a grain boundary diffusion mechanism is sustained up to higher temperatures. Kolster ascribes the corresponding activation energy to bulk diffusion. The low value of the activation energy is attributed to the high defect concentration in Cu_3Si.

Onishi et al.(lit.5) have eliminated the incubation time at low temperatures by the application of high compressive stresses. At 450°C we see (figs.4.2 and 4.37) that the reaction rate constant raises from a value consistent an extrapolation of our high temperature data, to a value that fits our data in the presence of phosphorus. The data Onishi et al. have obtained at temperatures above 450°C, and we have obtained at 500°C with pure copper at high stresses fit this CuiP plot. This suggests that this curve represents a kind of maximum reaction rate constant, when the reaction has become independent of compressive stress or phosphorus content (fig.4.8). In those cases many nuclei are formed at the reaction interface resulting in a closed reaction layer containing many grain boundaries.

At low stresses or in the absence of phosphorus only a few nuclei are formed resulting in a layer with a few grain boundaries. The diffusion of copper proceeds predominately through the bulk phase.

At low temperatures the diffusion through the bulk phase is so slow that many nuclei can form before the reaction layer is closed. This leads again to a reaction layer containing many grain boundaries, where the diffusion is very fast. The overall process will then be determined by grain boundary diffusion, but other factors, like for instance the compressive stress, will determine the amount of grain boundaries and therefore the reaction rate constant. Both the presence of phosphorus in the reaction interface and the presence of a compressive stress increase the amount of nuclei and therefore will enhance the contribution of grain boundary diffusion. In the absence of phosphorus and compressive stress bulk diffusion will be important.

Summarizing we can conclude that in copper-silicon diffusion couples Cu_3Si is the main product. It can be formed by grain boundary or bulk diffusion of copper through the already formed silicide layer. Which process occurs depends on the particular reaction conditions, although in general at low temperatures (T<450°C) grain boundary diffusion occurs while at high temperatures (T>550°C) bulk diffusion dominates. In the medium range a subtile interplay of reaction barriers, impurities and stresses determines the precise mechanism and thereby the morphology of the reaction layer.

References chapter 4

1] P.J.C. Vosters, M.A.J.Th. Laheij, F.J.J. van Loo, R. Metselaar; Oxid. Met. 20(1983),147

2] F.A. Veer, B.H. Kolster, W.G. Burgers; Trans. Met. Soc AIME 242(1968),669

3] B.H. Kolster; Thesis Technische Hogeschool Delft (1968)

4] W.J. Ward, K.M. Carroll; J. Electrochem. Soc. 129(1982),227

5] M. Onishi, H. Miura; Trans. Jap. Inst. Met. 18(1977),107

6] R. Frech; Thesis Max-Planck-Institut für Metallforschung (1983)

7] R. Hultgren, P.D. Desai; Selected thermodynamic values and phase diagrams for copper and some of its binary alloys. International Copper Research Association Inc. (1971)

8] M. Hansen; Constitution of binary alloys. McGraw-Hill, New York (1958)

9] K. Arrhenius, L. Westgren; Z. Phys. Chem. 14(1931),66 ASTM syst.nr. 4-0841

10] K.P. Mukherjee, J. Bandyopadhyaya, K.P. Gupta; Trans. Met. Soc. AIME 245(1969),2335

11] J.K. Solberg; Acta Cryst. A34(1978),684

12] G.F. Bastin, H.J.M. Heijligers, F.J.J. van Loo; Scanning 6(1984),58

13] W.F. Banholzer, M.C. Burrell; Surf. Sci. 176(1986),125

14] see for instance R.W. Baluffi in Interfacial Segregation; ed. W.C. Johnson, J.M. Blakely; American Society for Metals, Metals Park Ohio (1979)

15] Handbook of chemistry and physics, 51st ed. Chemical Rubber Co. Cleveland Ohio (1970)

16] J.G.M. Becht, F.J.J. van Loo, R. Metselaar;
Reactivity of Solids, ed. P. Barret, L.-C. Dufour;
Elsevier Publishers BV, Amsterdam (1985), 941
17] C. Wagner;
Acta Metal. 17(1969), 99
18] Y.Adda, J. Philibert; La diffusion dans les solides;
Institut national des sciences et techniques nucleaires
(1966), II, p 1163
19] Th. Heumann, S. Dittrich; Z. Metallk. 50(1959), 617
20] P.G. Shewmon; Diffusion in solids;
McGraw-Hill Book Company Inc., New York (1963)
21] K.K. Ng, W.J. Polito, J.R. Ligenza
Appl. Phys. Lett. 44(1984), 626
22] J.D. McBrayer; Thesis Stanford University (1984)
23] H. Makart; Helv. Chem. Acta 50(1967), 399

chapter 5 the reaction between copper phosphide and silicon

§ 5.1 Introduction

In the previous chapter we have studied the influence of a trace of phosphorus in copper on the solid state reaction between copper and silicon. We have found that the segregation of phosphorus changes the reaction kinetics. The copper surface resembles a copper phosphide surface. We have studied the reaction between copper phosphide and silicon, in order to get more insight in the details of the influence of phosphorus on the reaction. The solid state reaction itself has proven to contain many interesting aspects. Again it is the behaviour of phosphorus that dominates the reactions that take place. In this case it is the volatility of phosphorus that determines the reaction.

We have determined the low phosphorus part of the ternary phase diagram Cu-Si-P by preparing and analyzing ternary alloys. Also the products formed in diffusion couples give information on the shape of the ternary phase diagram.

The solid state reaction between Cu_3P and silicon has been studied both in vacuum and in closed evacuated capsules, in the temperature range between 400 and 550 °C.

§ 5.2 Ternary phase diagram Cu-Si-P

§ 5.2.1 *Literature survey*

The binary phase diagram Cu-Si has been discussed in the previous chapter.

In the binary system Cu-P two phosphides are known (lit.1) : Cu_3P and CuP_2 (fig.5.1). The solubility of phosphorus in copper is considerable : at 350°C 1.2 at% and at 714°C (the eutectic temperature) 3.5 at% (lit.2). Because of the high phosphorus content CuP_2 is of no concern to the study discussed in this chapter. Cu_3P has a hexagonal crystal structure (lit.3), with a = 0.694 nm and c/a = 1.028. The structure shows resemblance to the Cu_3Si structure (lit.4).

The most recent silicon-phosphorus phase diagram (fig.5.2) as published in Muffatt's handbook in 1986 (lit.5) states SiP as the only compound in this system. But depending on the preparative techniques SiP_2 (lit. 6), Si_3P_2 (lit. 7) and Si_2P (lit. 8) are reported. Confusion exists about the structures of these compounds: an orthorhombic structure with a = 1.36 nm, b = 2.05 nm and c = 0.35 nm is attributed both to SiP (lit.9) and to SiP_2 (lit.6), while for SiP_2 also an alternative orthorhombic structure with a = 1.399nm, b = 1.009nm and c = 0.343nm (lit.10) is reported.

The data on the stability of SiP are contradictory: SiP is reported to be stable in water and air (lit.11), but on the other hand SiP has to be considered as an hazardous material (lit.12), decomposing into SiO_2 and PH_3 in contact with humid air (lit.13).

One ternary compound has been described in the literature : $CuSi_2P_3$, a semiconductor (lit.14) which crystallizes in the sphalerite structure with random distribution of copper and silicon atoms on the cation sites (lit.15). The lattice constant a = 0.525 nm. No further information has been found on the ternary system.

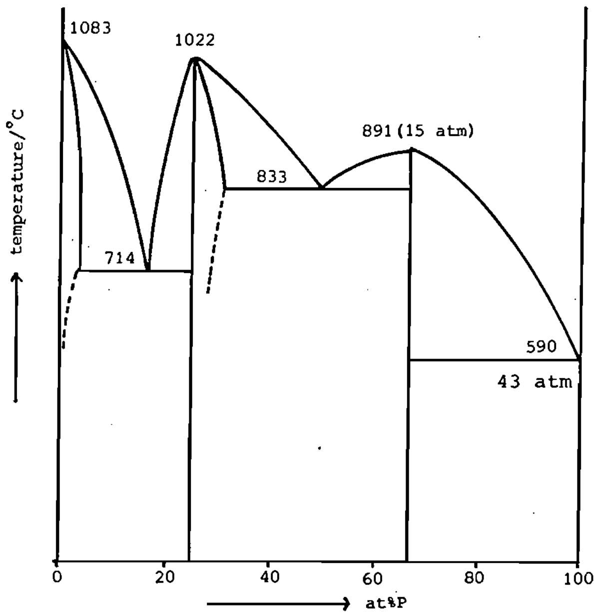

Fig.5.1 The binary system copper-phosphorus (lit.1) in a non-isobaric representation.

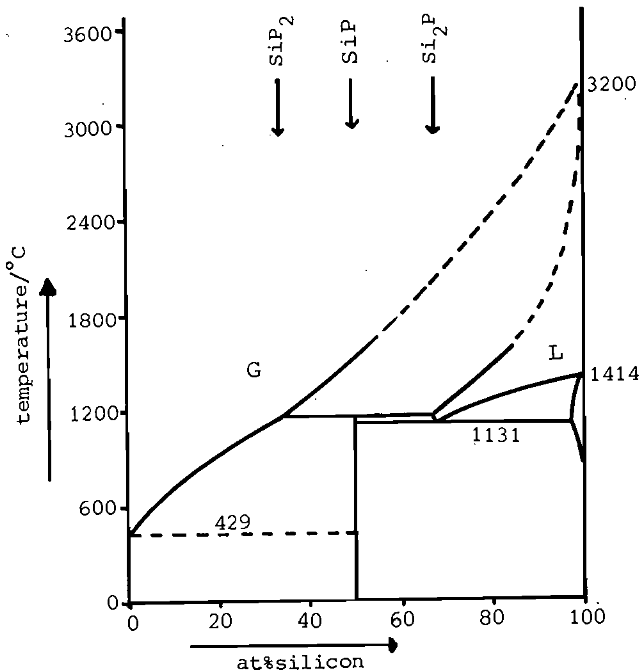

Fig.5.2 The binary system silicon-phosphorus, according to Muffatt, (lit.5) at atmospheric pressure.

§ 5.2.2 Determination of the ternary system at 500 °C

Alloys have been prepared by arc melting lumps of copper, silicon and copper phosphide. During the melting considerable losses occur, presumably phosphorus vapour, which condenses on the glass container of the apparatus. The choice of the raw materials limits the overall compositions of the alloys: the maximum phosphorus content lies below the line Cu_3P/Si. Series of alloys have been prepared containing less than 30 at% silicon and variable (2-15 at%) amount of phosphorus. Alloys containing high amount of silicon (about 40 at%) have been prepared without the addition of copper to the silicon and Cu_3P. Alloys containing 75 at% copper and varying amount of silicon and phosphorus will be discussed in § 5.2.3.

The alloys are equilibrated in evacuated silica capsules for one to two months at 500 °C. The closed capsules ensure that the alloys are annealed under equilibrium phosphorus pressure. No losses occur during the annealing treatment. After quenching in salted water the specimens are cut with a water cooled SiC saw, ground on SiC paper, and polished with diamond paste. Occasionally the characteristic odour of PH3 has been perceived.

The composition of the phases is determined with EPMA. The results are shown in fig. 5. 3. As the diagram shows, there exists an equilibrium between Cu_3P and $Cu_{15}Si_4$ and between Cu_3P and Cu_5Si; both silicides contain some phosphorus. Furthermore a three phase triangle exists between Cu_3P, Cu_3Si and $CuSi_2P_3$. Another equilibrium exists between Cu_3Si, silicon and a ternary compound containing 16 at% Cu, 43 at% Si and 41 at% P, denoted F in the phase diagram. This last compound lies nearly on the connection line between $CuSi_2P_3$ and Si.
Three explanations for the composition are thinkable:

- F is a microscopic mixture of $CuSi_2P_3$ and Si.
  A variable composition would strongly support this idea, but in all alloys with an overall composition within the

triangle Cu_3Si-Si-F the same compound has been found.

- F is in fact $CuSi_2P_3$, but with a maximum of dissolved Si. This idea is based on the analogous system Cu-Ge-P, where it is known that considerable amounts of Ge dissolve in $CuGe_2P_3$ (lit. 16).
- F is a true ternary compound.

Since we have not been able to prepare alloys with an overall composition in the triangle Cu3Si-CuSi2P3-F, which is very small within the composition range at our disposal, we can not decide against either of the two latter possibilities.

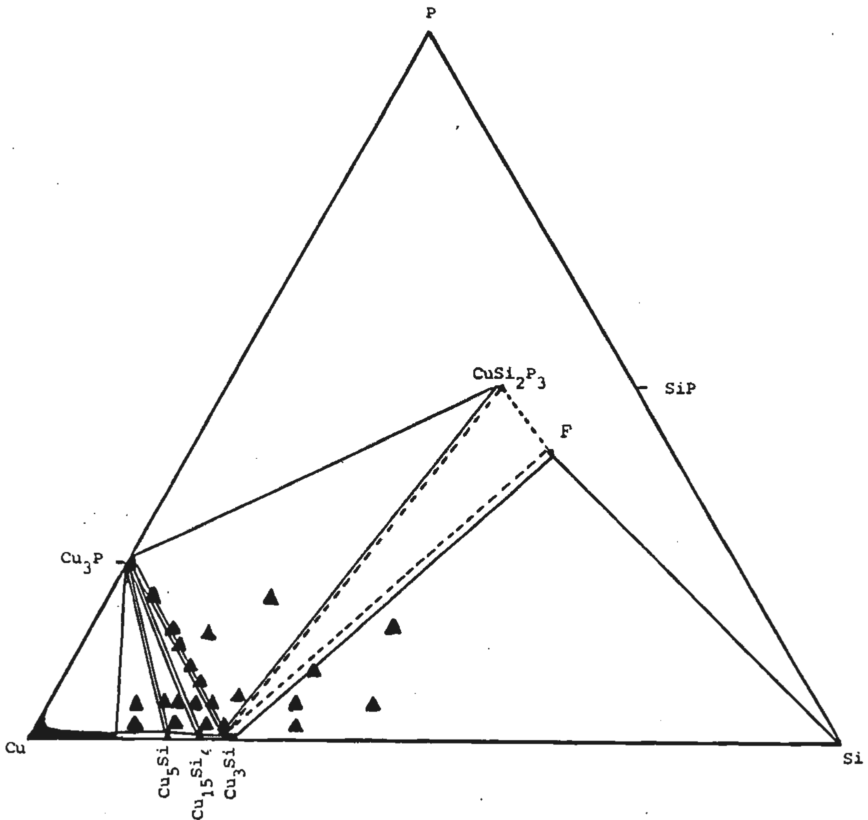

Fig.5.3. Phase relations in the ternary system Cu-Si-P as determined with EPMA in alloys, equilibrated in evacuated silica capsules at 500°C.

§ 5.2.3 The Cu_3Si-Cu_3P pseudo binary system

The crystal structures of Cu_3Si and Cu_3P are related (lit. 4). Both compounds show the same anisotropic behaviour in polarized light. During the analyses discussed in §5.2.2. data are found, which suggest the formation of a continuous range of compositions between Cu_3Si and Cu_3P, all with 75 at% copper.

Alloy have been prepared by arc melting Cu_3Si and Cu_3P and are equilibrated in evacuated silica capsules at 500 °C. Non of these are homogeneous. They either decompose in Cu_3P, $Cu_{15}Si_4$ and Cu_3Si or in Cu_3Si, $CuSi_2P_3$ and Cu_3P. Cu_3Si and Cu_3P in these alloys show a slight mutual solubility, but it never exceeds 1 at%.

A diffusion couple has been prepared between Cu_3P and Cu_3Si. Fig. 5.4 shows the concentration profile through the reaction layers as determined with EPMA, while fig. 4.14 shows a detailed picture of similar reaction layer. The diffusion path leads from Cu_3Si via $Cu_{15}Si_4$ and Cu_5Si to the solid solution of phosphorus and silicon in copper ending in Cu_3P. Phosphorus can only be detected in the solid solution, the silicides are virtually phosphorus free. No sign of mutual solubility has been found. It should be noted here, that the starting materials Cu_3P and Cu_3Si contain a little excess of copper, meaning that the diffusion couple is completely on the copper-rich side of the line Cu_3Si-Cu_3P.

Alloys containing less than about 70 at% copper (the other side of the Cu_3Si-Cu_3P line) also contain either Cu_3P with 1 at% Si or Cu_3Si with 1 at% P.

A critical reexamination of the original data on the composition of the alloys indeed raises doubts, whether this mutual solubility really exists. The analyses are performed with EPMA and although it is a micro-analyzer, the analyzed volume has a finite extent. If two crystals are mixed on a scale of comparable or smaller size, an average composition will be determined. A consequence is that the composition changes from area to area. This is the case with at least

part of the analyses in the $Cu_3(P,Si)$ alloys: within what appears to be one crystal, the composition changes. We have to conclude that this is not an equilibrium composition and that no mutual mixability exists between Cu_3Si and Cu_3P, in agreement with the diagram of fig. 5.3.

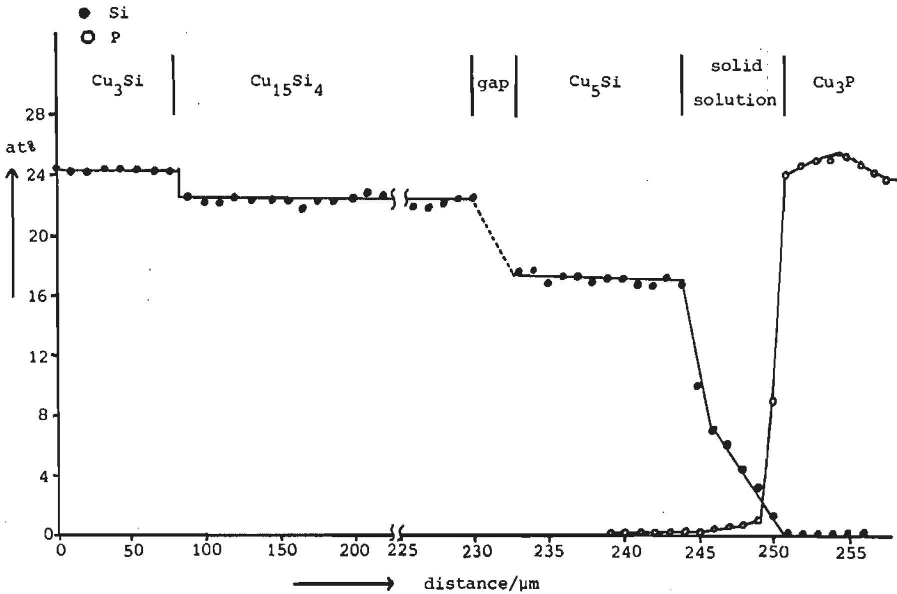

Fig.5.4 Concentration profile through a Cu_3Si-Cu_3P diffusion couple, as determined with EPMA. The diffusion couple has been annealed for 70 h at 500°C in vacuum.

§ 5.3 The solid state reaction between Cu_3P and Si in vacuum

We have prepared diffusion couples with Cu_3P and Si platelets. The reaction takes place in the vacuum furnace as described in chapter 3. The vacuum pressure is less than 0.1 mPa. The experiments are conducted in the temperature range between 400 and 550°C.

§ 5.3.1 *Product formation*

If we look at the phase diagram as determined in §5.2, we see that the slope of the tielines changes on going from Cu_3P via Cu_3Si to $CuSi_2P_3$. Therefore we expect the following layer sequence in a Cu_3P-Si diffusion couple:

Cu_3P - $CuSi_2P_3$ - Cu_3Si - Si

as explained in chapter 2.

However, we only observe the formation of Cu_3Si, growing in columns that separate the original platelets, although the platelets are pressed together with a weight of 20kg. This is shown for a real couple in fig.5.5 and schematically in fig.5.6.The separation of the Cu_3P and Si platelet, deserves attention, since in a diffusion couple where the reaction is hampered and only proceeds locally, the original interface stays intact. This is shown schematically in fig.5.7. This latter morphology has been discussed in § 4.8.2.

The Cu_3Si crystals in a Cu_3P/Si diffusion couple are embedded in the silicon layer, showing a perfect pore free interface, but the contact with the Cu_3P layer is remarkable: the smallest crystals have lost contact with the Cu_3P layer, as if the Cu_3P platelet had already been lifted away by faster growing crystals before the particular crystal could react, so the little one has lost contact with the Cu_3P layer and has stopped growing. The contact with the large crystals is also rather unusual. The Cu_3Si column only touches the Cu_3P platelet, but is not embedded in it. This morphology indicates that the whole of the Cu_3P surface takes part in the reaction, instead of only the immediate contact area. So the surface diffusion of copper on the Cu_3P surface is very fast.

At 550°C a different morphology occurs (fig.5.8): the columns formed are bulgy instead of straight. We attribute this to plastic deformation, since the reaction tempe-

rature is relatively high, T $\cong$ 0.73 T_m, and the load of 20 kg is carried by only a few mm^2 of product layer, leading to stresses in the range of about 20 MPa.

The product formed is Cu_3Si, containing less than 0.02 at%P. No concentration gradient is found in the product layer (fig.5.9) and the histogram of the distribution of the silicon content in the layer is similar to those determined for Cu/Si diffusion couples (fig.5.10)

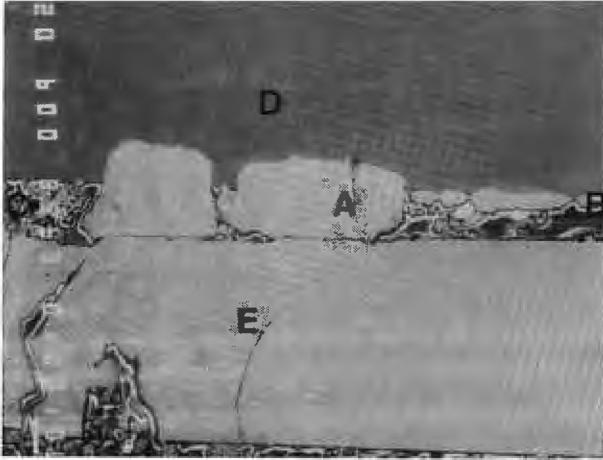

Fig.5.5 Back scattered electron image of a Cu_3P/Si diffusion couple, annealed at 430 °C for 145 h, showing large columns[A] and small crystals[B] of Cu_3Si and the gap[C] between the original Si[D] and Cu_3P[E] platelets. Bar indicates 100 μm.

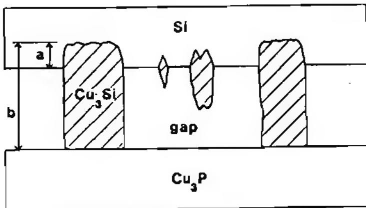

Fig.5.6 Schematic drawing of a Cu_3P-Si diffusion couple.
a denotes the amount of silicon consumed.
b denotes the amount of Cu_3Si formed

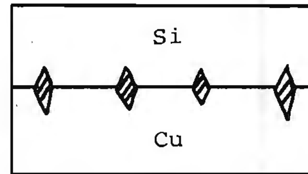

Fig.5.7 Schematic drawing of a Cu/Si diffusion couple, when reaction occurs at only part of the contact area.

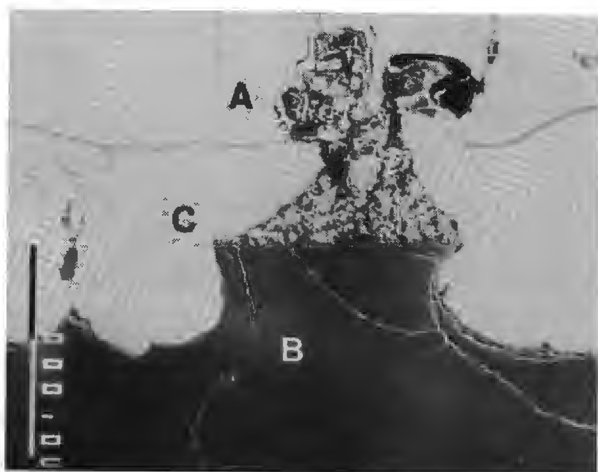

Fig.5.8 Cu_3P^A/Si^B diffusion couple annealed at 550°C for 73h showing plastically deformed Cu_3Si columns^C. Bar indicates 1000µm, secondary electron image.

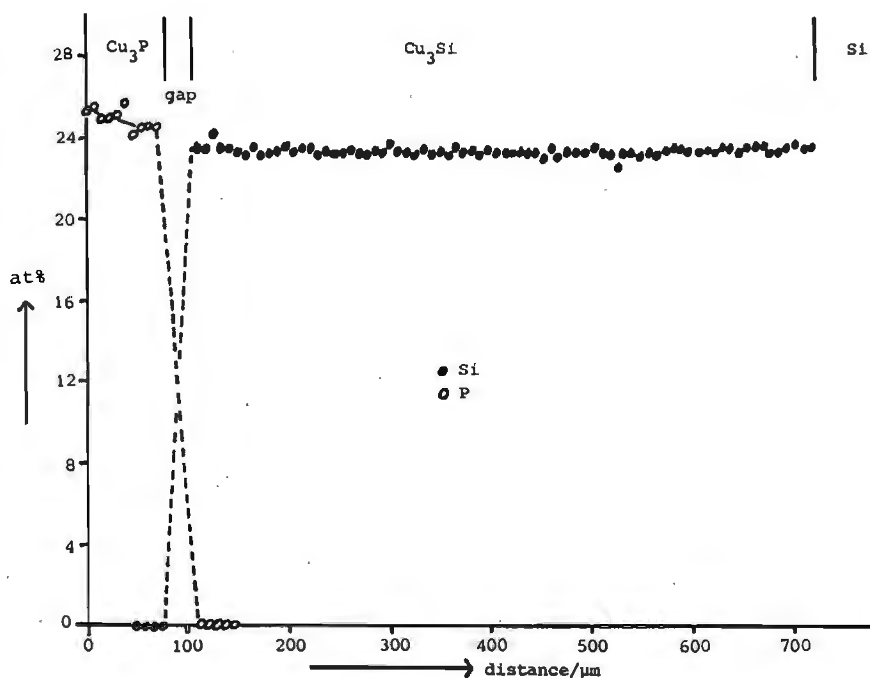

Fig.5.9 Concentration profile through the reaction layer of a Cu_3P/Si diffusion couple, annealed at 500°C.

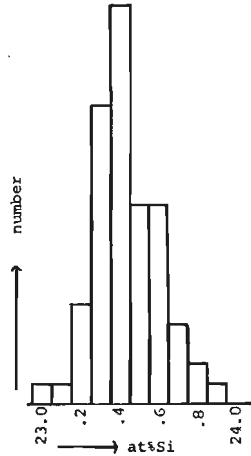

Fig.5.10 Histogram of the distribution of the silicon concentration in Cu_3Si formed in a Cu_3P/Si diffusion couple.
$n = 78$, $\bar{x} = 23.49$ at%Si
$s = 0.02$

So in Cu_3P/Si diffusion couples Cu_3Si is formed, that contains negligible amounts of phosphorus. This observation contradicts the mass balance: if Cu_3P is decomposed and the copper reacts with silicon, we expect the formation of a phosphorus containing compound. Based on the shape of the ternary phase diagram (fig. 5. 3) we expect the formation of this compound at the Cu_3P/Cu_3Si interface.

Since the reaction takes place inside a vacuum system, it is possible that a gaseous product is formed, that will be removed, so that no layer will be detected. We can think of some different reactions, for instance :

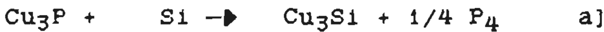

$$Cu_3P + Si \rightarrow Cu_3Si + 1/4\ P_4 \qquad a]$$

$$3\ Cu_3P + Si \rightarrow Cu_3Si + 3\ Cu_2P \qquad b]$$

$$Cu_3P + 2\ Si \rightarrow Cu_3Si + SiP \qquad c]$$

$$9\ Cu_3P + 14\ Si \rightarrow 8\ Cu_3Si + 3\ CuSi_2P_3 \qquad d]$$

We know the volumes per formule unit of Cu_3Si (lit.17) = $0.049 nm^3$ and Si (lit.18) = $0.021 nm^3$. Therefore we can calculate the ratio between the amount of silicon consumed (fig.5.5,a) and the amount of Cu_3Si formed (fig. 5.5,b). Both for reaction a] and b] this ratio is 21/49 = 0.41. Both reactions are similar with respect to

the products formed : i.e. the second product (beside Cu_3Si) does not contain silicon. If silicon is part of the second product the ratio raises to 0.71 for reaction d] and 0.82 for reaction c].

This ratio can be determined in the diffusion couples if we know where the original silicon surface is after the reaction. Since the unreacted silicon surface is still mirror-like, we assume that the surface we observe in the side view is the original silicon surface. The average ratio as determined in the diffusion couples at 400, 430 and 500 °C is 0.43. Only couples at 550 °C deviate from this value, probably because of the deformation of the Cu_3Si columns. From this ratio we conclude that the gaseous product does not contain any silicon.

No Cu_2P could be detected. This leaves as the most probable reaction the formation of phosphorus vapour, which will be accompanied with weight losses in the diffusion couples. The weight losses determined at 500°C are compatible with the formation of phosphorus vapour.

The phosphorus formation is not in agreement with the phase diagram as presented in fig.5.3. This may be caused by the difference in reaction conditions, especially with respect to the vapour pressure: the alloys are equilibrated in closed capsules, resulting in an equilibrium phosphorus pressure. The diffusion couples, however, are annealed in a vacuum system, which will remove any phosphorus vapour formed.

SiP is on the borderline of stability under the circumstances in the vacuum furnace, as can be seen from its Gibbs energy (for data see Barin and Knacke, lit.19):

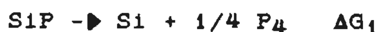

$$SiP \rightarrow Si + 1/4\ P_4 \quad \Delta G_1$$

700 K: $\Delta G_1 = -17489 - 1/4 * 151306 + 93303 = +37987 J$

800 K: $\Delta G_1 = -21480 - 1/4 * 186234 + 100742 = +32703 J$

From these values it follows that:

700 K: $-RT \ln[P_{P_4}]^{1/4} = +37987$; $P_{P_4} = 4.6*10^{-7}$Pa

800 K: $-RT \ln[P_{P_4}]^{1/4} = +32703$; $P_{P_4} = 2.9*10^{-4}$Pa

Therefore, in the dynamic vacuum in the furnace of 10^{-4} Pa the decomposition of SiP into Si and P_4 is likely.

This is more so in the presence of Cu_3P, since then the reaction

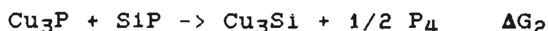

$$Cu_3P + SiP \rightarrow Cu_3Si + 1/2\ P_4 \qquad \Delta G_2$$

takes place.

We can estimate whether SiP is stable in the presence of Cu_3P by calculating the change in Gibbs energy ΔG_2. We need a value for the Gibbs energy of Cu_3Si. This is not known, but an estimate can be made based on the correspondence in structure between Cu_3Si on one hand and Cu_3P and Cu_3As on the other hand.

According to Barin and Knacke (lit.19) the following values for the Gibbs energy of Cu_3P and Cu_3As apply:

	G_{Cu_3P}(J/mol)	G_{Cu_3As}(J/mol)
700 K	-223664	-222057
800 K	-244274	-244893

These values are very close to each other, therefore we take as an estimate for the values of Cu_3Si those of Cu_3P.
This leads to the following calculation of ΔG_2:

$$\Delta G_1 = G_{Cu3Si} + 1/2 G_{P4} - G_{Cu3P} - G_{SiP}$$

$$= -23664 - 0.5*151306 + 223664 + 93303 = 17650 \text{ J (700K)}$$

or

$$= -244274 + 0.5*186234 + 244274 + 100742 = 7625 \text{ J (800K)}$$

Thus, if only pure compounds occur in the reaction:

700K : $-RT \ln[P_{P_4}]^{1/2} = +17650$; $P_{P_4} = 230$ Pa

800K : $-RT \ln[P_{P_4}]^{1/2} = +7625$; $P_{P_4} = 1*10^4$ Pa

From these values we conclude that, if SiP is formed during the reaction of Cu_3P and Si, it will decompose in the presence of Cu_3P with the formation of phosphorus vapour in a dynamic vacuum system, where the pressure is 0.1 mPa. A consequence is that the phase realtions in a closed system will be different from those in a vacuum system. In fig.5.11 a schematic diagram is drawn that applies for a vacuum system. The diffusion path in Cu_3P/Si diffusion couples is denoted, showing the formation of Cu_3Si and phosphorus vapour.

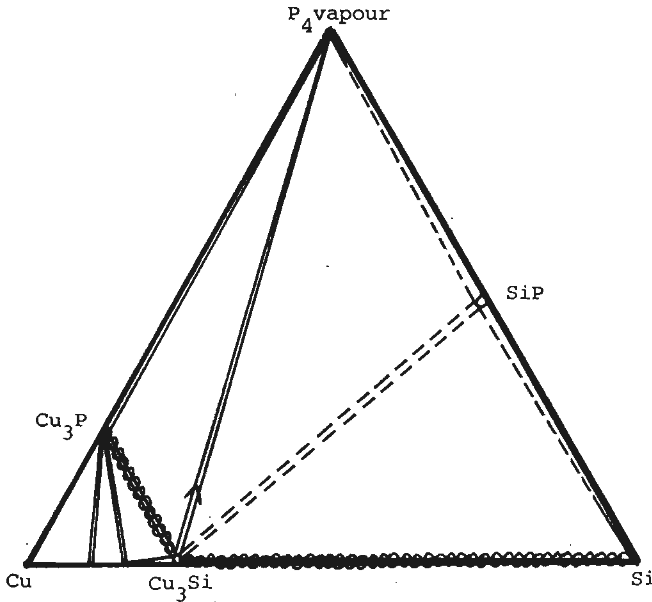

Fig.5.11 A ternary diagram that illustrates the formation of phosphorus vapour in a Cu_3P/Si diffusion couple in a vacuum system. The arrow denotes the formation of vapor, the dotted lines denote a possible instability, the circles denote the diffusion path.

§ 5.3.2 The kinetics of the solid state reaction between Cu_3P and Si in vacuum

The time dependence of the thickness of the Cu_3Si layer has been determined at 4 different temperatures. The results are summarized in fig.5.12.

The spread in the data is rather large, since the crystals are thin and scarce. Therefore it is difficult to decide whether a particular crystal is really the largest one obtained at a specific time and temperature.

The thicknesses for the couples at 550 °C are corrected for the plastic deformation. This is done by measuring the thickness of Cu_3Si in the silicon slice and multiplying this value by 1/0.41, being the ratio between the amount of silicon consumed and the amount of Cu_3Si formed if the columns are straight.

It is clear that the reaction in Cu_3P/Si couples is never faster than in Cu Marz/Si couples at the same temperature (if necessary extrapolated to higher temperatures). Only at 550°C if a closed reaction layer has been formed, and at 400°C the reaction rate is similar to Cu Marz. This indicates that the reaction has slowed down, because some hinderence occurs. At 430°C a linear time dependence is found, indicating that an interfacial reaction is the rate determining step, instead of the diffusion of copper through the already formed silicide layer.

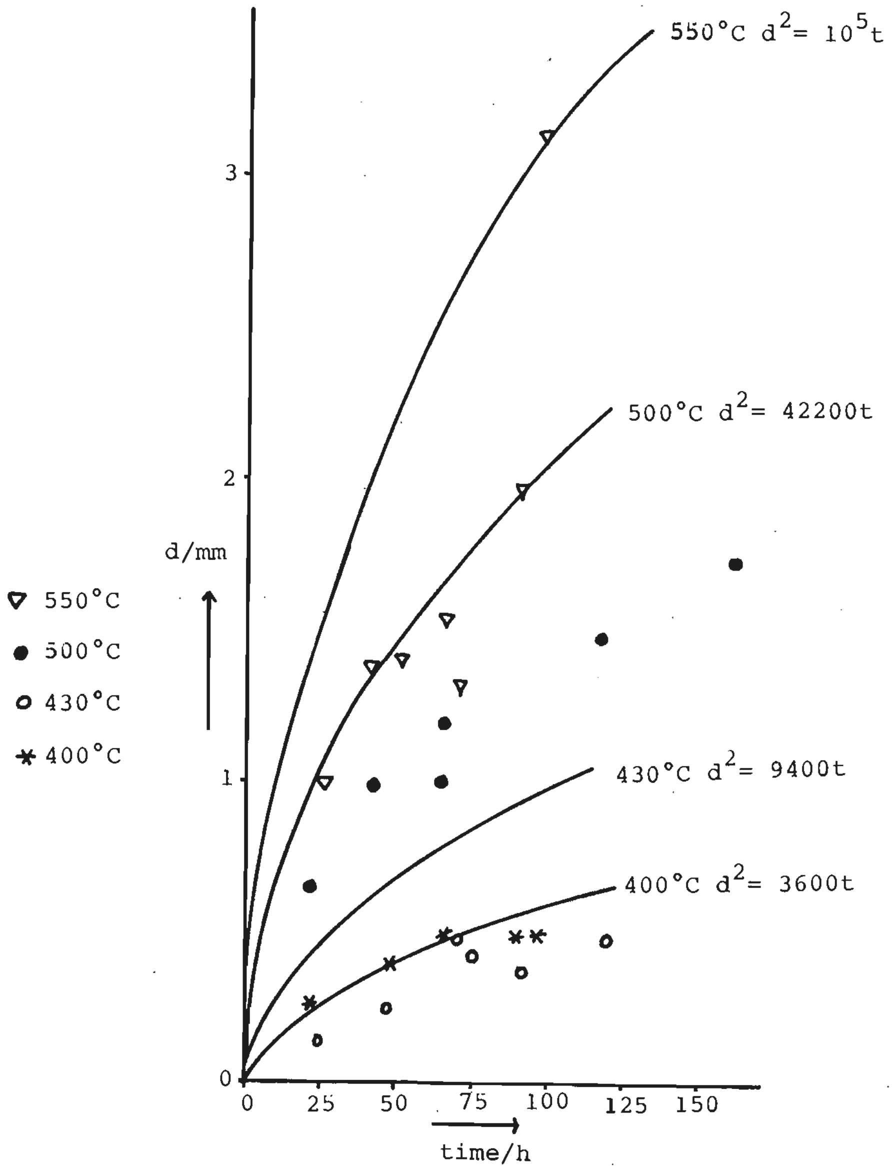

Fig.5.12 The thickness of the Cu_3Si layer in Cu_3P/Si diffusion couples, plotted as a function of reaction time for several temperatures. The couples have been annealed in a vacuum system. For comparison parabolic growth curves are plotted, using the reaction rate constant being determined from the Arrhenius plot for Cu Marz/Si as shown in fig.4.36.

§ 5.3.3 *Morphology of the reaction layer in Cu_3P/Si diffusion couples annealed in vacuum*

The formation of gaps in the reaction layer in Cu_3P/Si diffusion couples provokes curiosity, since this is certainly not a usual situation. We see that the overall growth is retarded in such cases. Furthermore the shape of the Cu_3Si-Cu_3P interface shows, that the whole Cu_3P platelet is involved in the reaction instead of just the contact area.

If a closed reaction layer is formed, the diffusion couple must shrink in height, since phosphorus vapour is lost at the Cu_3Si-Cu_3P interface. The layer thickness will be determined by the diffusion of copper through the silicide layer as long as the contact between Cu_3Si and Cu_3P remains good.

When the contact between Cu_3Si and Cu_3P is lost, Cu_3P will be removed towards a point where the reaction still continues. Then the contact between Cu_3Si and Cu_3P is definitely lost, leaving a Cu_3Si crystal that has only contact with silicon. The gap that is left behind, is the space originally taken by Cu_3P. The overall reaction rate is retarded compared to a couple where a closed layer is formed.

§ 5.4 The solid state reaction between Cu_3P and Si in a closed system

A diffusion couple has been prepared in a stainless steel clamp, and annealed in an evacuated silica capsule at 500°C. After 65 h the capsule was allowed to cool down slowly and was carefully opened. The specimen became warm in contact with air and the characteristic smell of PH_3 spread around. Inspection by optical microscopy showed that the outside of the reaction layer was covered with small, white crystals, definitely different from Cu_3Si. Metallographic preparation of the specimen turned out to be difficult, since the second phase formed (fig.5.13) either is crushed under the pressure during the heat treatment or decomposed in contact with water and air.

EPMA analyses show that one product is Cu_3Si, which is in contact with silicon. A second phase has been formed. No quantitative analyses can be performed. Qualitatively only silicon and oxygen can be detected, no copper or phosphorus. This suggests that this second phase originally consisted of SiP, which decomposes into SiO_2 and PH_3 (lit.13) as is supported by the characteristic smell. This reaction would account for the fact that the specimen became warm and for the impossiblity to polish the specimen.

According to the phase diagram determined in § 5.2, we expect the formation of $CuSi_2P_3$ at the Cu_3P-Cu_3Si interface. In that case, however, even if this compound decomposes, some copper would be left behind in the products. Since no copper has been detected, probably no $CuSi_2P_3$ has been formed. We have to conclude that the diagram of fig.5.3 is irrelevant for this experiment, because of difference in phosphorus pressure and that the diagram of fig.5.14 is more likely for the circumstances used in this experiment.

The thickness of the reaction layer is smaller than in case of a vacuum annealed couple: the diffusion of copper through SiP might be rate determining.

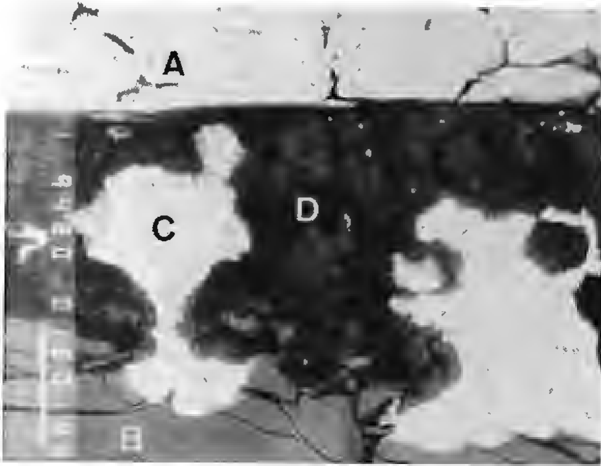

Fig.5.13 Secondary electron image of a Cu_3P^A/Si^B diffusion couple annealed in a closed capsule at 500°C for 65 h. The bright reaction product is Cu_3Si^C, the second crumbly phase is probably SiP^D. Bar indicates 100 µm.

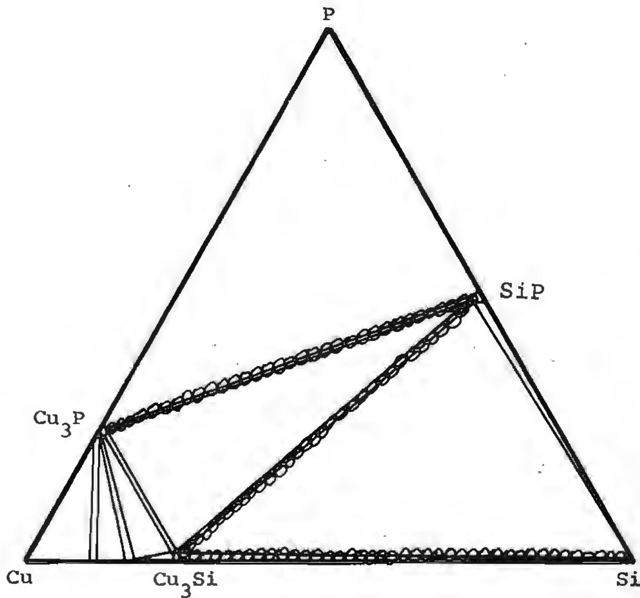

Fig.5.14 Ternary phase diagram for Cu_3P/Si diffusion couples in closed evacuated capsules.

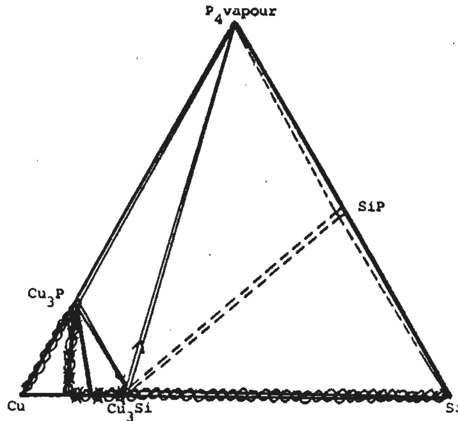

Fig.5.15 Schematic ternary diagram for a vacuum system at 500°C showing the diffusion pathes of a CuIP/Si couple (o), and a Cu_3Si/Cu_3P couple (x)

§ 5.5 Conclusions

The central problem in this chapter is the phosphorus pressure: it is certain that the phosphorus pressure during the annealing treatment of the alloys is different from the vacuum diffusion experiments and there exist doubts whether the situation for the alloys is comparable with a diffusion couple annealed in a closed capsule. In all three cases Cu_3Si is formed, but phosphorus is found in different compounds: in the alloys $CuSi_2P_3$ (and maybe a second ternary compound) is formed, in diffusion couples in a vacuum system phosphorus vapour is formed, while during annealing of a diffusion couple in a closed capsule SiP seems to be formed.

The diffusion couples annealed in a vacuum system exhibit an extraordinary morphology: often gaps are formed between the original platelets. They are created when Cu_3P diffuses away when the reaction is obstructed at a certain point. This morphology is accompanied by an overall retarded growth rate if we compare it with results on grain boundary diffusion of copper through the silicide layer.

References chapter 5

1] M. Hansen; Consitution of Binary Alloys, McGraw-Hill, New York (1958)

2] V.M. Rozenberg, I.A. Voloshko; Fiz.Metal.Metalloved 53(1982),198 (English translation)

3] Gmelins Handbuch der Anorganischen Chemie; Kupfer,60 B II; 8th ed. (1961) Verlag Chemie GMBH, Weinheim/Bergstrasse

4] R. Hultgren, P.D. Desai; Selected thermodynamic values and phase diagrams for copper and some of its binary alloys. International Copper Research Association Inc. (1971)

5] W.G. Muffat; Handbook of binary phase diagrams,(1976-..) General Electric Co., Schenectady N.Y.

6] A.J. SpringThorpe; Mat.Res.Bull 4(1969),125

7] K. Maser, J. Dubnack, U. Siegel; Z.Phys.Chemie 265(1984),225

8] G. Fritz, H.O. Berkenhoff; Z.Anorg.Allgem.Chem. 300(1959),205

9] T. Wadsten; Acta Chem.Scand. 23(1969),2532

10] T. Wadsten; Acta Chem.Scand. 21(1967),593

11] Ya.A. Ugai, S.N. Miroshnichenko, E.P. Domashevskaya, M.A. Vasilevskaya;Inorg.Mater. 9(1973),6

12] W. Braun, A. Donhardt; Vergiftungsregister Georg Thieme Verlag Stuttgart (1970)

13] Gmelins Handbuch der Anorganischen Chemie; Phosphor,16 C; 8th ed. (1965) Verlag Chemie GmbH, Weinheim/Bergstrasse

14] H. Neumann, W. Kissinger, Falah S. Hasoon, B.R. Pamplin, H. Sobotta, V. Riede; Phys.Stat.Sol.(b) 127(1985),K9

15] O.G. Folberth, H. Pfister; Acta Cryst. 14(1961),325

16] N.A. Goryunova, V.I. Sokolova, Ping-Hsi Tsing Dokl.Acad.Nauk.SSSR 152(1963),363

17] B.H. Kolster; Thesis Technische Hogeschool Delft (1968)

18] Handbook of chemistry and physics, 51st ed. Chemical Rubber Co. Cleveland Ohio (1970)

19] I. Barin, O. Knacke;
Thermochemical Properties of Inorganic Substances,
Springer Verlag, Berlin (1973)
I. Barin, O. Knacke, O. Kubaschewski;
Thermochemical Properties of Inorganic Sustances,
Supplement; Springer Verlag, Berlin (1977)

chapter 6 the solid state reaction between copper and germanium

§ 6.1 Introduction

In the previous chapters we have studied the solid state reaction between copper and silicon. The reaction is characterized by the presence of large incubation times at low temperatures, which are removed when a trace of phosphorus is present in the copper.

We have wondered whether such a large influence of an impurity would also occur in similar systems. An obvious example seemed to be the reaction between copper and germanium. Silicon and germanium are very much alike: they have the same crystal structure and have a similar chemical behaviour. Furthermore the phase diagrams of the copper-silicon and copper-germanium systems as well as the diagrams of the phosphorus-silicon and phosphorus-germanium systems are much alike.

The solid state reaction between copper and germanium has not yet been described, to our knowledge. Therefore we have studied the reaction between copper and germanium in diffusion couples between 400 and 575°C. Special attention has been paid to the occurrence of incubation times and the influence of compressive stress and the presence of phosphorus on the reaction kinetics.

§ 6.2 Phase diagrams

§ *6.2.1 Literature survey*

Fig. 6.1 shows the binary copper-germanium phase diagram according to Hansen (lit. 1), adopted by Hultgren (lit. 2). The solubility of germanium in copper is considerable: 9.5at% at 300°C, and with a maximum of 11.8at% at 823°C. The solubility of copper in germanium is negligibly small: the maximum copper content is less than $3*10^{-4}$at% at 875°C (lit. 1).

In the low temperature range two compounds exist: the ζ-phase or Cu_5Ge and the ε-phases or Cu_3Ge. Some confusion exists about the composition of these phases. Hansen (lit. 1) states that the ζ-phase ranges from 11.4 to 18.7at%, but Schubert (lit. 3) places the boundaries at 11.9 and 19.4at% Ge. The ζ-phase has a h.c.p. structure (A3 type). It is to be considered a 3:2 electron compound, based on the composition Cu_5Ge (16.7at% Ge) (lit. 4).

The ε-phases form a group of three compounds. The ε-phase is the only one existing at low temperatures. It has a orthorhombically distorted A3 type structure with a=0.2645nm, b=0.4553nm and c=0.4202nm at 25at% Ge (lit. 3). Hansen does not give homogeneity boundaries (which is copied by Hultgren) but suggests them to be 24.25 and 25.5 at%Ge (lit. 1). Above 570°C the ϵ_1-phase is formed, h.c.p. with a=0.420nm, c/a=1.20. The ϵ_2-phase is cubic with about 27.5at%Ge (lit. 1).

Reynolds and Hume-Rothery (lit. 5) give a different interpretation for this region as is shown in fig. 6.2. The homogeneity region of the e phase is much wider, and the transformation to ϵ_1 occurs at 550°C.

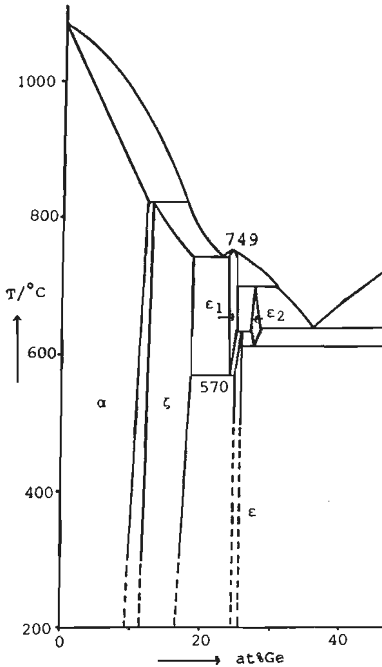

Fig.6.1
The binary phase diagram copper - germanium according to Hansen (lit.1).

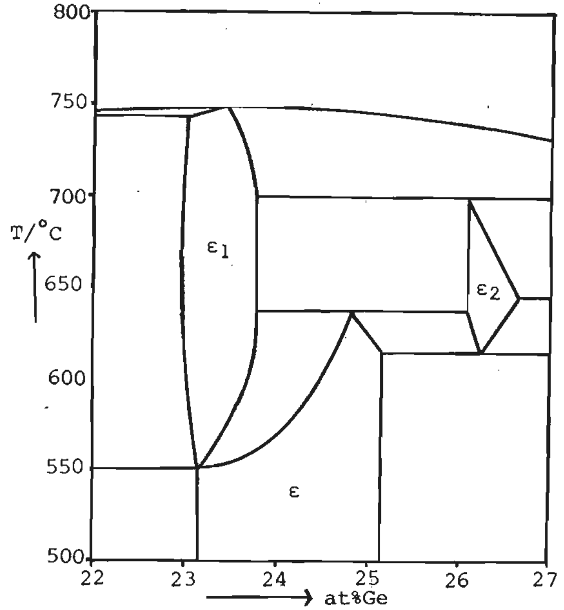

Fig.6.2.
Detail of the binary phase diagram copper - germanium according to Reynolds et al(lit.5).

The Cu-Si and Cu-Ge phase diagrams show great resemblance (lit.5). In both systems the complicated sequence of solid phases is confined in the first 27at% of the solute. A maximum in the solidus-liquidus curve is found at approximately 24at%. The extent of the primary solid solutions is of the same order. In the copper-germanium diagram the range of compositions 11-19at%Ge is occupied by the one h.c.p. ζ-phase. In the copper-silicon diagram almost exactly the same range of compositions is covered by the κ, β, ∂, γ phases, some having a h.c.p. structure, while the γ-phase has to be considered a 3:2 electron compound, like the ζ Cu-Ge compound. The copper-silicon η-phases occupy composition ranges similar to the copper-germanium ε- and ε_1-phases. In each there are high and low temperature

modifications. The ϵ_2 Cu-Ge compound does not find a counter part in the Cu-Si system, and the reverse applies for $Cu_{15}Si_4$.

In the germanium-phosphorus system only one compound is known: GeP (lit. 1).

No information has been found on the ternary Cu-Ge-P phase diagram. One ternary compound is known: $CuGe_2P_3$ (lit. 6), a semiconductor (lit. 7) with a zincblende type structure having a lattice parameter of 0.5375nm (lit. 6). Germanium can dissolve in the compound, in which case the lattice parameter can vary significantly (lit. 8).

§ 6.2.2 *Determination of the phase diagrams at 500°C*

Alloys are prepared by arc melting lumps of copper and germanium for binary and lumps of copper, germanium and copperphosphide for ternary compositions. The alloys are equilibrated for 1 month in evacuated silica capsules at 500°C. They have a tendency to stick together when they accidentally touch each other during the annealing. This phenomenon has not been observed with silicon containing alloys. After the heat treatment the alloys are metallographically prepared, as described in § 3.2. The composition of the constituting phases is determined with EPMA. Quantitative analyses are performed with the BAS correction program (lit.9) and elementary copper and germanium as calibration standards.

The maximum solubility of germanium in copper is determined to be 10.5at% at 500°C. The low germanium limit of Cu_5Ge has not been detected in Cu-Ge alloys, since the gap between this phase and the primary solid solution is that small that no two phased alloys could be prepared in this region. In diffusion couples where Cu_5Ge is formed as well, the composition ranges from 11.6 to 17.8at%. In alloys the germanium rich side of Cu_5Ge has been determined to contain 17.2at%Ge, which is less than has been described in the literature (lit.1, 3). The boundaries of

Cu_3Ge as determined in alloys with EPMA are 21.7 and 24.2at%Ge, again rather low compared with the literature values. In diffusion couples 24.8 at% germanium has been found as the maximum germanium content of the Cu_3Ge phase. Within experimental error these values are equal to those found in alloys. The width of the homogeneity region is in agreement with the results obtained by Reynolds (lit.5), but is shifted towards the copper side. This can be a result of the use of elements as calibration standards. No other binary compounds are found.

The ternary alloys have an overall composition below the line Cu_3P-Ge, since Cu_3P is the only phosphorus source used. In fig.6.3 the ternary phase diagram is depicted as is determined from the ternary alloys. Cu_3P contains 1at%Ge at the most. The compound is in equilibrium with Cu_3Ge, Cu_5Ge and with the primary solid solution. Both germanides contain 1at%P as maximum at the corner of the three phase triangles. Another three phase triangle exists between Cu_3P, Cu_3Ge and Ge.

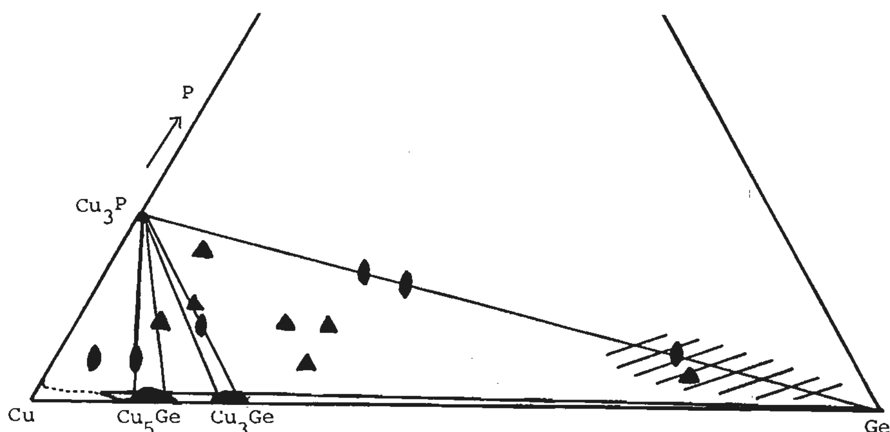

Fig.6.3 Low phosphorus part of the ternary phase diagram Cu-Ge-P. The alloys are equilibrated at 500°C in evacuated silica capsules. The compositions are determined with EPMA. The hatching indicates an area of non-equilibrium "compositions" sometimes observed and will be discussed in the text.

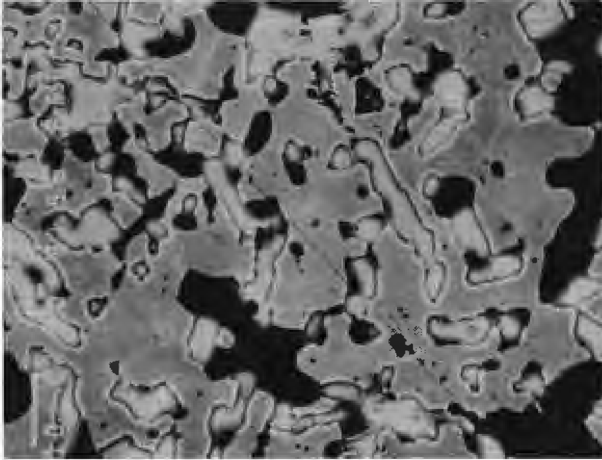

Fig.6.4 Back scattered electron image of a ternary alloy with the overall composition of $Cu_{60}Ge_{30}P_{10}$. The alloy contains Cu_3P (dark), Cu_3Ge (grey) and a ternary composition (bright, bounded by black and white lines). Bar indicates 10µm.

This situation exists in most germanium rich alloys, but sometimes a peculiar material has been found. In the back scattered electron image (fig.6.4) this material appears as bright areas, although the brightness is not constant. Furthermore the areas are surrounded with white and black lines. This may point to a conductivity problem occurring in these specific spots. If we try to make quantitative analyses of this material, we see a very large spread in composition, even within one "crystal". In fig.6.3. the compositions (normalised atomic percentages) are plotted as a hatched area. As is to be expected the brightest areas are related to the highest germanium content. The average atomic number is the highest there and this gives the greatest brightness in a back scattered electron image. If we study the results more closely, notably the measured weight percentages, we see that the total amounts are not 100%. Sometimes they are as low as 95% although the specimen is in focus, the overall conductivity is good, and no other components can be detected with EDS (energy dispersive

spectrometry). But even more odd : the totals can be as high as 105%. No explanation exists for this phenomenon. We have to conclude that this is a non-equilibrium situation, perhaps a microscopic mixture so finely divided that the electron probe also irradiates "grain boundaries". The normalised compositions suggest that this is a mixture of the original Cu_3P and Ge used to prepare the alloy. Since it is clearly not an equilibrium compound, we have not included it in the ternary phase diagram.

Contrary to the Cu-Si-P system, no ternary compounds are found by us in the Cu-Ge-P system in evacuated silica capsules at relatively low phosphorus content at 500°C.

§ 6.3 Diffusion reaction between copper and germanium

§ 6.3.1 *General remarks*

Diffusion experiments are conducted in the temperature range from 400 to 575°C in the vacuum furnace described in § 3.3.2. Below 570°C the reaction between copper and germanium is considerably slower than between copper and silicon, but seems less vulnerable for perfect slice preparation. This was already suggested by the fact that alloys stick together, although they only touch each other. High mechanical stresses are induced in the diffusion couples, sometimes resulting in spectacular flee-like jumps of the germanium platelet away from the couple after the annealing.

The influence of the compressive stress has been tested explicitely and found to be non-existent: between 2 and 9.5MPa the layer thickness is independent of the compressive stress. The influence of the phosphorus concentration in copper has been tested and again no influence has been found. Copper containing less than 1 ppm (Cu MRC Marz), 1 at% (Cu1P) and 25 at% (Cu_3P) phosphorus all react at the same rate within the experimental error.

As is shown in figs.6.5 and 6.6 straight-lined reaction

layers are formed. In all cases the main product Cu_3Ge is coarse grained. Also Cu_5Ge is formed in thin layers.

In diffusion couples with Cu1P, the Cu_3P crystals are present at the copper-germanides interface (fig.6.6). Copper is the only diffusing component in the copper-germanium system.

Since no differences in reaction rate exist between the various diffusion couples, all will be discussed together.

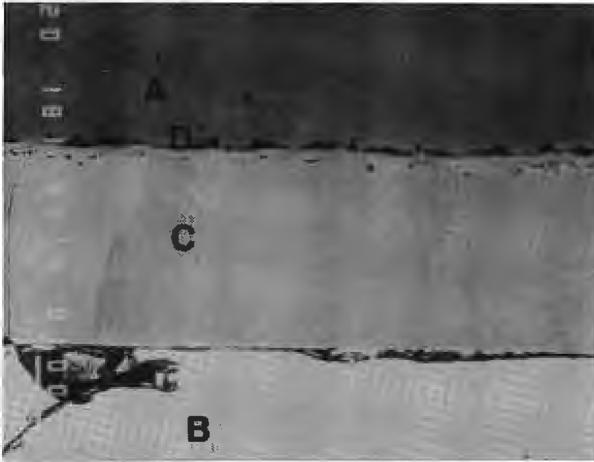

Fig.6.5 Cu MRC Marz^A/Ge^B;500,48,IV. back scattered electron image, showing the straight lined interfaces, and the coarse Cu_3Ge grains^C. Bar indicates 100 μm.

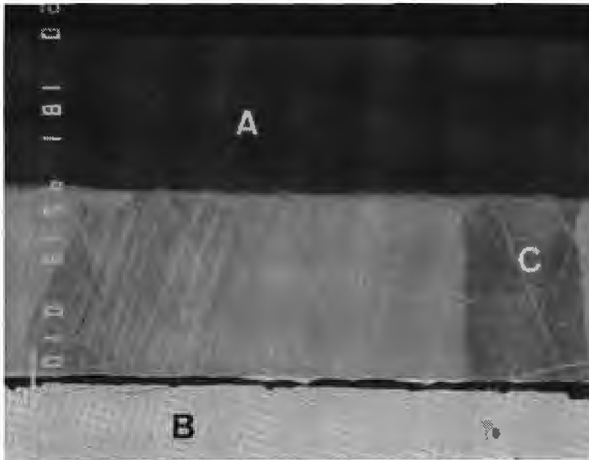

Fig.6.6 Cu1P^A/Ge^B;500,48, back scattered electron image, showing the large Cu_3Ge crystals^C, and the formation of Cu_3P at the copper-germanides interface^D. Bar indicates 100 μm.

§ 6.3.2 *Time dependence of the reaction between copper and germanium*

In figs.6.7 and 6.8 the time dependence of the layer thickness in Cu/Ge diffusion couples is plotted. It is obvious that significant experimental errors exists. This can be illustrated with the thickness of three different Cu MRC Marz/Ge diffusion couples annealed at 500°C for 48 hours. The thicknesses are respectively 219, 180 and 168 μm. If we square these values we get for d^2 (in μm^2) 47961, 32400 and 28224. Nevertheless fig.6.8 shows that these values still fit within the range set by the other diffusion couples. It is this experimental error which forces us to treat all the types of copper as equal, since we can not distinguish between them.

Fig.6.7 and 6.8 show that at both temperatures probably the parabolic growth law is obeyed, so diffusion through the already formed layer is the rate limiting step. The absence of an incubation time indicates that the reaction is not hindered by a reaction barrier. The reaction between copper and germanium is much slower than the reaction between copper and silicon: at 400°C, after 100 h about 80 μm of germanides are formed, while about 550 μm silicides are formed under the same conditions.

§ 6.3.3 *Temperature dependence of the reaction between copper and germanium*

The temperature dependence of the reaction rate constant has been determined in the temperature range between 400 and 550°C. The results are plotted in fig.6.9. The activation energy derived from this plot with the least-squares method is 104 kJ/mol. The standard deviation is 12 kJ/mol. Since the diffusion of copper through the germanides is the rate determining step in the process, this activation

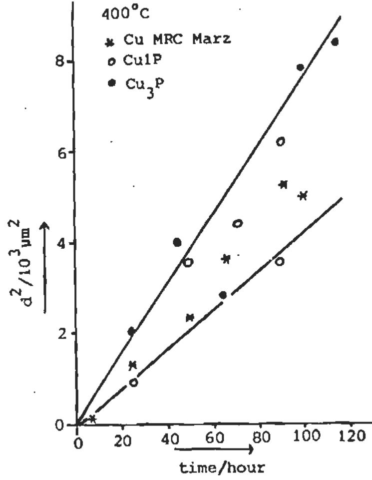

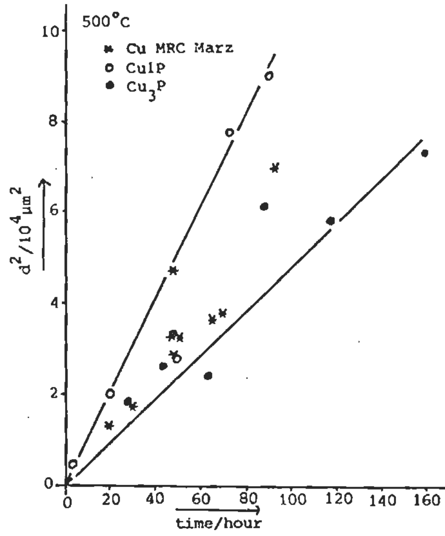

Fig.6.7 400°C *Fig.6.8 500°C*

The layer thickness in Cu/Ge diffusion couples as a function of time.

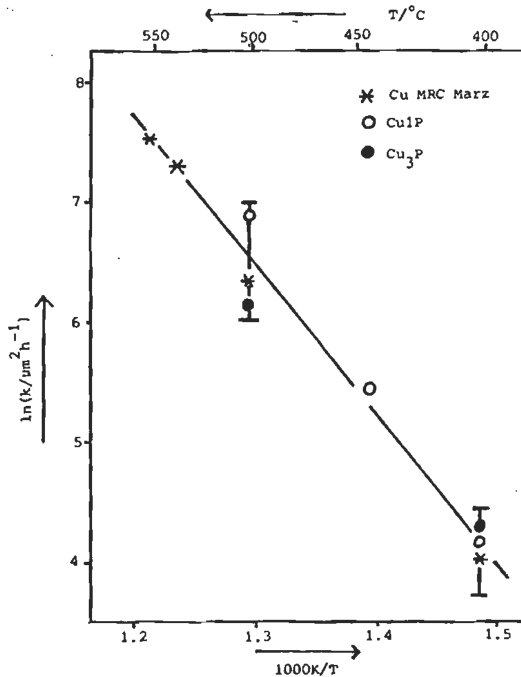

Fig.6.9 Arrhenius plot of the reaction rate constant of copper-germanium diffusion couples.

energy has to be attributed to this copper diffusion. From the pictures in figs. 6.5 and 6.6 it is clear that the Cu_3Ge is coarse grained and that diffusion is likely to occur through the bulk of the crystals, since there are not enough grain boundaries to supply the reaction interface with copper atoms. The observed activation energy is a rather low value for bulk diffusion. A vacancy mechanism seems unlikely; it may be possible that the crystal structure of Cu_3Ge offers routes for easy diffusion.

At 570 (lit. 1) or 550°C (lit. 5) a structure change occurs in Cu_3Ge. We recognize this structure change in a sudden enhancement of the reaction rate above 570°C. The excessive growth of Cu_3Ge occurs for both Cu1P and Cu MRC Marz. At 575°C a layer of 616µm grows in 10 minutes time, leading to ln k = 16.4. The reaction is so fast that experiments are virtually impossible: the few minutes necessary to reach a temperature over 570°C and to cool down afterwards will result in thick layers, that clearly influence the determined layer thickness. Furthermore very thick pieces of copper and germanium are necessary to let such large amount of germanides grow, but these will result in mechanically instable diffusion couples, where a good contact cannot be guaranteed. Therefore only a few short experiments are conducted at 575°C.

The enhancement is clearly a discontinuity in the reaction rate. Two explanations are conceivable:

- Above 570°C the ϵ_1 is formed, which has a different crystal structure. Therefore the diffusion coefficient and the frequency factor may be different (fig. 6.10)
- The Hedvall efffect (lit. 10) a sudden enhancement of the reaction rate occurs if the solid undergoes a structure change (fig. 6.11). The acceleration has been ascribed to the formation of metastable defects, which facilitates the reaction. At temperatures above the transformation the reaction rate is reduced to the expected value. In our experiments probably the formation of vacancies is facilitated near the transformation, thereby increasing the diffusion rate.

The fact that we observe this enhancement in reaction rate above 570°C suggests that the structure change occurs at 570°C (lit. 1) or a little higher temperature instead of at 550°C (lit. 5).

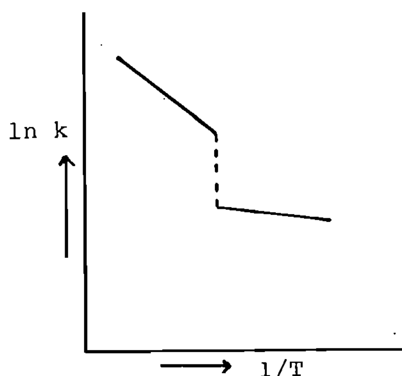

Fig. 6.10 Possible dependence the reaction rate constant on the temperature. Above 570°C a different phase is formed with a different activation energy and frequency factor.

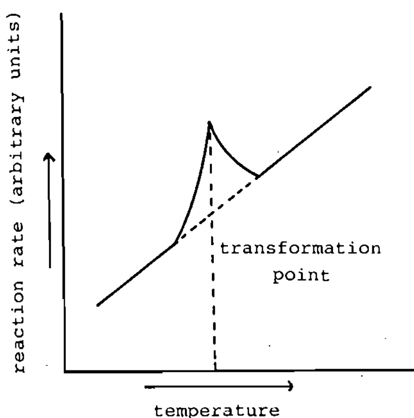

Fig. 6.11 The Hedvall effect. The reaction rate is enhanced when a structure change occurs.

§ 6.3.4 Determination of the diffusion coefficient in copper-germanium diffusion couples

In Cu/Ge diffusion couples all expected compounds are formed (the (Cu, Ge) solution, Cu_5Ge, and Cu_3Ge) and all layers show a concentration gradient. This gives the possibility to determine the inter diffusion coefficient according to formula [2. 8].

The molar volumes of Cu_3Ge and Cu_5Ge are calculated from lit. 11. For Cu_3Ge it is given that the volume of a unit cell is 0.10116 nm^3. This cell contains 2 molecules of Cu_3Ge,

so the volume per atom is 0.01264nm^3, the molar volume is then 7.61cm^3/mol $Cu_{0.75}Ge_{0.25}$. For Cu_5Ge this value is 7.55cm^3/mol $Cu_{0.83}Ge_{0.17}$. For pure copper and germanium these values are, respectively (lit.12): 7.11 and 13.63 cm^3/mol. This means that the reaction between copper and germanium to Cu_3Ge causes a shrinkage of 13%.

In fig.6.12 the concentration profile of a copper/germanium diffusion couple is given. The couple has been annealed 30 hours at 500°C. With graphical integration the diffusion coefficients can be determined according to equation [2.8]. The results are summarized in fig.6.13. Two sets of values are given, both deduced from the same profile, with the same technique. The differences show the experimental error made in this kind of determinations. The problem is that at the phase boundaries the concentration gradient is usually the steepest, but that EPMA may result in less reliable concentrations at these boundaries. Furthermore, there exists always an experimental error in the determination of the concentration which gives some uncertainty in the drawing of the concentration profile.

The average diffusion coefficient in the solid solution is $6*10^{-12}$cm^2/s, while in the Cu_5Ge phase the diffusion coefficient is $4*10^{-11}$cm^2/s. In Cu_3Ge the diffusion coefficient raises from about $1*10^{-10}$cm^2/s at 22at%Ge to about $1*10^{-8}$cm^2/s at 25at%Ge. In the diffusion couples this high diffusion coefficient leads to a thick layer of Cu_3Ge containing about 24-25at%Ge, with a small concentration gradient.

We can compare these values with those given in the literature on the catalytic activity of copper-germanium alloys in the formation of germanes (lit.13). From the amount of germanes formed, the diffusion coefficients in the alloys can be deduced. Although Chong and Skaates assume that germanium diffuses, contradictory to our findings, the interdiffusion coefficient they determine does give a measure for the total transport in the alloys. At 700K they derive the following values: in Cu_5Ge D = $5*10^{-11}$cm^2/s, in Cu_3Ge D = $5*10^{-10}$cm^2/s.

From these values and the value for the activation energy. determined in § 6.3.3 (104 kJ/mol), we can calculate a value for 773K leading to $D(Cu_5Ge)=2.7*10^{-10}cm^2/s$ and $D(Cu_3Ge)=2.7*10^{-9}cm^2/s$.

These values are comparable with those determined in this study.

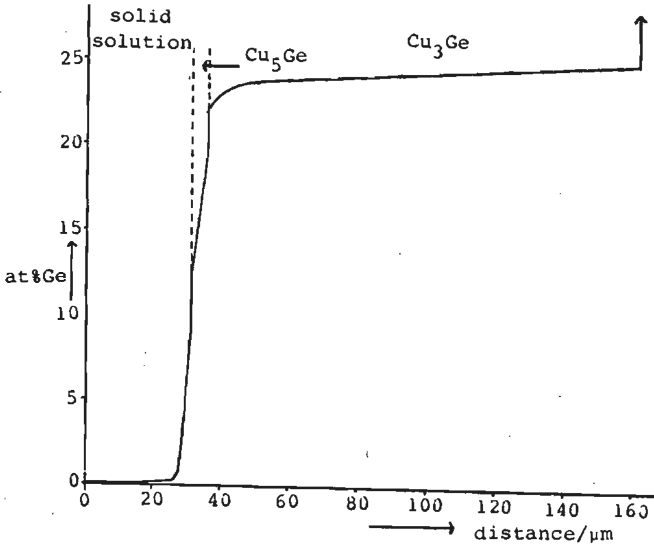

Fig.6.12 Concentration profile of a Cu/Ge diffusion couple, annealed at 500°C, for 30h, determined with EPMA.

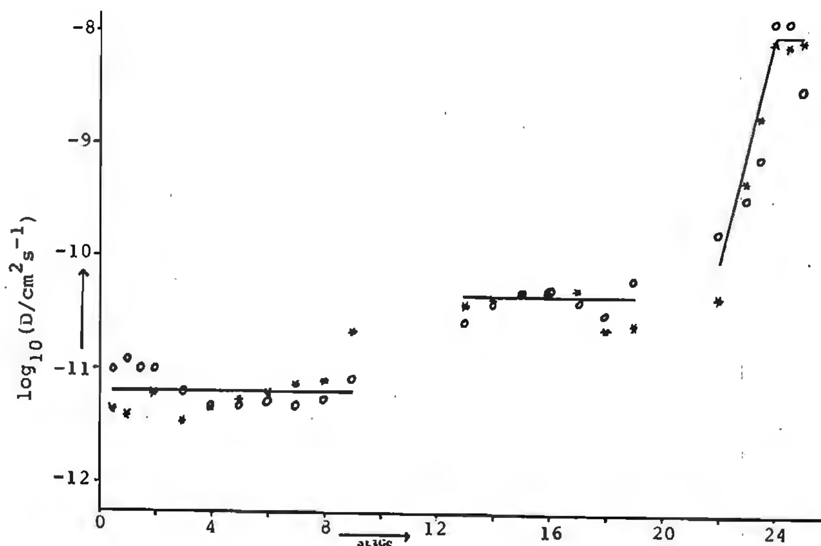

*Fig.6.13 Calculated diffusion coefficients as a function of the concentration in a Cu/Ge diffusion couple at 500°C. o and * denote two different sets of values calculated from the same profile (fig.6.12),- denotes an average value.*

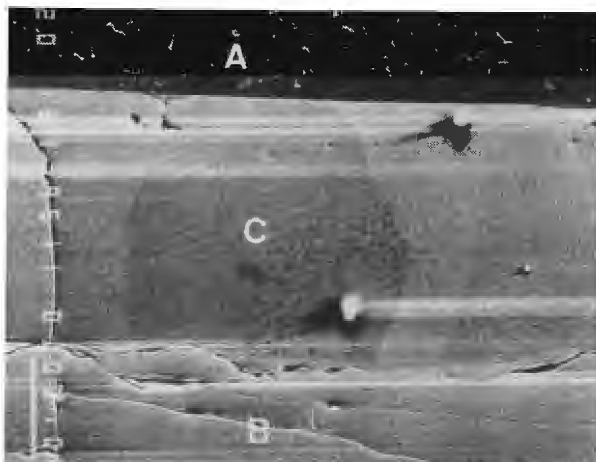

Fig.6.14. Secondary electron image of a Cu_3P^A/Ge^B diffusion couple, annealed at 500°C for 162 hours, showing the large crystals of Cu_3Ge^C. Note the absence of Cu_5Ge and the primary Cu-Ge-P solid solution. Bar indicates 100 μm.

§ 6.4 The reaction between Cu_3P and germanium in a vacuum system

So far we have considered Cu_3P as a type of copper containing a lot of phosphorus, but similar to the other types of copper. Obviously this is not true.

If we inspect the ternary phase diagram of fig.6.3, we see that there exists an equilibrium between Cu_3P and germanium, so it is not immediately clear at all how a reaction can occur in a Cu_3P/Ge diffusion couple. Furthermore the absence of a phosphorus containing reaction product contradicts the mass balance. Contrary to the copper -germanium couples, in copper phosphide-germanium couples neither the solid solution of germanium in copper nor Cu_5Ge has been formed (fig.6.14). So again we have to conclude, that the phase diagram as determined with ternary alloys, equilibrated in evacuated capsules, does not apply to diffusion couples annealed in a vacuum system. We do not have thermodynamic data on GeP or Cu_3Ge, so we can not calculate whether GeP is stable against Cu_3Ge in a vacuum system. The fact that GeP melts incongruently at 725°C shows, that this compound is not particularly stable (lit.14). Therefore we propose a phase diagram (fig. 6.15) applying for the vacuum system, analogous to the Cu-Si-P diagram: in the reaction between Cu_3P and Ge Cu_3Ge is formed and GeP, which is not stable against Cu_3P in a vacuum system and reacts to Cu_3Ge and phosphorus vapour.

From the observed reaction rate it follows, that the formation of phosphorus does not hamper the reaction. Also the morphology of the reaction layer suggests that the contact at the Cu_3P/Cu_3Ge interface remains good.

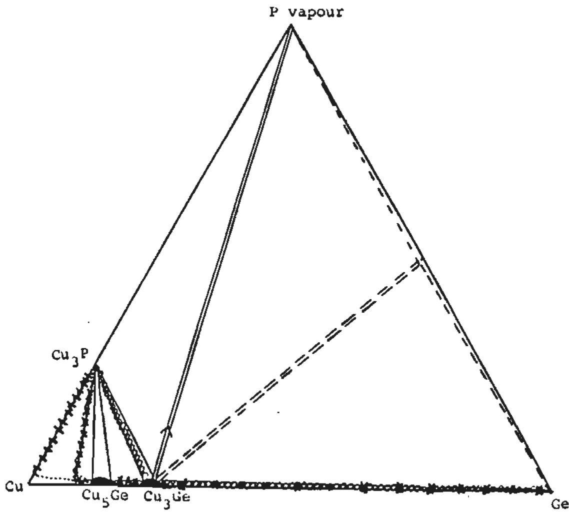

Fig.6.15 Part of the ternary Cu-Ge-P diagram prososed to apply for diffusion couples in a vacuum system. The diffusion pathes in Cu_3P/Ge couples (o) and Cu1P/Ge (x) are denoted, the arrow denotes the evolution of phosphorus vapor, GeP is considered to be instable.

§ 6.5 Conclusions

The results on the solid state reaction between copper and germanium can be summarized as follows.

Copper and germanium react in a diffusion limited process between 400 and 550°C. Copper is the only diffusing component. The activation energy for the diffusion of copper through Cu_3Ge is 104+/-12 kJ/mol. The morphology of the reaction layer suggests that bulk diffusion occurs. All expected phases are formed. No influence of the compressive stress has been found. The presence of phosphorus in copper does not influence the reaction rate, or the morphology of the reaction layers. The reaction between copper and germanium proceeds without an incubation time. All expected reaction layers are formed, since the diffusion coefficients in the various layers are such that layers with observable thicknesses can form.

At temperatures above 570°C the reaction undergoes a sudden acceleration, probably due to a structure transformation in Cu_3Ge.

Copper phosphide and germanium are in equilibrium which each other in closed silica capsules. In a vacuum system, however, they react to form Cu_3Ge and phosphorus vapour. In this case Cu_5Ge has not been found. The rate determining step is the diffusion of copper through the germanides, reaction rates being equal to those found for Cu/Ge couples.

references chapter 6

1] M. Hansen; Constitution of Binary Alloys, McGraw-Hill, New York (1958)

2] R. Hultgren, P.D. Desai; Selected thermodynamic values and phase diagrams for copper and some of its binary alloys. International Copper Research Association Inc. (1971)

3] K. Schubert, G. Brandauer; Z.Metallk. 43(1952),262

4] W. Hume-Rothery, P.W. Reynolds, G.V. Raynor; J.Inst.Met.66(1940),19

5] J. Reynolds, W. Hume-Rothery; J.Inst.Met. 85(1956),119

6] O.G. Folberth, H.Pfister; Acta Cryst. 14(1961),325

7] T.Hailing, G.A. Saunders, M.S. Omar, B.R. Pamplin; J.Phys.Chem.Solids 45(1984),163

8] N.A. Goryunova, V.I. Sokolova, T. Ping-Hsi; Dokl.Acad.Nauk.SSSR 152(1963),363

9] G.F. Bastin, H.J.M. Heijligers, F.J.J. van Loo; Scanning 6(1984),58

10] J.A. Hedvall; Reaktionsfahigkeit fester Stoffe; Verlag von Johann Ambrosius Barth, Leipzig (1938)

11] P.Villars, L.D. Calvert; Pearson's Handbook of Crystallographic Data for Intermetallic Phases, vol 2, American Society for Metals, Metals Park, Ohio (1985)

12] Handbook of Chemistry and Physics, 51st ed. Chemical Rubber Co., Cleveland Ohio (1970)

13] T. Chong, J.M. Skaates; J.Catal. 28(1973),20

14] Ya.A. Ugai, L.I. Sokolov, E.G. Goncharov, V.R. Pshestanchik; Russ.J.Inorg.Chem; 23(1978),1048

chapter 7 a comparison between silicon and germanium in their reaction with copper

When we see the results discussed in the previous chapters, we can distinguish four aspects, in which silicon differs from germanium in the reaction with copper.

a] In copper-silicon diffusion couples only Cu_3Si is formed, while in copper-germanium couples the (Cu,Ge) solid solution, Cu_5Ge and Cu_3Ge are formed. Furthermore the layer thicknesses in copper-silicon couples are much larger than in copper-germanium couples at the same time and temperature.

b] In copper-silicon couples we can distinguish two activation energies, 175 and about 100 kJ/mol, attributed to bulk- and grain boundary diffusion of copper through Cu_3Si, respectively. In the copper-germanium couples only one activation energy has been found. Based on the morphology of the product layer we attribute it to bulk diffusion of copper through Cu_3Ge, although the value of 105 kJ/mol for the activation energy is much lower than for the bulk diffusion through Cu_3Si.

c] Copper phosphide-silicon diffusion couples exhibit a remarkable morphology. Gaps are formed in the product layer, which consists of columns of Cu_3Si, separating the original platelets. Only at high temperatures sometimes a closed product layer has been found.
The product layer in copper phosphide-germanium couples, however, is closed in the whole temperature range.

d] In copper-silicon diffusion couples a reaction barrier is present, which results in the occurrance of an incubation time at low temperatures. Connected with this the reaction is influenced by the presence of phosphorus in copper and by the applied compressive stress. These phenomena are absent in copper-germanium diffusion couples.

ad a]

The layer thicknesses in copper-silicon and copper-germanium couples depend on the respective diffusion coefficients. Unfortunately, the Cu_3Si as well as the $Cu_{15}Si_4$ layers do not show a concentration gradient, so we can not determine an interdiffusion coefficient. However, we can determine an integrated diffusion coefficient by eq. [2.9].

For the copper-germanium compounds we can determine the interdiffusion coefficients for Cu_5Ge and Cu_3Ge using eq. [2.8]. We get the following values at 500°C:

Cu_3Si:	D_{int}	$\approx 2.2*10^{-8}$	cm^2/s
$Cu_{15}Si_4$:	D_{int}	$\approx 1.6*10^{-11}$	cm^2/s
Cu_3Ge:	$\tilde{D}$	$\approx 10^{-10} - 10^{-8}$	cm^2/s
Cu_5Ge:	$\tilde{D}$	$\approx 4*10^{-11}$	cm^2/s

From these data we derive that, since the integrated diffusion coefficient in $Cu_{15}Si_4$ is over 1000 times smaller than in Cu_3Si, the $Cu_{15}Si_4$ layer will be invisibly thin compared to the Cu_3Si layer in a Cu/Si diffusion couple. The same is true, to a lesser extent, for the layer thicknesses of Cu_5Ge and Cu_3Ge. Therefore Cu_5Ge can be observed in Cu/Ge diffusion couples, albeit very thin.

A direct comparison between the diffusivities in Cu_3Si and Cu_3Ge is not possible from the data cited above. However, we can estimate a minimum value for the interdiffusion coefficient $\tilde{D}$ in Cu_3Si from a modification of eq[2.9]:

$$D^{int} \approx \tilde{D}_{av} * \Delta N$$

Since the difference in mole fraction ΔN in the growing Cu_3Si layer from the silicon to the copper side is less than 0.001, it follows that the average interdiffusion coefficient $\tilde{D}_{av}$ in $Cu_3Si > 2.2*10^{-6}$ cm^2/s. This is about 100 times as large as the interdiffusion coefficient in

Cu_3Ge.

From these values for the interdiffusion coefficients and the activation energies, we can determine the frequency factor D_0 for Cu_3Ge and Cu_3Si by appling eq[2.15].

$$\tilde{D} = D_0 \exp{-Q/RT}$$

We get for Cu_3Ge that $D_0 \approx 0.06$ cm^2/s and for Cu_3Si that $D_0 > 1.5*10^6$ cm^2/s. The value for Cu_3Ge is quite normal for bulk diffusion (lit.1), but that for Cu_3Si is very high.

The difference in diffusion coefficients between the germanides and the silicides may be related with differences in structure.

ad b]

When we want to compare the activation energies for the copper diffusion in Cu_3Si and Cu_3Ge, we have to take into consideration the fact that the melting point T_M of Cu_3Ge (1022K) is about 100°C lower than that of Cu_3Si (1132K). We can allow for this difference by plotting the results as a fucntion of the relative temperature, T/T_M, in the same way as Tiwari has done when comparing the selfdiffusion coefficients in f.c.c and b.c.c metals (lit.2).

Fig.7.1 gives an Arrhenius plot for the reaction rate constants as a function of the reciprocal temperature. The slope obtained from this plot gives Q/T_M.

Several remarks can be made. The relative temperature ranges, where Cu_3Si and Cu_3Ge are formed in coarse-grained layers, seem to be identical. The activation energies for the bulk diffusion of copper in Cu_3Ge and Cu_3Si are unequal (104 resp. 175 kJ/mol). The values for Q/T_M are also different, but to a lessr extent: 100 and 150 J/mol.K for Cu_3Ge and Cu_3Si respectively. For comparison, Tiwari has found 145 J/mol.K for the selfdiffusivity in f.c.c. and b.c.c. metals (lit.2).

These values suggest, that bulk diffusion occurs, but that in Cu_3Si fast diffusion routes exist, expressed in the high frequency factor. In Cu_3Ge bulk diffusion occurs

with a relative low activation energy.
The reaction rate constant for the Cu/Ge reaction at 575°C fits an extropolation of the Cu_3Si bulk diffusion at higher relative temperatures. This suggest that the ϵ_1 phase formed in Cu/Ge couples has a diffusivity comparable with Cu_3Si. Furthermore we expect a change in slope in the Cu_3Ge curve similar to the Cu_3Si curve, occurring at low temperatures, for instance, above $T_M/T \approx 1.5$. In order to determine this transition experiments ought to be conducted in the temperature range between 400 and 200°C. Unfortunately, the reaction rate will then be that small, that experiments are virtually impossible.

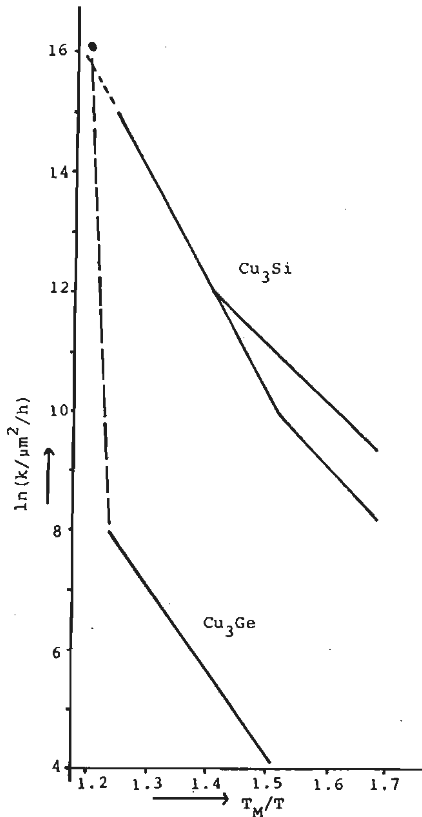

Fig.7.1 Arrhenius plot of the reaction rate constants in Cu/Si and Cu/Ge diffusion couples as a function of the reciprocal relative temperature.

ad c]

In Cu3P/Si diffusion couples, annealed at 550 °C, we observed plastic deformation of the columns, sometimes leading to a closed layer, with a reaction rate comparable with the reaction rate in Cu/Si diffusion couples. In Cu_3P/Ge diffusion couples we observe only closed product layers and reaction rates comparable with Cu/Ge couples. Since the Cu_3P/Ge couples are annealed at higher relative temperature, plastic deformation is more likely to occur. This may be the reason for the difference in morphology of the product layers.

ad d]

The reaction of silicon with copper is charaterized by interfacial problems. Silicon is covered with a silicon dioxide layer, which is nearly inpenetrable for copper. If the reaction conditions are such that this layer is removed (high compressive stress, phosphorus in copper or after long incubation times) the reaction proceeds, but the morphology of the reaction product is strongly influenced by nucleation phenomena.

The reaction between germanium and copper proceeds like a text book example: all expected products are formed, no incubation time exists, no influence of compressive stress or phosphorus content. The copper-germanium interface seems hardly vulnarable for obstructions. The same phenomenon has been observed during heat treatment of alloys, which stick together although they only touch each other. Extensive diffusion occurs then. The reactions of silicon are dominated by the presence of an oxidation layer. Evidently the stability of the oxidation layer on germanium is different.

Some experimental prove for this statement is found in the literature, where the oxidation of copper-silicon respectively copper-germanium alloys has been studied. When Cu_3Si is oxidized SiO_2\ is formed, while Cu remains unchanged (lit.3). After 2 weeks even 0.4µm of SiO2 has been formed. The layer underneath is enriched in copper. If however Cu_3Ge is oxidized GeO and Cu_2O are formed

(lit. 4) at 400 and 500K. Only at 600K this surface is transformed to Cu + GeO_2.
For the diffusion couples this means that SiO_2 on the silicon surface will be stable with respect to Cu, but that GeO_2 will be transformed in the presence of Cu to Cu_2O and GeO, thereby breaking the oxidation layer. No reaction barrier will exist, as the results of the copper germanium diffusion couples clearly show. Since no reaction barrier exists, the reaction between copper and germanium is not influenced by the phosphorus content of the copper or by the application of compressive stress.

In this thesis we have seen a large influence of only a trace of an impurity on a solid state reaction. The influence can be that large since segregation causes a high enrichment of the impurity at the surface of the reactant. Therefore the reaction interface is different from what is suggested by the bulk composition. It is precisely at this interface where the copper-silicon reaction deviates from the copper-germanium reaction by the presence of a large reaction barrier. And so the whole of the reaction is changed by the presence of the impurity.

Generalizing the results, one can say, that in solid state reactions, exact knowledge of the reaction interface is necessary to understand the course of the reactions. Or the other way around: if a reaction proceeds different from what has been expected it might well be that impurities play a major role.

References chapter 7

1] Y. Adda, J. Philibert; La diffusion dans les solides; Institut national des sciences et techniques nucleaires (1966), I, p 490

2] G. P. Tiwari; Z. Metallk. 72(1981), 211

3] W. F. Banholzer, M. C. Burrell; Surf. Sci. 176(1986), 125

4] T. S. Sampath Kumar, M. S. Hegde; Surf. Sci. 150(1985), L123

summary

This thesis describes a research concerning the influence of a trace of a third element on the reaction in a binary system. The solid state reaction between copper and silicon is studied in diffusion couples. Copper and silicon slices are pressed together in a vacuum furnace. We have worked with a constant load, because the compressive stress appears to influence the thickness of the product layer.

The reaction rate is determined by the diffusion of copper through the already formed product layer. At high temperatures the diffusion proceeds with a bulk mechanism, at low temperatures ($T<470°C$) copper diffuses through the grain boundaries. In the latter case also an incubation time occurs. If a trace (ppm) of phosphorus is present in copper, the incubation time disappears and the grain boundary diffusion mechanism is operative until 530°C. Based on our experiments we explain this incubation time with the presence of an oxyde layer on the silicon, which is removed by segregation of phosphorus to the reaction interface.

Both in the absence and in the presence of phosphorus the only reaction product is Cu_3Si, although the phase diagram also predicts the formation of $Cu_{15}Si_4$ and Cu_5Si. The absence in diffusion couples can by explained by the kinetics of the formation: these compounds are formed in principle, but the reaction rate is that low, that the layer thickness is too small to be detected in normal Cu/Si diffusion couples. In diffusion couples between copper and Cu_3Si, however, these compounds are found.

Ternary diffusion couples between Cu_3P and silicon and ternary Cu-Si-P alloys are studied. Also in these diffusion couples only Cu_3Si is formed. Based on the mass balance we expect the formation of phosphorus or a phosphorus containing compound. In alloys, which have been annealed in evacuated silica capsules, ternary compounds are found. These compounds are absent in the product layer. The couples lose weight during the reaction, so a gasous product is formed.

Based on the morphology of the product layer it can be determined, that this product does not contain silicon. If we also take the weight losses into consideration it can be concluded, that phosphorus vapor is formed. It appears, that isothermal sections of the Cu-Si-P phase diagram are dependent on the experimental conditions: the phase relations in the vacuum furnace differs from those in a closed capsule.

The reactions between copper and silicon are compared with those between copper and germanium. The reaction between copper and germanium is not influenced by the presence of phosphorus, or by the applied compressive stress. The reaction is diffusion limited, no incubation times have been found. Copper diffuses with a bulk diffusion mechanism between 400 and 570°C. At higher temperatures the reaction rate is much larger and makes experiments impossible. All germanides, existing according the phase diagram, are formed in copper-germanium diffusion couples.

No ternary compounds are found in Cu-Ge-P alloys. In Cu_3P/Ge diffusion couples only Cu_3Ge is formed. Also in this case phosphorus is lost as a vapor.

The differences between binary copper-silicon and copper-germanium couples can be explained by the differences in the properties between the oxydes of silicon and germanium: germanium oxyde does not hinder the reaction with copper, while silicon oxyde is an effective diffusion barrier for copper. Therefore, the factors that influence the reaction with silicon because of removal of this barrier, do not influence the reaction between copper and germanium.

A comparison has been made between our results ans those reported in literature on the reaction between copper and silicon. These literature data, which seemed to be conflicting, appear to be intepretable, when we take the above mentioned oxyde layer on silicon into account as well as the occurrance of grain boundary respectively bulk diffusion in temperature ranges, which depend on the purity of the copper used.

samenvatting

Dit proefschrift beschrijft een onderzoek naar de invloed van een spoor van een derde element op de reaktie in een binair systeem. Met behulp van de diffusiekoppeltechniek is de vaste stof reaktie tussen koper en silicium bestudeerd. In een vacuumoven zijn koper en silicium plaatjes tegen elkaar aan geklemd met behulp van konstant gewicht.

Het blijkt dat de klemdruk van invloed is op de dikte van de produktlaag. De snelheid van de reaktie wordt bepaald door de diffusie van koper door de reeds gevormde reaktielaag. Bij hoge temperatuur vindt diffusie plaats via een bulkmechanisme, bij lage temperatuur (T < 470°C) diffundeert koper via de korrelgrenzen. In dit laatste geval treedt ook een incubatie tijd op. Indien het koper een spoor (30 ppm) fosfor bevat, verdwijnt deze incubatietijd en het korrelgrensdiffusie mechanisme treedt op tot 530°C. Op grond van onze experimenten verklaren wij deze incubatietijd met de aanwezigheid van een oxidelaag op het silicium, welke verwijderd wordt door de segregatie van fosfor naar het reaktie grensvlak. Zowel in aan- als afwezigheid van fosfor is het enige reaktieprodukt Cu_3Si, hoewel het fasendiagram ook de vorming van $Cu_{15}Si_4$ en Cu_5Si voorspelt. De afwezigheid in diffusiekoppels kan verklaard worden op grond van de kinetiek van de vorming : deze verbindingen worden in principe wel gevormd, maar de snelheid is zo laag, dat in Cu/Si koppels de reaktielaag te dun is om te detecteren. In koppels tussen koper en Cu_3Si worden ze wel aangetroffen.

Ternaire diffusiekoppels tussen Cu_3P en silicium en Cu-Si-P legeringen zijn bestudeerd. In deze diffusiekoppels wordt alleen Cu_3Si gevormd. Op grond van de massabalans zou ook fosfor of een fosforhoudende verbinding gevormd moeten worden. In legeringen, die verhit zijn in geevacueerde silicacapsules, zijn wel ternaire verbindingen aangetroffen. De koppels verliezen gewicht tijdens de reaktie, dus wordt er een gasvormig produkt gevormd. De morfologie van de reaktielaag laat zien, dat dit produkt geen silicium bevat. Ook op

basis van de grootte van het gewichts verlies kan geconcludeerd worden dat fosfordamp gevormd wordt. Het blijkt dat de isotherme doorsnede door het fasendiagram Cu-Si-P afhankelijk is van de proefomstandigheden: in de vacuumoven zijn de fasenrelaties anders dan in een gesloten capsule.

De reakties van koper met silicium zijn vergeleken met die van koper met germanium. De reaktie tussen koper en germanium wordt niet beinvloed door de klemdruk tijdens de reaktie, evenmin heeft de aanwezigheid van fosfor enige invloed. De reaktie is diffusiegelimiteerd, er treedt geen incubatietijd op. Koper diffundeert via een bulkmechanisme tot T = 570°C. Bij hogere temperaturen wordt de reaktiesnelheid veel groter en is dan experimenteel niet meer toegankelijk. Alle germaniden die volgens het fasendiagram bestaan worden ook daadwerkelijk gevormd in koper-germanium diffusiekoppels.

In Ge-Cu-P legeringen zijn geen ternaire verbindingen gevonden. In diffusiekoppels tussen Cu_3P en germanium wordt alleen Cu_3Ge gevormd. Ook in dit geval verdwijnt de fosfor als damp.

De verschillen tussen de binaire Cu/Si en Cu/Ge koppels kunnen verklaard worden door het verschil in eigenschappen van het oxide van silicium en germanium : germaniumoxide vormt geen belemmering voor de reaktie met koper, terwijl siliciumoxide een effectieve diffusiebarriere vormt. Daarom hebben faktoren, die in het geval van silicium een grote invloed hebben juist door de verwijdering van deze oxidelaag, geen invloed op de reaktie tussen koper en germanium.

Er is een vergelijking gemaakt tussen onze resultaten en die, welke in de literatuur vermeld worden omtrent de reactie tussen koper en silicium. Deze literatuurgegevens, die vaak strijdig leken, blijken geinterpreteerd te kunnen worden als men rekening houdt met de genoemde oxidehuid op silicium en het voorkomen van korrelgrens- en bulkdiffusie in temperatuurtrajekten, die afhankelijk zijn van de zuiverheid van het gebruikte koper.

LEVENSBERICHT

van Hanneke Becht, geboren 9 juli 1957

Na het behalen van het diploma ongedeeld VWO aan het Avond Lyceum te Breda, ben ik in 1976 begonnen aan de studie voor scheikundig ingenieur aan de Technische Hogeschool te Eindhoven. Het afstudeerwerk, met als onderwerp "Mechanistische aspekten van vitamine B_{12}-afhankelijke reakties" heb ik uitgevoerd binnen de vakgroep Organische Chemie, onder leiding van prof. dr. H.M. Buck. In april 1983 werd het ingenieursexamen afgelegd.

In mei 1983 ben ik begonnen aan het onderzoek, zoals beschreven in dit proefschrift, onder leiding van prof. dr. R. Metselaar. Van 1 mei 1983 tot 1 mei 1987 ben ik in dienst geweest van de Nederlandse Organisatie voor Zuiver Wetenschappelijk Onderzoek.

NAWOORD

Een proefschrift schrijven doet men niet alleen. Velen ben ik dank verschuldigd bij het tot stand komen van dit proefschrift: Ru Metselaar voor zijn inspirerende leiding, Frans van Loo voor alle adviezen op praktisch en theoretisch gebied en voor de vele stimulerende diskussies. Hans Heijligers heeft me ter zijde gestaan bij de bediening van de microprobe. Giel Bastin heeft me geleerd analyse resultaten kritisch te bekijken. Joop Horbach heeft het fotografische werk verricht. Hans de Jonge Baas en Fred Kruger wil ik danken voor het vele röntgen werk dat zij voor mij gedaan hebben. Sjef Vrolijk heeft voor de programmatuur gezorgd voor het verwerken van deze tekst. Alle leden van de vakgroep Fysische Chemie hebben bijgedragen aan de ontzettend fijne tijd, die ik bij hen heb doorgebracht.

Frits, dank je voor je vertrouwen en voortdurende steun in deze laatste moeilijke maanden.

STELLINGEN

1 In tegenstelling tot de bewering van Guy, biedt het gebruik van een "mole-fixed" referentiesysteem voor het beschrijven van een binair diffusieproces, geen voordelen boven het gebruik van een "volume-fixed" referentiesysteem.

A. G. Guy; J. Mater. Sci. 20 (1985), 4317-4328

2 De uitscheidingen, die door Quinn et al. worden gevonden in de titaancarbide laag, die wordt gevormd in diffusiekoppels van het type TiC-Ti duiden eerder op verontreinigingen met zuurstof en/of stikstof, dan op uitscheidingen van Ti_2C, zoals door hen wordt aangenomen.

C. J. Quinn, D. L. Kohlstedt;
J. Am. Cer. Soc. 67 (1984), 305-310

3 Bij de door Armigliato et al. voorgestelde deconvolutiemethode om de bijdrage van de TiLl röntgenemissielijn te scheiden van de NKα door gebruik te maken van een constant veronderstelde verhouding tussen de TiLα en de TiLl lijn, wordt voorbij gegaan aan het feit, dat deze verhouding sterk gewijzigd wordt door de aanwezigheid van de N-Kα absorptie kant in het emissiespectrum.

A. Armigliato, L. Dori, A. Garulli, P. Venturi;
J. Microsc. Spectrosc. Electron. 7 (1982), 593-603

4 In de ontwikkeling van een model, dat de warmteoverdracht en de depositiesnelheden gedurende laser-CVD beschrijft, wordt door Esrom en Wahl ten onrechte geen rekening gehouden met de mogelijke beschadiging van het substraat door thermoshock.

H. Esrom, G. Wahl; Proc. Euro-CVD VI, Jerusalem (Irsael), 30 mrt-20 apr 1987, ed. R. Pirat, pp 367-380

5 Gedurende de vaste stof reaktie tussen Ni en SiC bij 800°C ontstaat naast Ni_5Si_2(+C), zoals gevonden door Yamada et al., ook Ni_3Si en Ni_2Si(+C).

T. Yamada, H. Sekiguchi, H. Okamoto, S. Azuma, A. Kitamura; Proc. 2nd Intern. Symp. Cer. Mat. Compon. Engines, Lübeck (FRG), 14-17 apr 1986, ed. W. Bunk, H. Hausner, pp 441-448

6 Bij de verklaring van de elektrische eigenschappen van samenstellingen in het systeem Na_2SO_4-Li_2CO_3 gaat Dissanayake ten onrechte voorbij aan de rol van de anion dotering.

M. A. K. L. Dissanayake;
Solid State Ionics 23(1987), 49-51

7 De door N. S. Rasor gebruikte uitdrukking voor de uittree-arbeid van de collector in een thermionische energie-omzetter bevat alleen de collectortemperatuur en de cesiumreservoirtemperatuur als parameters; ten onrechte wordt hierbij de chemische constitutie van de collector geheel buiten beschouwing gelaten.

N. S. Rasor; Appl. Atom. Coll. Phys. 5(1982), 169-200

8 Het verdient aanbeveling onderzoek te verrichten naar de vraag of de voordelen van het gebruik van amidine beschermende groepen voor de exocyclische aminogroepen van de nucleotidebasen adenine, guanine en cytosine ook gehandhaafd blijven in de automatische DNA synthese.

L. J. McBride, R. Kierzek, S. L. Beaucage, M. H. Caruthers;
J. Am. Chem. Soc. 108(1986), 2040-2048

9 De door Frank et al. geconstateerde diffusielimitering tijdens de vorming van silaan uit methylchloride en Cu_3Si moet niet worden toegeschreven aan de diffusie van silicium in Cu_3Si maar aan de trage diffusie in de koperverrijkte fase aan het oppervlak van de Cu_3Si korrels.

T. C. Frank, K. B. Kester. J. L. Falconer;
J. Catal. 91(1985), 44-53

10 Hoewel Moissan in de door hem ontwikkelde vlamboogoven voor zijn tijd ongekend hoge temperaturen heeft bereikt, is het gezien zijn opstelling technisch onmogelijk, dat hij over gesmolten ijzer van 4000°C heeft beschikt, zoals Snelders stelt.

H. Moissan; Comptes Rendus de l'Academie des Sciences, 115(1892), 1031-1033
H. A. M. Snelders; Chemie en Techniek, 21(1966), 400-402

11 Mensen, die het eng vinden om een karkas van een klein dier als een kip of konijn zelf aan stukken te snijden, zouden ook geen vlees moeten eten dat door anderen in lapjes is gesneden.

Eindhoven 22 mei 1987 J. G. M. Becht